

Rowan University

Rowan Digital Works

---

Theses and Dissertations

---

6-20-2023

## EVALUATING THE IMPACT OF OXIDATION ON MOISTURE RESISTANCE OF ASPHALT COMPONENTS AND MIXTURES

Ahmad Alfalah  
*Rowan University*

Follow this and additional works at: <https://rdw.rowan.edu/etd>



Part of the [Civil and Environmental Engineering Commons](#)

---

### Recommended Citation

Alfalah, Ahmad, "EVALUATING THE IMPACT OF OXIDATION ON MOISTURE RESISTANCE OF ASPHALT COMPONENTS AND MIXTURES" (2023). *Theses and Dissertations*. 3137.  
<https://rdw.rowan.edu/etd/3137>

This Dissertation is brought to you for free and open access by Rowan Digital Works. It has been accepted for inclusion in Theses and Dissertations by an authorized administrator of Rowan Digital Works. For more information, please contact [graduateresearch@rowan.edu](mailto:graduateresearch@rowan.edu).

**EVALUATING THE IMPACT OF OXIDATION ON MOISTURE RESISTANCE  
OF ASPHALT COMPONENTS AND MIXTURES**

by

Ahmad Alfalah

A Dissertation

Submitted to the  
Department of Civil and Environmental Engineering  
College of Engineering

In partial fulfillment of the requirement

For the degree of

Doctoral of Philosophy in Civil Engineering

at

Rowan University

Dissertation Chair: Yusuf Mehta, Ph.D., P.E., Department of Civil and Environmental  
Engineering

Committee Members:

Cheng Zhu, Ph.D., P.E., Assistant Professor, Department of Civil and Environmental  
Engineering

Gilson Lomboy, Ph.D., P.E., Assistant Professor, Department of Civil and Environmental  
Engineering

Theresa Loux, Ph.D., P.E., Adjunct Faculty, Department of Civil and Environmental  
Engineering, and CTO, Aero Aggregate of North America

Nasrine Bendjilali, Ph.D., Associate Professor, Department of Mathematics

© 2023 Ahmad Alfalah

## **Dedications**

I dedicate this work to the most important people in my life, my father Ghazi, my mother Nadia, my brother Laith, and my sisters Areen and Nadeen, and their families. Their unwavering love, support, and encouragement have been a constant source of inspiration throughout my academic journey. I am forever grateful for their guidance and belief in me. To all those who have played a part in my growth, both personally and academically, thank you from the bottom of my heart.

## **Acknowledgements**

I am deeply grateful to Dr. Yusuf Mehta, Director of CREATES and my advisor, and Dr. Ayman Ali, Associate Director of CREATES, for their invaluable guidance and assistance throughout this research project. Their unwavering support and mentorship have been instrumental in my growth as a researcher.

I would also like to express my appreciation to the entire faculty of Rowan University Civil and Environmental Engineering Department, especially to my thesis committee members, Dr. Cheng Zhu, Dr. Gilson Lomboy, and Dr. Theresa Loux, as well as Dr. Nasrine Bendjilali from the Mathematics Department. Their insightful comments, time, support, and assistance have been invaluable to the completion of this research.

Furthermore, I would like to extend a special thank you to Dr. Daniel Offenbacher, who has been a constant source of guidance and assistance throughout my research. I also want to thank my lab mates and postdocs for their unwavering support throughout my graduate career and wish them success in their future endeavors.

Finally, I am grateful to the team at U.S. Army Engineer Research and Development Center (ERDC) and Cold Regions Research and Engineering Laboratory (CRREL), led by Ms. Danielle Kennedy, Dr. Ben Cox, Dr. Mohamed Elshaer, and Dr. Wade Lein, for their support and assistance throughout this project.

## **Abstract**

Ahmad Alfalah

### **EVALUATING THE IMPACT OF OXIDATION ON MOISTURE RESISTANCE OF ASPHALT COMPONENTS AND MIXTURES**

2022-2023

Yusuf Mehta, Ph.D., P.E.

Doctoral of Philosophy in Civil Engineering

This study investigated the effects of asphalt oxidation and testing temperature on moisture damage in asphalt mixtures, using AASHTO T283 and Surface Free Energy (SFE) testing. The study assessed the impact of three asphalt binder grades (PG 64-22, PG 76-22, and PG 52-34) and three test temperatures (ALT, AIT, and CIT) on the susceptibility to moisture damage. Additionally, three oxidation levels (OTC, STOC, and LTOC) were evaluated to determine the optimal level of oxidation and testing temperature for AASHTO T283 to detect moisture damage. Load-displacement curve parameters and IDEAL-CT were analyzed to better understand the effects of oxidation and moisture conditioning on asphalt mixtures. The study also evaluated the effects of three oxidative levels (OB, RTFO, and PAV20) on moisture damage susceptibility using SFE testing. Fourier transform infrared spectroscopy (FTIR) attenuated total reflectance (ATR) was also used to quantify the effects of oxidative conditioning on asphalt binder chemical properties. The findings suggest that asphalt mixtures are more susceptible to moisture damage at STOC and LTOC than OTC, and that oxidation and CIT have the greatest impact on moisture damage susceptibility. The study highlights the need for an alternative oxidation conditioning and testing at CIT to detect moisture damage more accurately in asphalt mixtures.

## Table of Contents

Abstract.....	v
List of Figures.....	ix
List of Tables .....	xi
Chapter 1: Introduction.....	1
Background.....	1
Problem Statement.....	2
Research Hypothesis.....	3
Significance of Study.....	4
Goal & Objectives.....	5
Research Approach.....	6
Chapter 2: Literature Review.....	8
Introduction.....	8
Tests Performed on Mixtures to Quantify Moisture Damage.....	9
Loose-Mix Test: Static Immersion Test (AASHTO T182).....	10
Loose-Mix Test: Boiling Water Test (ASTM D3625).....	11
Compacted-Mix Test: Hamburg Wheel Tracking Test (HWTT).....	11
Compacted-Mix Test: Saturated Ageing Tensile Stiffness (SATS).....	14
Compacted-Mix Test: Environmental Conditioning System (ECS).....	15
Compacted-Mix Test: Moisture Induced Sensitivity Test (M.I.S.T).....	17
Compacted-Mix Test: Modified Lottman Test (AASHTO T283).....	20
Compacted-Mix Test: Indirect Tensile Asphalt Cracking Test (IDEAL-CT).....	25
Surface Free Energy (SFE).....	27

## Table of Contents (Continued)

Calculations of SFE .....	30
Fourier Transform Infrared Spectroscopy-Attenuated Total Reflectance (FTIRATR) .....	41
Summary of Literature Review .....	43
Chapter 3: Description of Materials.....	44
Asphalt Binders and Aggregate .....	44
Probe Liquids .....	47
Chapter 4: Experimental Plan .....	48
Introduction.....	48
AASHTO T283 Experimental Plan .....	48
General Scope .....	48
AASHTO T283 Specimen Preparation.....	52
AASHTO T283 Conditioning Procedures .....	52
AASHTO T283 Moisture Conditioning .....	53
Additional Parameters for Moisture Damage Evaluation.....	54
SFE and FTIR-ATR Experimental Plan .....	56
General Scope .....	56
Binder Oxidation Procedures .....	57
SFE Calculations.....	57
SFE Test Equipment and Sample Preparation .....	59
FTIR-ATR Test Equipment and Sample Preparation.....	61
Chapter 5: Laboratory Performance Test Results.....	63
Introduction.....	63



## Table of Contents (Continued)

AASHTO T283 Test Results .....	64
Indirect Tensile Strength (ITS) and Tensile Strength Ratio (TSR%) .....	64
IDEAL-CT Interaction Charts .....	70
Statistical Analysis.....	76
Additional Load-Displacement Parameters .....	78
SFE and FTIR-ATR Results .....	81
SFE Results.....	81
FTIR-ATR Results.....	88
Regression Analysis Between Mixture and Binder Tests.....	91
Chapter 6: Summary of Findings, Conclusions, Recommendations & Future Work.....	97
Summary of Findings.....	97
Conclusions.....	102
Recommendations.....	104
Study Limitations and Future Work .....	105
References.....	107
Appendix: List of Abbreviations .....	120

## List of Figures

Figure	Page
Figure 1. Schematic Illustration of The HWTT Failure Phases (Tavassoti & Baaj, 2020). .....	13
Figure 2. Pressure Vessel and Test Setup for SATS (Khan et al., 2013).....	15
Figure 3. ECS Test Schematic Diagram (Solaimanian et al., 2007).....	16
Figure 4. Picture of M.I.S.T Device (The M.I.S.T.TM, 2022). .....	19
Figure 5. Load-Displacement Curve Parameters. ....	27
Figure 6. Applying Contact Angle to Get The Variables In Young’s Equation. ....	34
Figure 7. The Energy Required to Separate Two Surfaces Of The Same Material, Identified As The Work Of Cohesion. ....	34
Figure 8. The Energy Required to Separate Two Surfaces Of Different Material, Identified As The Work Of Adhesion.....	35
Figure 9. FAA P-401 Gradation.....	46
Figure 10. AASHTO T283 Laboratory Experimental Plan.....	51
Figure 11. AASHTO T283 Laboratory Experimental Plan.....	55
Figure 12. SFE and FTIR-ATR Laboratory Experimental Plan.....	56
Figure 13. Example Of Contact Angle Measurement from Both Right And Left Sides ..	59
Figure 14. Asphalt binder and Aggregate Preparation for Contact Angle Measurement.....	61
Figure 15. ITS And TSR% Results for Asphalt Mixtures Tested At 25°C. ....	67
Figure 16. ITS And TSR% Results for Asphalt Mixtures Tested At AIT.....	69
Figure 17. IDEAL-CT Interaction Diagram (25°C) Results.....	73
Figure 18. IDEAL-CT Interaction Diagram AIT Results.....	75
Figure 19. Results For Pre-Peak Parameters of PG 64-22 At The LTOC. ....	79

**List of Figures (Continued)**

Figure 20. Work Of Cohesion Results ..... 86

Figure 21. Work Of Adhesion, Debonding, And Energy Ratio Results ..... 88

Figure 22. FTIR-ATR Test Results ..... 90

## List of Tables

Table	Page
Table 1. Properties of Selected Granite Aggregate.....	45
Table 2. Mix Design Results.....	46
Table 3. Properties of Probe Liquids .....	47
Table 4. Temperatures Used when Conducting AASHTO T283 Testing .....	50
Table 5. ANOVA Results for Indirect Tensile Strength (ITS) .....	77
Table 6. Tukey’s HSD Results for Indirect Tensile Strength (ITS) .....	78
Table 7. Pre-Peak Parameters Analysis Results at 25% .....	80
Table 8. Contact Angle Measurements .....	82
Table 9. SFE Components Results.....	84
Table 10. Aging Levels for Regression Analysis .....	92
Table 11. ANOVA Results for Tests Performed on Asphalt Binders .....	92
Table 12. Regression Analysis (R <sup>2</sup> ) Between TSR% with SFE and FTIR-ATR Components .....	93
Table 13. Predicted And Actual TSR% Values .....	95

## **Chapter 1**

### **Introduction**

#### **Background**

Asphalt pavements are exposed to environmental factors such as precipitation, temperature extremes, and UV radiation, which can cause structural damage. Moisture damage is a major concern, as it can lead to cracking, rutting, and potholes. Water enters the asphalt mixture through surface cracks, causing the components to expand and contract, accelerating pavement deterioration. Moisture damage reduces cohesion in the asphalt binder and adhesion between the binder and aggregate, which accelerates deterioration. Highway agencies and the pavement industry have established criteria for designing asphalt mixtures that are resistant to moisture damage.

To identify asphalt mixtures' moisture damage susceptibility, performance evaluation tests have been implemented. Two types of tests are qualitative tests performed on loose-mix asphalt mixtures and quantitative tests performed on compacted asphalt specimens. Qualitative tests are carried out on asphalt-coated aggregates submerged in water. However, these experiments cannot reproduce pore pressure, traffic conditions, or mix design parameters needed to understand moisture susceptibility. Quantitative tests, such as the modified Lottman test (AASHTO T283), determine the reduction in indirect tensile strength (ITS) resulting from water saturation and accelerated water conditioning, followed by a freeze-thaw cycle of compacted asphalt specimens. Several agencies use AASHTO T283 as the primary test criterion for field acceptance of

asphalt mixtures' moisture susceptibility. A minimum Tensile Strength Ratio (TSR%) of 80% is recommended for a mixture to be considered resistant to moisture damage.

### **Problem Statement**

- The oxidative conditioning procedure (to simulate pavement aging) in the current AASHTO T283 test may not be representative of field climatic conditions. There is a lack of research on determining appropriate levels of oxidative conditioning for asphalt mixtures where moisture damage has the greatest impact.
- The AASHTO T283 test is performed at the laboratory ambient temperature of 25°C, which may not be representative of the actual intermediate temperature of the asphalt binder or the intermediate temperature of the climate where the pavement would be built.
- While AASHTO T283 relies on one parameter, TSR%, as the deciding factor for moisture damage evaluation, other parameters, such as those from the Indirect Tensile Asphalt Cracking Test (IDEAL-CT), can be evaluated for their ability to show the impact of moisture damage of asphalt mixtures.
- There is a lack of an accurate, practical, and reliable material property technique for examining the degree of moisture damage at the asphalt-aggregate interfaces, which is essential for understanding the causes of moisture damage at different oxidation levels.
- While AASHTO T283 measures the TSR% through ITS reduction, it does not provide a comprehensive understanding of the chemical changes in the asphalt binder

that can result in a change in material properties with oxidation, which limits the ability to evaluate moisture damage.

Therefore, further research is needed to address these knowledge gaps and establish a consensus among researchers and state agencies regarding moisture damage in asphalt mixtures. This research involves incorporating surface free energy (SFE) as a material property test and Fourier transform infrared spectroscopy – attenuated total reflectance (FTIR–ATR) spectroscopy as a chemical test to gain a more comprehensive understanding of the mechanisms causing moisture damage in asphalt mixtures.

### **Research Hypothesis**

This study is initiated to question and verify the following hypotheses:

- A modified laboratory test procedure based on AASHTO T283 that accounts for asphalt oxidation and testing temperature allows more accurate and reliable measurements of asphalt mixtures with higher response to moisture damage.
- Additional AASHTO T283 load-displacement curve parameters can be utilized in greater detail using IDEAL-CT parameters than with indirect tensile strength alone to characterize moisture damage in asphalt mixtures.
- The SFE and FTIR-ATR characterization methods are practical for determining how oxidative conditioning impacts the degree of moisture-induced damage at the asphalt-aggregate interfaces, and to determine the chemical changes that occur because of oxidation in the asphalt binder, respectively.

- Based on the SFE and FTIR-ATR findings, it is possible to assess moisture damage at the asphalt-aggregate interface by recommending an appropriate oxidation level for the asphalt binders to evaluate moisture damage.
- The results obtained from this research may help to establish a more accurate and practical material property test for examining moisture damage susceptibility in asphalt mixtures.

### **Significance of Study**

This study is conducted to address several knowledge gaps related to the moisture susceptibility of asphalt mixtures. By developing a modified laboratory test procedure based on AASHTO T283, this study can provide more accurate measurements of moisture sensitivity in asphalt mixtures. This can have several benefits, including:

- Provide recommendations to revise AASHTO T283 test to consider an alternative oxidative conditioning for characterizing moisture damage in asphalt mixtures when conducting TSR% testing, leading to improved design of moisture-resistant asphalt mixtures,
- Improved sustainability by reducing the need for frequent pavement rehabilitation and reconstruction.
- Provide a more comprehensive understanding of the mechanisms causing moisture damage in asphalt mixtures, which can lead to the development of more effective pavement design and maintenance strategies, contributing to the long-term sustainability of the transportation infrastructure.



- The study assessed asphalt binder types that are commonly used in two different climatic regions, including cold regions like Alaska and Canada, and warmer regions like New Jersey. This allows for a more comprehensive understanding of the performance of moisture-sensitive asphalt mixtures across a broader range of climatic conditions.

### **Goal & Objectives**

The goal of this research study is to Evaluate the effectiveness of a modified laboratory test procedure based in AASHTO T283 that better captures moisture sensitivity of asphalt mixtures. To address this goal, this study presents the following objectives:

- Assess the impacts of asphalt oxidation conditioning and testing temperature on the severity of moisture-induced damage of asphalt specimens using AASHTO T283,
- Evaluate the effectiveness of using additional AASHTO T283 load-displacement curve parameters in characterizing moisture damage in asphalt mixtures,
- Evaluate how asphalt binder oxidation affects the material and chemical properties and susceptibility to moisture damage, and
- Assess the correlation between the results obtained from the material and chemical properties of asphalt binder and the AASHTO T283 for assessing moisture damage in asphalt mixtures.

## **Research Approach**

The research approach adopted to address the study goal and objectives consisted of the following tasks:

Task 1: Conduct a comprehensive literature review to determine the current state of knowledge regarding the limitations of the AASHTO T283 test and the influence of oxidative conditioning and testing temperature on the severity of moisture-induced damage in asphalt specimens. This task included:

- Reviewing test procedures used to evaluate moisture damage of asphalt mixtures,
- Reviewing previous studies on the limitations of AASHTO T283 test,
- Reviewing studies on the influence of oxidative conditioning on the severity of moisture-induced damage in asphalt specimens, and
- Reviewing previous studies on IDEAL-CT and the impact of oxidation and moisture conditioning on its parameters.
- Reviewing previous studies on SFE used for moisture damage evaluation at the asphalt-aggregate interface, and FTIR-ATR used for detecting the chemical changes in asphalt binders.

Task 2: Identify and select representative materials that will be used in preparing asphalt mixtures for testing. This task involved:

- Identifying and selecting asphalt binder types that are used in two different climatic regions (New Jersey vs Alaska), and
- Preparing asphalt mixtures using the selected materials.

Task 3: Develop an experimental program to assess the effect of oxidation and moisture conditioning on the performance of asphalt specimens using AASHTO T283. This task included:

- Determining the suitable oxidation conditioning and testing temperature that should be applied in AASHTO T283,
- Assessing the load-displacement curve parameters and detect parameters that show susceptibility to moisture damage,

Task 4: Assess the material properties of asphalt-aggregate interfaces and chemical changes in asphalt using SFE and FTIR-ATR, respectively. This task included:

- Determining an acceptable oxidation level for application to asphalt binder to assess moisture damage at the asphalt-aggregate interface,
- Describing the chemical changes in the asphalt binder due to the impact of oxidation.

Task 5: Develop recommendations for modifications to be applied to AASHTO T283 to show higher susceptibility to moisture damage. This task involved:

- Recommending an oxidation conditioning and testing temperatures that should be applied in AASHTO T283 to better capture moisture damage in asphalt mixtures,
- Identifying additional parameters that can indicate the susceptibility of asphalt mixtures to moisture damage, and
- Developing recommendations for future studies based on the findings of the research.

## **Chapter 2**

### **Literature Review**

#### **Introduction**

Environmental factors such as heavy precipitation, extreme temperatures, and exposure to UV radiation can have a significant impact on the durability of asphalt pavements (Abdulrahman et al., 2019; Das & Singh, 2017; Maadani et al., 2021; Rafiq et al., 2020; Saedi & ORUÇ, 2020). Moisture damage can weaken the pavement's structure and cause cracking, rutting, and potholes. Moisture can enter the asphalt mixture through surface cracks and cause the individual components to expand and contract, thereby accelerating the pavement's deterioration. Moisture can also lead to the growth of vegetation and the formation of ice, both of which can cause additional pavement damage. Moisture damage occurs in asphalt pavement in two ways: by reducing the cohesion in the asphalt binder (cracks within the asphalt binder) and by compromising the adhesion between the asphalt binder and aggregate (also known as stripping). Reduced cohesion and adhesion bonding can significantly accelerate asphalt pavement deterioration (Copeland et al., 2007). Consequently, highway agencies and the pavement industry have established criteria for designing asphalt mixtures resistant to moisture damage.

In this chapter, results of a comprehensive literature review for evaluating moisture damage are provided. The following subsections present a discussion about tests

used to evaluate moisture damage, oxidation effect on moisture damage, and parameters used to evaluate moisture damage.

### **Tests Performed on Mixtures to Quantify Moisture Damage**

The development of laboratory performance to evaluate moisture damage started in the 1930s (Alam, 1998). Since then, several performance evaluation tests have been utilized to determine how susceptible asphalt mixtures are to moisture damage (Abo-Qudais, 2007; Alam, 1998; S. H. Al-Swailmi, 1992; Amelian et al., 2014; Birgisson et al., 2005; Collop et al., 2004; Diab & You, 2013; Terrel & Al-Swailmi, 1994). These tests can be categorized into two types; qualitative tests performed on loose mixes, and quantitative tests performed on compacted specimens. The most common tests on loose samples are: 1) the static immersion test (AASHTO T182) (Airey & Choi, 2002; Solaimanian et al., 2003), and 2) the boiling water test (ASTM D3625) (Xiao, Polaczyk, & Huang, 2022; Xiao, Polaczyk, Wang, et al., 2022). Qualitative tests are carried out on asphalt-coated aggregates mixes submerged in water. These tests lack quantitative testing in their ability to replicate mix design, traffic conditions, and pore pressure characteristics required to comprehending asphalt mixtures' sensitivity to moisture. These tests provide largely qualitative answers, and their interpretation is subjective since it relies on the expert opinion of the evaluator.

Quantitative moisture-induced damage tests can be carried out on lab-compacted specimens, field cores, or slabs. Test procedures basically carry out different types of moisture conditioning to asphalt specimens, followed by a comparison of indirect tensile

strength between the unconditioned and conditioned asphalt specimens. The modified Lottman test (AASHTO T283) is the most widely used procedure for assessing moisture-damage in asphalt mixtures. Other tests, such as the immersion-compression test (ASTM D1075/AASHTO T165) (Eid, 2000; Jakarni et al., 2016) and tunnicliff-root test (ASTM D4867) (Emery & Seddik, 1997; Taib et al., 2019) were also developed. The immersion-compression test was withdrawn from the ASTM database in 2019 (ASTM, 2011), and tunnicliff-root test is like the widely-used AASHTO T283 (Kandhal, 1992; Solaimanian et al., 2003). Other quantitative tests such as Hamburg wheel tracking test (AASHTO T324) (Ali et al., 2022; Aschenbrener, 1995), saturated ageing tensile stiffness (SATS) (Airey et al., 2005; Khan et al., 2013), environmental conditioning system (ECS) (AASHTO TP34) (Tandon et al., 1996; Vemuri, 1996), and moisture induced sensitivity test (M.I.S.T) (Kaukuntla, 2014; Tarefder et al., 2014) are also available. A summary of asphalt moisture damage tests is presented in the following subsections:

***Loose-Mix Test: Static Immersion Test (AASHTO T182)***

AASHTO T182 test procedures rely on measuring the percentage of total measured visible area of aggregate surface that keeps its asphalt binder coating. This process is carried out by immersing an asphalt loose-mix sample in water after 16 to 18 hours and then seeing it through the water. After being cured for 2 hours at 60°C and cooled to room temperature, asphalt mixes are then submerged in a jar filled with 600 mL of distilled water. The jar is then sealed and placed in a water bath at 25°C for 16 to 18 hours. While the mixture is still in the jar, the degree of stripping is visually assessed

(Airey & Choi, 2002; Solaimanian et al., 2003). This test is likewise straightforward yet subjective, and it does not need the measurement of strength.

***Loose-Mix Test: Boiling Water Test (ASTM D3625)***

ASTM D3625 procedure consists of stirring loose asphalt mixes in hot water with a glass rod. The mixture is then allowed to cool down for ten minutes before the stripped bitumen is removed. After 24 hours, the mixture is removed from the water and dried at room temperature. The inspector visually determines what fraction of the aggregate surface still has its asphalt binder layer intact. Simple but subjective, assessing strength is not part of ASTM D3625, and analyzing fine aggregate is challenging under this standard. The importance of visual examination in loose-mix tests and specifically in ASTM D3525 is the fundamental drawback of qualitative testing. For that reason, previous studies have used computational technologies such as digital image analysis and MATLAB to design systems and detect the stripping occurring after the boiling water test (Amelian et al., 2014; Caputo et al., 2020; Nazirizad et al., 2015; Vinet-Cantot et al., 2019; Yusoff et al., 2014). For instance, Nazirizad et al., 2015 have used digital images analysis methods taken from coated aggregate particles, after performing ASTM D3625, to evaluate the effect of anti-stripping material on asphalt mixtures' moisture susceptibility.

***Compacted-Mix Test: Hamburg Wheel Tracking Test (HWTT)***

The HWTT test was conducted to examine the permanent deformation characteristics and sensitivity to moisture of asphalt mixtures. In this test, compacted

asphalt samples of 150 mm in diameter and 75 mm in height are subjected to a force of 702N applied by a steel wheel. Asphalt samples were loaded at a constant rate while submerged in warm water. 20,000 loading passes are applied until specimen failure, or specimens reaching 12.5 mm maximum rut depth. In terms of rutting assessment, the pass/fail criteria, and the rut depth difference between specimens until sample failure or after 20,000 passes.

Stripping Inflection Point (SIP) is a method used for moisture damage evaluation. The SIP is the number of wheels that pass at the beginning of the stripping process. As seen in Figure 1, it is illustrated visually as the intersection of two lines that best reflect the creep and stripping phases. SIP occurs when a material begins to sustain severe water-induced degradation. Tavassoti & Baaj, 2020 have developed a schematic illustrating the detection of SIP during HWTT. As can be seen from Figure 1, the SIP parameter was determined by the number of wheel passes at which the Creep Slope and Stripping Slope intersect. Maine DOT reported that a stripping inflection point larger than 15,000 passes would indicate good performance, and less than 10,000 passes indicating bad performance. Inflection points for stripping between 10,000 and 15,000 passes were associated with average performance of these mixes (Hajj et al., 2021). As illustrated in Figure 1, the SIP is the intersection of the slope of the creep phase via the visco-plastic inflection point and the slope of the stripping phase. SIP represents the rate at which the material begins to incur substantial moisture-induced damage, whereas the strip slope reveals the rate at which the material degrades once considerable moisture-induced damage has occurred.



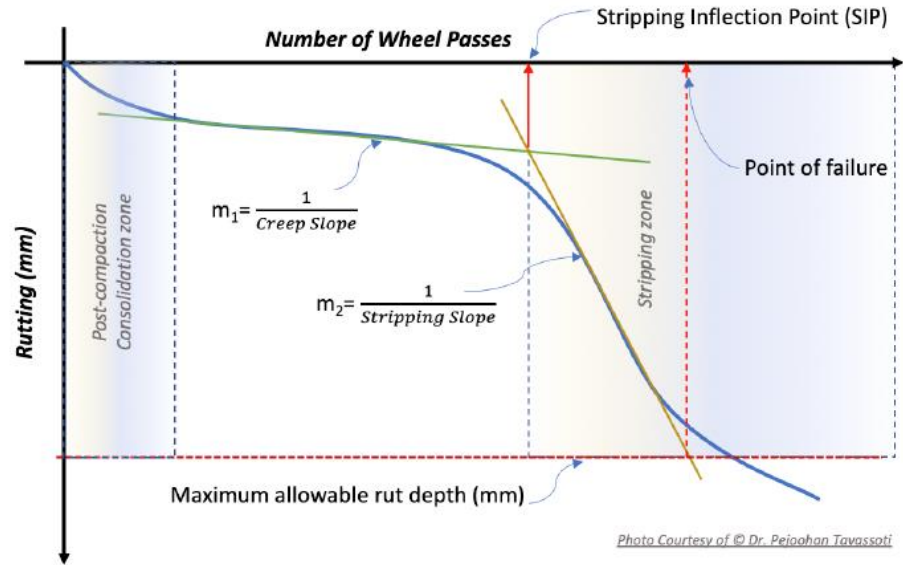


Figure 1. Schematic Illustration of The HWTT Failure Phases (Tavassoti & Baaj, 2020).

NCHRP Project 9-49 considers asphalt mixes with higher SIP values and smaller rut depths to have good performance in the HWTT (Yin et al., 2014). Several research studies have used HWTT and SIP to evaluate moisture damage of asphalt mixtures (Giwa et al., 2021; F. Rahman & Hossain, 2014; Schram & Williams, 2012; Swiertz et al., 2017; Yin et al., 2020). While this method has been adopted by several transportation agencies, AASHTO T324 does not give a precise method of analysis; hence, the conclusions tend to be subjective, varied, and difficult to replicate. NCHRP project 20-07/task 361 reported that there is no standard method for calculating SIP using creep phase and stripping phase data (Mohammad, 2015).

### ***Compacted-Mix Test: Saturated Ageing Tensile Stiffness (SATS)***

SATS test was developed by Collop et al., 2004. The SATS test was first created at the Nottingham Transportation Engineering Centre (NTEC), and its objective was to simulate the aging and moisture damage processes under laboratory conditions by adding water at high pressure and temperature (Collop et al., 2004). The SATS test combines oxidative and moisture conditioning in asphalt specimens (Airey et al., 2008; Grenfell et al., 2012).

As observed in Figure 2, the conditioning technique of SATS was provided by Zaidi et al., 2022. The SATS test involves placing asphalt samples in a pressure vessel and subjecting them to 0.5 MPa of pressure and 85°C for 24 hours. Specimens of asphalt are cooled at 30°C and for 24 hours under 0.5 MPa of pressure. Following a determination of the saturated surface dry (SSD) mass. After four hours of conditioning at 20°C, specimens were put through tests measuring indirect tensile stiffness modulus (ITSM). Previous studies have used SATS to evaluate moisture-induced damage of asphalt mixtures (Badal et al., 2020; Grenfell et al., 2014, 2015; Khan et al., 2013; Nicholls et al., 2011).

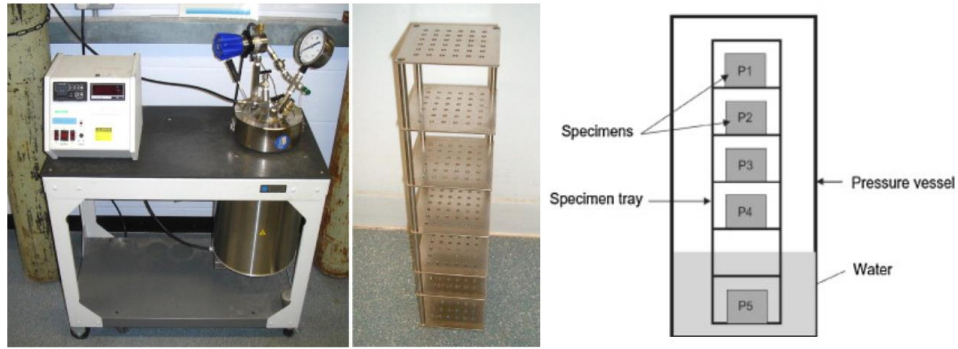


Figure 2. Pressure Vessel and Test Setup for SATS (Khan et al., 2013).

The SATS procedure is mainly useful for evaluating moisture damage in asphalt mixtures made with low penetration grade (hard) bitumen, and not in those with a high penetration grade (soft) binder. As a workaround, the SATS test was adapted to accommodate asphalt mixes with softer binders (those with a greater penetration grade) (Grenfell et al., 2012).

***Compacted-Mix Test: Environmental Conditioning System (ECS)***

The Strategic Highway Research Program (SHRP) funded the implementation of various moisture damage laboratory tests in 1992. The ECS was developed in previous study (S. Al-Swailmi & Terrel, 1992). The Asphalt Research Program at Oregon State University (OSU) is responsible for the creation of the ECS test procedure. This method (which was formerly known as AASHTO TP34, "Determining Moisture Sensitivity of Compacted Bituminous Mixtures Subjected to Hot and Cold Climate Conditions") was developed to assess the sensitivity of asphalt mixtures to moisture damage under simulating pavement conditions (Solaimanian et al., 2003). Solaimanian et al., 2003 have

developed a schematic diagram of ECS test presented in Figure 3. In this procedure, a membrane-encapsulated specimen is heated, loaded, and moisture conditioned. Loose asphalt mixtures are short-aged per AASHTO PP2-94, then compacted to 102 mm diameter and height samples. A silicone sealant is used to seal a latex membrane around the specimen. Specimens are dried for at least 15 hours.

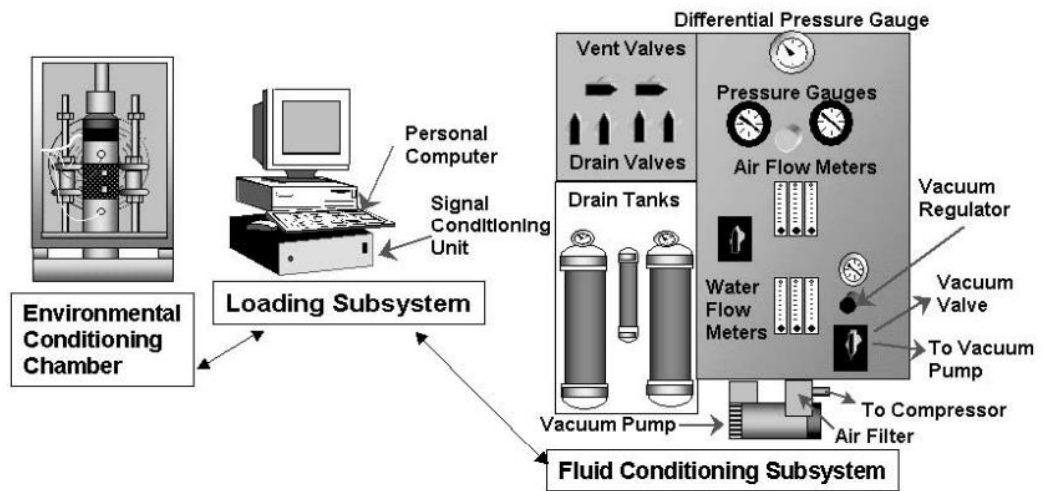


Figure 3. ECS Test Schematic Diagram (Solaimanian et al., 2007).

In the ECS load frame, air permeability and dry resilient modulus are measured. The resilient modulus is determined by applying a haversine load for 0.1 second and resting for 0.9 second. With distilled water and a 68 kPa vacuum, specimens were saturated, then is water permeability determination. Saturated samples are heated to 60°C for six hours while loaded with haversine. Sample cooled to 25°C for two hours. MR and water permeability are measured after 8 hours. The process is repeated twice (six hours

loading, 60°C heating, two hours cooling).  $MR > 70\%$  is the acceptable resistance to moisture damage of conditioned to unconditioned specimens. This procedure is too long and complex to be used for routine mixture design or quality control testing.

Although the ECS showed promise, this form of conditioning system did not produce findings that were much more exact or accurate than the AASHTO T283. Solaimanian et al., 2007, in their NCHRP 9-34 research, further assessed ECS. Based on these findings, Tandon & Nazarian, 2001 updated an ECS system that was used in the NCHRP experiment. To determine the extent of damage in asphalt mixes caused on by moisture, the dynamic modulus of the mixes was used with the revised and enhanced ECS.

Researchers found that the ECS/dynamic modulus process has several limitations that need to be addressed before it can be used as a standard mix design test to identify a mixture's susceptibility to moisture damage, despite the approach's advantages. The main challenges were the conditioning time of required water/load, the required temperature during conditioning, and the total conditioning load (Dave et al., 2018).

#### ***Compacted-Mix Test: Moisture Induced Sensitivity Test (M.I.S.T)***

Asphalt mixes' susceptibility to moisture damage can be measured with the use of a new conditioning technology called the M.I.S.T. InstroTek manufactures the M.I.S.T as a self-contained conditioning device (The M.I.S.T.TM, 2022). M.I.S.T can identify water moisture damage by simulating cyclic field traffic at in-situ hot pavement temperatures. Each loading cycle injects water into the sample and then removes it, like a tire rolling

over a wet surface. When a tire rolls over wet asphalt, the water is forced into the surface and then extracted when the tire comes to a stop.

M.I.S.T. is a water-filled tank that can accommodate two 150 mm x 100 mm samples (Figure 4). This test rapidly duplicates in the lab the field characteristics that promote moisture damage. Other test methods require 24 hours, but the M.I.S.T requires only six. The machine's test temperature can be controlled from 300°C to 600°C, and the tank's pressure can reach 75 psi. Pressure cycles between one and 50,000 can be specified for the test. The standard test requirements are 600°C. and 40 psi.

The M.I.S.T process consists of two components: the adhesive cycle and the cohesive cycle. The adhesive cycle starts by placing specimens in a 60°C water-filled chamber for 20 hours. The specimens are then subjected to 270 kPa (40 psi) hydraulic pumping for 3,500 cycles at a rate of 3.5 seconds each pressure cycle while remained in the heated water tank at 60°C. After M.I.S.T conditioning, the samples' height and diameter are measured. In addition to obtaining the conditioned specimen's tensile strength and bulk specific gravity, the Volume Change and TSR% values are also determined. The minimum TSR% recommendation for M.I.S.T is 80% (LaCroix et al., 2016). According to the manufacturer, a volume change of 1% indicates that the specimen is sensitive to stripping.



*Figure 4.* Picture of M.I.S.T Device (The M.I.S.T.TM, 2022).

Several research studies have used M.I.S.T conditioning to evaluate moisture damage (Kaukuntla, 2014; H. Li et al., 2020; M. A. Rahman et al., 2021; Tayebali et al., 2017; Twagira & Jenkins, 2009). Tayebali et al., 2017 compared the AASHTO T283 and M.I.S.T conditioning standards to the Boiling Water Test. According to the study's findings, asphalt mixes' moisture damage limitations can be suggested using the % stripping from the Water Boiling Test and the % change in volume from the M.I.S.T. to provide an adhesive and cohesive failures occurred.

Li et al., 2020 studied the effect of fibers on the durability and healing performance using M.I.S.T device. The mechanical properties and strength recovery ratios of specimens before and after M.I.S.T were evaluated using the semi-circular bending (SCB) test. Sample conditioning in M.I.S.T device varied in temperature, cycles, and chamber pressure. Li et al., 2020 reported that M.I.S.T device showed that fibers

enhance the moisture resistance of asphalt mixtures. Further, the change in conditioning temperature showed the most effect caused by M.I.S.T Device.

***Compacted-Mix Test: Modified Lottman Test (AASHTO T283)***

The Standard Method of Test for Resistance of Compacted Asphalt Mixtures to Moisture-Induced Damage (AASHTO T283), as a part of Super-pave mix design, has been known to be the most common quantitative test conducted by researchers and highway agencies to evaluate moisture damage (AASHTO, 2009). The test involves determining the reduction in ITS (ASTM D6931) resulting from water saturation and accelerated water conditioning, followed by a single freeze–thaw cycle, of compacted asphalt mixtures. Several agencies specified AASHTO T283 as the primary test criterion for field acceptance of asphalt mixtures’ moisture susceptibility (Azari, 2010). For field performance correlation, minimum 80% TSR% is recommended (Ameri et al., 2018; Schram & Williams, 2012). The TSR% equation is shown in Equation 1:

$$TSR\% = \frac{ITS_{MC}}{ITS_{UC}} \quad (1)$$

Where:

TSR%: The Tensile Strength Ratio

ITS<sub>MC</sub>: The Indirect Tensile Strength for Moisture Conditioned Specimens (MPa)

ITS<sub>UC</sub>: The Indirect Tensile Strength for Unconditioned Specimens (MPa)

**History of AASHTO T283.** The A substantial number of pavements in the United States began to suffer from moisture sensitivity of hot-mix asphalt (HMA)



components in the late 1970s and early 1980s. Many asphalt pavements develop distresses such as rutting, cracking, as well as pavement releveling which were mainly developed because of moisture-induced degradation. The reasons for this abrupt rise in pavement distresses due to water sensitivity have yet to be determined. AASHTO T 283, developed in 1978, is a test used for determining if materials are susceptible to stripping and moisture-induced degradation as well as determining the efficiency of additives. The AASHTO T283 performance test is based on research performed by R. P. Lottman under the National Cooperative Highway Research Program (NCHRP) Project 4-08(03) and subsequent research performed by D. G. Tunncliffe and R. E. Root under NCHRP Project 10-17.

Specimens are compacted until they have an air void content (AVC%) between 6% and 8% for the test. An unconditioned control group of three samples is evaluated, while a conditioned group of three samples (three that were previously frozen) are thawed and immersed in warm water. After that, the specimens are placed through an in-direct tensile strength test, where the force required to break them is measured while being loaded at a constant 50 mm/min. TSR% is determined by comparing the tensile strength of conditioned and unconditioned samples. Pavement cores obtained after construction are also suitable for this examination.

In 2002, the Colorado department of transportation surveyed 50 state departments of transportation, three Federal Highway Administration (FHWA) federal offices, one Canadian province, and the District of Columbia to demonstrate the widespread use of AASHTO T283. According to the survey, 87% of these organizations conduct moisture

damage tests. 82 percent of these agencies employ tensile tests (e.g., AASHTO T283, ASTM D4867, etc.) as their principal test for assessing moisture damage. According to the poll, 10% of respondents utilize tensile testing (such as AASHTO T115), 4% use retained stability tests, and 4% use combined tensile tests and wheel tracking tests (Hicks et al., 2003).

**Shortcomings of AASHTO T283.** AASHTO T283 is still the most extensively utilized test procedure for assessing asphalt mixtures' moisture damage. Highway organizations have pointed out various shortcomings regarding the testing procedure. Shortcomings of AASHTO T283 have been reported in literature (Azari, 2010; Brown et al., 2001; Buchanan et al., 2004; Epps, 2000; Solaimanian et al., 2007).

Despite the widespread use of AASHTO T283, several potential improvements can still be made to address some of its shortcomings. Researchers and highway agencies alike pointed out various limitations of the AASHTO T283 test. Some of these limitations include that AASHTO T283:

- Does not always predict moisture sensitivity as observed in the field (Bausano & Williams, 2009; Epps, 2000; Kringos, Azari, et al., 2009; Schram & Williams, 2012; Solaimanian et al., 2007);
- Shows disagreement in results obtained from 100-mm Marshall and 150-mm Superpave gyratory samples (Epps, 2000);
- Does not offer a clear justification for poor or good performance (Brown et al., 2001); and,

- Allows for only a narrow range of water-saturation levels and one single freeze-thaw cycle.

With regards to lack of relatability of AASHTO T283 results to the field, researchers observed that mixes might satisfy the laboratory TSR% criterion (e.g., min. 80%); however, that was not reflected in field performance (Bausano & Williams, 2009; Epps, 2000; Kringos, Azari, et al., 2009; Schram & Williams, 2012; Solaimanian et al., 2007). Solaimanian et al., 2007 reported that laboratory TSR% values for good-performing field asphalt specimens were unexpectedly low, whereas those for bad-performing mixtures were unexpectedly high. There is also no consensus among studies on the agreement between AASHTO T283 results obtained from Marshall- and Superpave gyratory-compacted samples. For example, a survey conducted by the AASHTO materials reference laboratory (AMRL) reported that using 100 mm (4 in.) Marshall specimens for the AASHTO T283 test had better agreement with field performance (Kringos, Scarpas, et al., 2009). On the contrary, Epps et al. 2000 reported that using 150 mm Superpave Gyratory Compactor (SGC) specimens when conducting the AASHTO T283 test showed better correlation with field performance than using 100 mm Marshall-compacted specimens. In terms of subjectivity of testing and not offering a clear justification for poor or good performance, the evaluation criterion for AASHTO T283 relies only on a pass/fail type of criteria and allows a narrow saturation degree of 70%-80% and one cycle of freeze-thaw.

In addition to the above limitations, the oxidative conditioning procedure (to simulate pavement aging) in the current AASHTO T283 test may not necessarily be

representative of field climatic conditions. The original T283 procedure include 16 hours of oxidation at 60°C to simulate the pavement condition at the early life of asphalt pavement, whereas a severely aged asphalt binder (or mixture) can accelerate the occurrence of moisture damage in flexible pavements (Bazuhair et al., 2020; Rahmani et al., 2017; Sirin et al., 2018). After being built for many years, asphalt pavements suffer moisture damage, where aging has already taken place, and not at the service start of pavement life. In other words, aging is a major factor when characterizing the moisture damage of asphalt mixtures. This was observed by Bazuhair et al., 2020 where they monitored multiple performance characteristics of asphalt pavement over the course of eight years in the field. The early performance of the asphalt pavement was seen to be dominated by the stiffening effects of oxidation, with the tensile strength increasing throughout the first four to five years and Hamburg rutting decreasing. Whereas in future years, as the effects of moisture became more dominant, tensile strength started to decrease and Hamburg rutting began to increase.

Epps, 2000 also evaluated the effect of different oxidative conditioning variations of loose and compacted mix methods. Asphalt mix oxidization was identified as a significant factor influencing both unconditioned and moisture conditioned asphalt mixtures. Previous studies have reported that the sensitivity of moisture-induced damage is significantly affected by asphalt binder and mixture oxidative conditioning (Chindaprasirt et al., 2009; Jemere, 2010; Saltibus & Wasiuddin, 2017). Liang, 2008 evaluated the effect of oxidation on the susceptibility of asphalt mixtures to moisture-induced damage and found that oxidative conditioning increased their susceptibility.

Asphalt aging conditions vary between a cold region area and a warmer area as the oxidative effect is higher for warmer areas. These factors are not being taken into consideration while simulating field aging. Overall, previous studies have preferred performing oxidative conditioning on loose-mix than compacted specimens for higher uniformity in mixture and recommended loose-mix oxidation at the LTOC level (85°C for 5 days) (Braham et al., 2009; Elwardany et al., 2017; Kim et al., 2018; Partl et al., 2012; Rad et al., 2017). Also, applying conditioning temperatures above 100°C has been shown to affect reaction kinetics, break polar molecule interactions, lead to additional oxidation effect on asphalt mixtures (Elwardany et al., 2018; Kim et al., 2018; Petersen, 2000; Rad et al., 2017).

***Compacted-Mix Test: Indirect Tensile Asphalt Cracking Test (IDEAL-CT)***

In 2017, the InDirect TEnsile Asphalt Cracking Test (IDEAL-CT) was developed by F. Zhou et al., 2017. The test method adopted by ASTM D8225-19 describes the determination of the cracking tolerance index,  $CT_{index}$  at 25°C, and other parameters from the same load-displacement curve used in AASHTO T283 (Figure 3). Parameters from T283 and D8225 are investigated in this study for evaluating moisture damage. Multiple research studies have adopted IDEAL-CT to evaluate the  $CT_{index}$  and the post-peak performance of asphalt mixtures (Al-Badr, 2021; Alfalah et al., 2020, 2021; Polaczyk et al., 2021; C. Yan et al., 2020). Five different parameters were considered in the IDEAL-CT calculations, as shown in Equation 2:

$$CT_{index} = \frac{t}{62} \times \frac{l_{75}}{D} \times \frac{G_f}{|m_{75}|} \quad (2)$$

Where:

$CT_{index}$ : The cracking tolerance index

$G_f$ : fracture energy (J/m<sup>2</sup>)

$|m_{75}|$ : Absolute slope of load and displacement from 85% to 65% post-peak load (N/m)

$l_{75}$ : Displacement corresponding to 75% of the peak load at the post-peak stage (mm)

$t$ : Specimen thickness (mm)

$D$ : Specimen diameter (mm)

With regards to moisture damage evaluation, IDEAL-CT parameters do not consider the peak load ( $P_{100}$ ) accounted for in TSR% calculations to be the deciding factor for moisture damage performance in asphalt mixtures. Instead, IDEAL-CT detects other post-peak parameters obtained from the load-displacement curve, such as  $G_f$ , which reflects the energy required to break the specimen (considering the area under the curve and the work of fracture ( $W_f$ )), where higher  $G_f$  is desirable for better performance. Similarly,  $|m_{75}|$  provides an evaluation of the post-peak rate of failure in an asphalt specimen (i.e., crack propagation rate). As seen in Figure 5, a lower  $|m_{75}|$  is desirable for better resistance to crack propagation. Lastly,  $l_{75}$  gives an indication of the cracking deformation tolerance at 75% peak load ( $P_{75}$ ) after the peak, where a higher value is desired. These parameters used in the  $CT_{index}$  calculation can also be assessed individually to evaluate the effect of oxidative conditioning and testing temperature on moisture

damage.  $CT_{index}$  values are also sensitive to oxidation, where previous studies reported a decrease in  $CT_{index}$  as asphalt mixtures were exposed to oxidative conditioning (Al-Badr, 2021; Ali et al., 2022; Radeef et al., 2021).

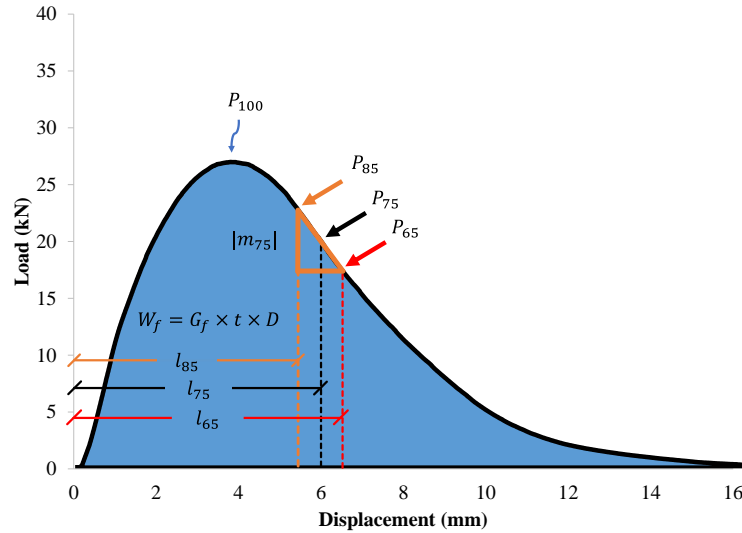


Figure 5. Load-Displacement Curve Parameters.

### Surface Free Energy (SFE)

Despite the benefits and popularity of moisture evaluation tests, these methodologies have shortcomings such as poor correlation with field performance (Bausano & Williams, 2009; Epps, 2000; Solaimanian et al., 2007), their inability to explain why an asphalt mix performs well or poorly (Bhasin et al., 2006), and the need for extensive time including the 16 hours of freezing and 24 hours of thawing required for sample conditioning. It is; therefore, vital to supplement moisture-induced damage

tests with an evaluation technique that is both accurate, practical, and reliable for examining the degree of water damage in asphalt-aggregate interfaces. Texas Department of Transportation (TxDOT) and Texas A&M University developed more fundamental testing methods to detect moisture susceptibility (CJ Zollinger, 2005; Hefer, 2004; Howson et al., 2009). Howson et al., 2009 assessed the cohesion behavior in asphalt binders and adhesion with aggregates. Howson et al., 2009 also reported that SFE, defined as the required energy to create a new unit surface area, was a successful measure of evaluating these cohesion and adhesion bonds.

SFE is a fundamental thermodynamic material property test that is useful for selecting materials that are more resistant to moisture damage. SFE is a material property that can accurately assess binder cohesion and its adhesive properties with aggregates (Ahmad N, 2011). The energy parameters derived from SFE (i.e., SFE components) also include the work of water-debonding, which relates to moisture damage characterization of asphalt-aggregate interfaces. This current study uses the term “water-debonding” to describe the weakening of the aggregate-binder adhesive bonds in the presence of water. Several research studies (Bhasin et al., 2007; Cheng et al., 2002; Liu et al., 2020; Masad et al., 2006; Tu et al., 2021) used SFE approaches on asphalt binder and aggregate to characterize the work of cohesion, adhesion, and water-debonding of asphalt-aggregate interfaces. Different methodologies were established to measure SFE. Sessile drop, Wilhelmy plate, atomic force microscopy (AFM), universal sorption device (USD), inverse gas chromatography, and microcalorimetry are some methods of measuring SFE.



Wilhelmy plate and sessile drop are often used to measure the SFE components. Both methods quantify surface free energy based on liquid contact angles.

Bhasin et al., 2006 measured the cohesion, adhesion, and water-debonding of 16 mixtures consisting of field cores and lab-prepared mixes. The study covered 14 asphalt binders and 10 aggregate types for producing asphalt mixtures. Bhasin et al., 2006 reported that SFE findings correlated well with field performance where good performing mixtures had high energy ratio and poor performing mixes had lower energy ratio obtained from SFE calculations. The researchers ultimately concluded that the SFE approach is a successful tool at evaluating moisture-induced damage of asphalt-aggregate interfaces. Using the Wilhelmy plate technique, Zhang & Luo, 2019 investigated the SFE of asphalt binders and aggregate types with and without additives. The Wilhelmy plate technique (for asphalt binder), vapor adsorption test (for aggregate), boiling water test (on loose asphalt mix), and Modified Lottman Test (on compacted specimens) were performed to evaluate the moisture damage of asphalt mixtures. According to Zhang & Luo, 2019, SFE and mixture moisture susceptibility tests showed equivalent rankings of different mixtures.

Most of the prior research studies have concentrated on determining the SFE properties of asphalt binders without considering an appropriate oxidation level (simulating short- and long-term aging that occurs in the field) to quantify moisture damage. However, it may be more appropriate to characterize the potential for moisture damage after some duration of oxidative conditioning. As mentioned earlier, Bazuhair et al., 2020 monitored multiple performance characteristics of asphalt pavement through

eight years of field aging and observed that in subsequent years of pavement construction, the tensile strength began decreasing and Hamburg rutting began increasing as effects of moisture became more dominant.

Hossain et al., 2019 examined the impact of oxidative conditioning on asphalt binders. They used PG 64-22 subjected to Rolling Thin Film Oven (RTFO) for 85 minutes and Pressure Aging Vessel oxidation levels for 20 hours (PAV20), along with two types of rejuvenators, to analyze cohesion properties of asphalt binders and adhesiveness with granite and limestone aggregates. Hossain et al., 2019 reported that oxidation reduced cohesion and adhesion at the asphalt-aggregate interface. However, rejuvenators helped to mitigate the negative effects of oxidation on asphalt binder properties. J. Wei & Zhang, 2010 evaluated the effect of short- and long-term asphalt oxidative conditioning on surface free energy. In their study, RTFO conditioning was carried out for 45, 85, 135, and 175 minutes as well as PAV conditioning for 20 hours on RTFO-conditioned binders. J. Wei & Zhang, 2010 reported that asphalt oxidation generally reduced the surface free energy of asphalt binders. However, some cases showed varied results without a clear explanation, which suggested that the relationship between oxidation and contact angle may be complex and require further investigation.

### ***Calculations of SFE***

SFE is based on the concepts of thermodynamic adsorption in which an adhesive will adhere to a substrate if contact is made (CJ Zollinger, 2005). SFE characterization of cohesion and adhesion are associated with the breaking of asphalt-aggregate interfaces

and the formation of cracks inside the binder, respectively. Characterizing materials and assessing their interfaces allows for the examination of their susceptibility to moisture damage, healing abilities, and fatigue cracking resistance and to predict their long-term performance and durability (Bahmani et al., 2022; Bhasin et al., 2007; Cheng, 2002; L. Li et al., 2021; Sarsam, 2021; J. M. Wei et al., 2009; L. Zhou et al., 2021).

Asphalt and aggregate SFEs consist of nonpolar (i.e., Lifshitz-van der Waals) and polar (i.e., acid-base) components. Good and Van Oss (van Oss et al., 1987) used equations to calculate aggregate and asphalt SFE. Total aggregate and asphalt binder SFE can be expressed separately as in Equation (3):

$$\gamma^{tot} = \gamma^{LW} + \gamma^{AB} \quad (3)$$

Where:

$\gamma^{tot}$ : total SFE of asphalt or aggregate

$\gamma^{LW}$ : Lifshitz-van der Waals component

$\gamma^{AB}$ : acid-base component

$l_{75}$ : Displacement corresponding to 75% of the peak load at the post-peak stage (mm)

Equation (3) separates dispersive and acid-base interactions, where  $\gamma^{tot}$  represents the total surface energy term. Good-van Oss-Chaudhury (GvOC) proposed that the Lifshitz-van der Waals forces are the London dispersion force, the Keesom dipole-dipole

force, and the much smaller Debye dipole-induced dipole force (van Oss et al., 1987). Equation (4) subdivides the acid-base component  $\gamma^{AB}$ .

$$\gamma^{AB} = 2\sqrt{\gamma^+\gamma^-} \quad (4)$$

Where:

$\gamma^+$ : Lewis's acid surface interaction component

$\gamma^-$ : Lewis's base surface interaction component

$\gamma^{AB}$ : acid-base component

Combining Equations (3) and (4), the surface free energy of a material can be defined as illustrated in Equation (5):

$$\gamma^{tot} = \gamma^{LW} + 2\sqrt{\gamma^+\gamma^-} \quad (5)$$

**Wettability and Contact Angle.** The wetting effect is a liquid's tendency to cover a solid surface, limiting surface contact (Shanahan, 1991). According to the thermodynamic adsorption hypothesis, adhesion occurs in moist conditions. Wetting is a bonding condition regardless of the type of material. Wetness is determined by the balance of cohesive and adhesive forces.

One way to quantify the surface wetting characteristics of a liquid is to measure the contact angle ( $\theta$ ) of a drop of liquid deposited on a solid's surface. A low contact angle  $< 90^\circ$  indicates good wetting and adhesion, and better resistance to moisture damage. If  $> 90^\circ$ , the liquid is non-wetting, causing inadequate wetting and adhesion.

Therefore, surfaces with low wetness will have a high contact angle, while surfaces with high wetness will have a low one. Consequently, the contact angle is a crucial parameter in moisture damage evaluation, and its measurement provides accurate SFE estimation. As seen in Equation (6), Young's equation (Schrader, 1995; Young, 1805) shows the connection between surface tension and contact angle as shown in Equation (6).

$$\gamma_S = \gamma_{SL} + \gamma_L \cos \theta \quad (6)$$

Where:

$\gamma_S$ : solid surface free energy

$\gamma_L$ : liquid surface tension

Figure 6 shows the contact angle approach to Young's Equation. Subscripts S, L, and SL, respectively, indicate solid, liquid, and solid-liquid, respectively.

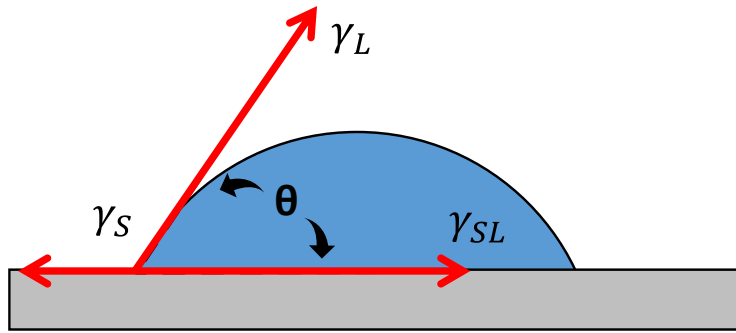


Figure 6. Applying Contact Angle to Get The Variables In Young's Equation.

**Work of Cohesion.** Cohesion can be defined as the intermolecular attraction between similar molecules. Figure 7 shows how cohesive liquids or solids separate from themselves, and Equation (7) shows the work of cohesion ( $W_c$ ).

$$W_c = 2\gamma^{tot} \quad (7)$$

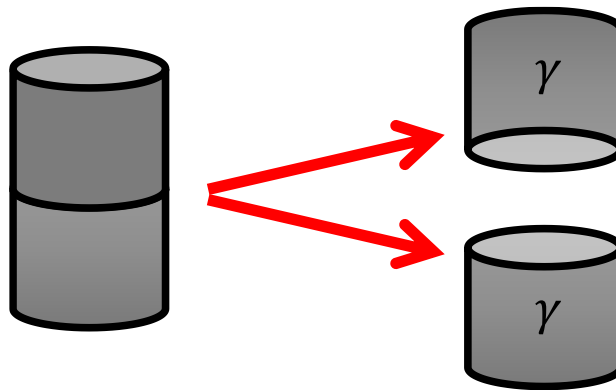
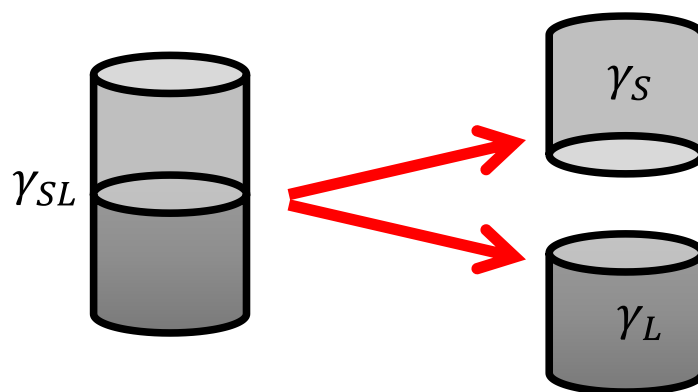


Figure 7. The Energy Required to Separate Two Surfaces Of The Same Material, Identified As The Work Of Cohesion.

**Work of Adhesion.** The thermodynamic work of adhesion ( $W_a$ ) measures intermolecular contact between two substances (Shanahan, 1991). The effort needed to divide a solid from a liquid is seen in Figure 8 (Schrader, 1995). Therefore, the breakdown of the preexisting liquid-solid surface is necessary for adhesion, along with the formation of new surfaces (vapor-liquid and solid-vapor).



*Figure 8.* The Energy Required to Separate Two Surfaces Of Different Material, Identified As The Work Of Adhesion.

Adhesion is a property of liquid-solid groups that depend on the nature of the liquid and the solid. Consequently, Dupré's (Dupré, 1869) equation derives adhesion work from interfacial free energy (Equation (8)).  $\gamma_{SL}$  is defined by Equation (9).

$$W_{SL} = \gamma_S + \gamma_L - \gamma_{SL} \quad (8)$$

Where:

$W_{SL}$ : the work needed to separate the solid and liquid surfaces

$\gamma_S$  and  $\gamma_L$ : the SFE component for solid and liquid, respectively

$\gamma_{SL}$ : solid-liquid interfacial energy

$$\gamma_{SL} = (\sqrt{\gamma_S^{LW}} - \sqrt{\gamma_L^{LW}})^2 + 2(\sqrt{\gamma_S^+ \gamma_S^-} + \sqrt{\gamma_L^+ \gamma_L^-} - \sqrt{\gamma_S^+ \gamma_L^-} - \sqrt{\gamma_S^- \gamma_L^+}) \quad (9)$$

Where:

$\gamma^{LW}$ : the apolar or Lifshitz-van der Waals component

$\gamma^+$ : surface energy Lewis's acid parameter

$\gamma^-$ : the Lewis base parameter

By combining Equations (6) and (8), the relationship between contact angle and surface free energy can be expressed as the Young-Dupré equation:

$$W_{SL}^a = \gamma_L(1 + \cos \theta) \quad (10)$$



The adhesion work can be rewritten by combining Equations (8), (9), and (10) with the relationship shown in Equation (11):

$$W_{SL}^a = \gamma_L(1 + \cos \theta) = 2(\sqrt{\gamma_S^{LW} \gamma_L^{LW}} + \sqrt{\gamma_S^+ \gamma_L^-} + \sqrt{\gamma_S^- \gamma_L^+}) \quad (11)$$

In Equation (11), there are three unknowns connected to the substrate:  $\gamma_S^{LW}$ ,  $\gamma_S^+$ , and  $\gamma_S^-$ . To calculate these values, it is necessary to measure the contact angles of at least three liquids with known surface energy characteristics ( $\gamma_S^{LW}$ ,  $\gamma_S^+$ , and  $\gamma_S^-$ ) on the proposed surface. For instance, if the contact angles of three known liquids are measured on a specific asphalt, Equation (11) shows the determination of the asphalt's surface energy components, from which the asphalt's total surface energy can be derived. A higher value of  $W_{SA}^a$  indicates higher resistance to moisture damage. At least two of the three liquids should be polar, and a high-energy polar liquid should also be used for the measurements (Good, 1992). In the case of asphalt and aggregate, Equation (11) can be rewritten as follows:

$$W_{SA}^a = 2(\sqrt{\gamma_S^{LW} \gamma_A^{LW}} + \sqrt{\gamma_S^+ \gamma_A^-} + \sqrt{\gamma_S^- \gamma_A^+}) \quad (9)$$

where

$W_{SA}^a$ : the adhesion work between aggregate stone (S) and asphalt binder (A),

The adhesion of asphalt-aggregate under dry conditions, as illustrated in Figure 8, can be simply computed from the interactions of the observed asphalt and aggregate SFE components.

**Work of Water Debonding.** Work of water-debonding ( $W_{SWA}^a$ ) is used to describe the surface energy components of water, aggregate, and asphalt binder. The Dupré equation, as shown in Equation (8), can be used to determine the work of adhesion between aggregates and asphalt binders in the presence of water (i.e., the work of debonding), as shown in Equation (12):

$$W_{SWA}^a = \gamma_{AW} + \gamma_{SW} - \gamma_{AS} \quad (12)$$

Where

subscripts A, W, and S: asphalt binder, water, and aggregate stone, respectively

$\gamma_{AW}$ : work required to create a new asphalt-water interface

$\gamma_{SW}$ : work required to create a new stone-water interface

$\gamma_{AS}$ : the external work required to remove the binder-aggregate interface

Equation (12) can be reformulated in terms of GvOC, energy components derived from SFE, as shown by Equation (13):

$$\begin{aligned}
 W_{SWA}^a = & -2 \left[ \sqrt{\gamma_S^{LW} \gamma_W^{LW}} + \sqrt{\gamma_A^{LW} \gamma_W^{LW}} - \sqrt{\gamma_S^{LW} \gamma_A^{LW}} - \gamma_W^{LW} \right. \\
 & + \sqrt{\gamma_W^+} (\sqrt{\gamma_S^-} + \sqrt{\gamma_A^-} - \sqrt{\gamma_W^-}) + \sqrt{\gamma_W^-} \left( \sqrt{\gamma_S^+} + \sqrt{\gamma_A^+} - \sqrt{\gamma_W^+} \right) \\
 & \left. - \sqrt{\gamma_S^+ \gamma_A^-} - \sqrt{\gamma_S^- \gamma_A^+} \right] \quad (13)
 \end{aligned}$$

Therefore, the work of adhesion in the dry state can be obtained using Equation (11), whereas the work of adhesion in the presence of water can be determined using Equation (13). The latter involves utilizing the three different parts of water's surface energy, which amounts to the work of water debonding.

The work of adhesion in the dry state can be determined using Equation (11), whereas the work of adhesion in the presence of water can be determined using Equation

(13). The latter involves understanding the three different parts of water's surface energy, which amounts to the work of water debonding.

Contact angle test results can be used to calculate the debonding energy of asphalt-aggregate and water interactions. This is done by measuring the contact angles between three distinct probe liquids and the asphalt binder and/or aggregates. Three linear equations for the asphalt binder and aggregate can be generated from these measurements. Unknown components of the asphalt binder surface energy and aggregate surface energy can then be found by solving these equations. Debonding work in the presence of water can be calculated using Equation (13) after the three surface energy components of the asphalt binder and aggregate are known. Water's function on the adhesion between asphalt binder and aggregate can now be better understood, which is important for the longevity and performance of asphalt pavements.

If the three components are known, it is feasible to determine the aggregate and asphalt binder surface energies using Equation (12), and the debonding work of these two materials in the presence of water using Equation (13). The extent of debonding work ( $W_{SWA}^a$ ) is a feature of each asphalt-aggregate system. As water displaces asphalt binder from the asphalt-aggregate interface, the magnitude of absolute value of work of debonding directly correlates with the amount of free energy released. This indicates that a greater quantity of free energy is released during the displacement process. As a result, if water has a greater propensity to remove asphalt binder from the asphalt-aggregate interface, it is an indication that the asphalt binder has a lower resilience to moisture damage. By

considering the effect of adhesion and water-debonding, the energy ratio (ER) can be shown in the following Equation (14) (Xu et al., 2018):

$$\text{Energy Ratio (ER)} = \left| \frac{W_{SA}^a}{W_{SWA}^a} \right| \quad (14)$$

Theoretically, a higher value of ER indicates a stronger resistance of an asphalt mixture to moisture damage because it indicates a higher adhesion between asphalt and aggregate and a lower energy release of the mixture system because asphalt is replaced by water on aggregates.

### **Fourier Transform Infrared Spectroscopy-Attenuated Total Reflectance (FTIR-ATR)**

The impact of oxidative conditioning is primarily determined by the asphalt binder's chemical composition, where the chemistry of the binder and aggregates has a direct influence on SFE measurements and in turn the resistance of asphalt-aggregate interfaces to moisture-induced damage. To further research the relationship between oxidative conditioning and moisture damage, researchers utilized the FTIR-ATR test (Hofko et al., 2017; Karlsson & Isacsson, 2003; Mullapudi & Sudhakar Reddy, 2020; Samara et al., 2022).

FTIR-ATR technology has become a popular asphalt binder test due to its ability to monitor asphalt binder oxidation (Karlsson & Isacsson, 2003; Mullapudi & Sudhakar

Reddy, 2020; Samara et al., 2022). The purpose of the test is to detect and quantify the functional group concentration in asphalt binder. FTIR measures the amount of infrared radiation absorbed by a sample. Various wavelengths correspond to the chemical components of samples. The oxidation of the binder increases the carbonyl and sulfoxide components. Carbonyl and sulfoxide groups compare the oxidative conditioning susceptibilities of asphalt binders. Asphalt binder comparisons are made using carbonyl and sulfoxide indices. Equations 15 and 16 provide the carbonyl and sulfoxide indices, respectively.

*Carbonyl Index*

$$= \frac{\text{Area around } 1700 \text{ cm}^{-1}}{\text{Area around } 1460 \text{ cm}^{-1} + \text{Area around } 1375 \text{ cm}^{-1}} \quad (15)$$

*Sulfoxide Index*

$$= \frac{\text{Area around } 1032 \text{ cm}^{-1}}{\text{Area around } 1460 \text{ cm}^{-1} + \text{Area around } 1375 \text{ cm}^{-1}} \quad (16)$$

Mullapudi & Sudhakar Reddy, 2020 investigated the relationship between FTIR-ATR and SFE. Mullapudi & Sudhakar Reddy, 2020 applied different oxidative conditionings on recycled asphalt pavement (RAP) material and reported a good correlation between carbonyl index and SFE, indicating the reliability of FTIR-ATR to provide justifications behind SFE findings in terms of the chemical behavior of asphalt binder due to oxidative conditioning.

## Summary of Literature Review

The following is a summary of the findings from the literature review:

- Oxidative conditioning and moisture damage of asphalt mixtures are frequent causes of pavement distresses.
- AASHTO T283 is the most commonly used test for evaluating moisture-induced damage of asphalt mixtures. However, previous studies highlighted several limitations of the AASHTO T283 test where conflicting observations were seen in literature.
- AASHTO T283 include an oxidative conditioning that simulates pavement performance at the early stages of construction, whereas moisture damage dominates after several years of construction, where higher oxidation was employed.
- Few studies have considered appropriate oxidative conditioning levels for asphalt mixtures where moisture damage has the most severe effect (highest sensitivity to moisture damage).
- Literature has shown that SFE characterization can be used to better evaluate the susceptibility of asphalt mixtures to moisture damage. However, there is a limited number of studies focusing on assessing the relationship between thermodynamic and chemical characterization determined through SFE and FTIR-ATR parameters.

## **Chapter 3**

### **Description of Materials**

In this chapter, a description of the materials selected for this study is presented. Furthermore, this chapter provides a discussion of aggregate and aggregate gradation as well as the binder types used. Moreover, the probe liquids used for the SFE evaluation are provided as well.

#### **Asphalt Binders and Aggregate**

Three different types of asphalt binders were selected for this study including: PG 64-22 and SBS modified PG 76-22, which are frequently used in New Jersey (Alfalah et al., 2020, 2021; Shackil, 2020), and PG 52-34, which is frequently used in cold regions like Alaska and Canada (Al-Badr, 2021; Ali et al., 2022). Granite aggregate with a nominal maximum aggregate size (NMAS) of 12.5 mm and obtained from a local source in New Jersey was utilized for this study. The aggregate and asphalt binders were mixed to obtain asphalt mixtures that meet the Federal Aviation Administration (FAA) P-401 specifications for low-weight aircraft (60,000 pounds or less) were prepared as part of this study (FAA, 2020). The decision to utilize FAA specifications for airfield asphalt mix was based on the accessibility of local materials and its resemblance to the asphalt mix specifications of the US Army Corps of Engineers (USACE) for airfields. The P-401 granite aggregate properties obtained from the job mix formula (JMF) are reported in Table 1.



**Table 1***Properties of Selected Granite Aggregate*

<b>Property</b>	<b>Specification</b>	<b>Value</b>	<b>Limit</b>
Wear Abrasion	ASTM C131	17.0 %	≤ 40 %
Sodium Sulfate	ASTM C88	0.2 %	≤ 12 %
Magnesium Sulfate	ASTM C88	0.0 %	≤ 18 %
Flat Elongated Pieces	ASTM D4791	0.8 %	≤ 8 %
Clay Lumps / Friable Particles	ASTM C142	0.0 %	≤ 1.0 %

The Asphalt mixtures were designed at 50 gyrations ( $N_{des}$ ) and an AVC% of 3.5%  $\pm$  0.5% with a minimum voids in mineral aggregate (VMA) of 15%. The dense-graded gradation used in this study is presented in Figure 9. The same aggregate blend was used with the three binder types to design three mixes (results shown Table 2). As seen from Table 2, the mixture prepared using PG 52-34 obtained an optimum binder content (OBC%) of 5.7%, which was slightly higher than the 5.5% obtained for mixtures prepared using PG 64-22 and PG 76-22.

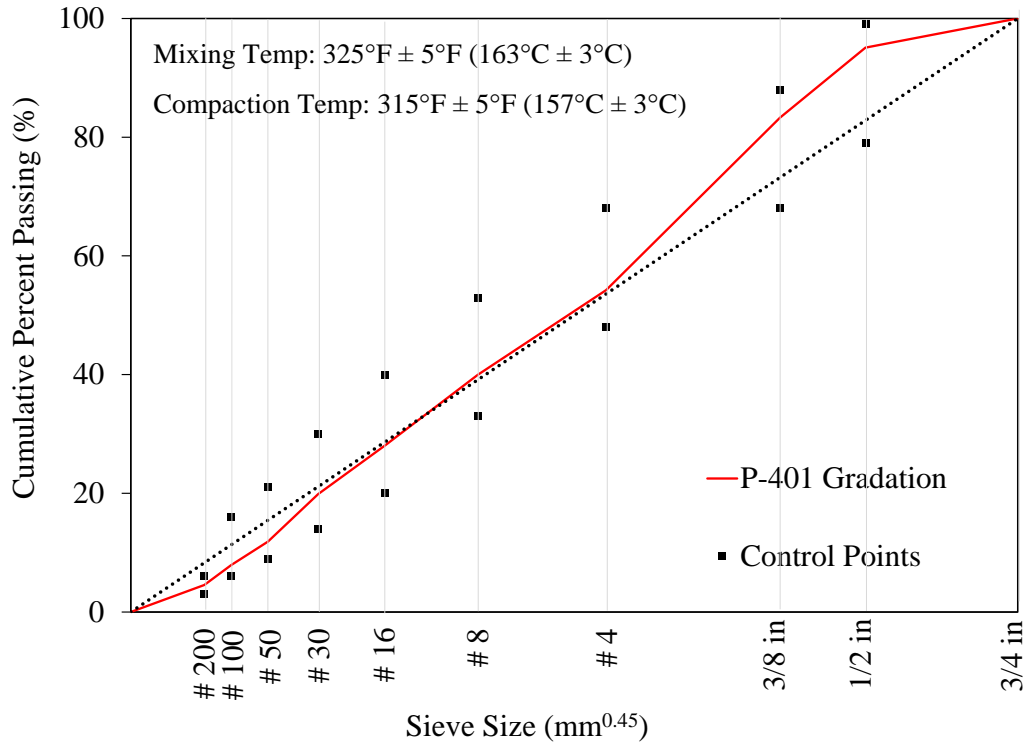


Figure 9. FAA P-401 Gradation.

**Table 2**

*Mix Design Results*

Binder Type	OBC (%) *	AVC (%)	VMA (%)
PG 64-22	5.5%	4.0%	16.4%
PG 76-22	5.5%	3.7%	16.4%
PG 52-34	5.7%	3.6%	16.6%

\* Optimum Binder Content by total mixing weight

## Probe Liquids

Based on ASTM Volume 40, Issue 5 recommendations (J. Wei & Zhang, 2012), three test probe liquids (distilled water, formamide, and ethanol glycol) were employed in this study due to their comparatively high surface free energy values and distinctive surface free energy components. Table 3 provides the surface free energy components for the three probe liquids at the ALT. Eight separate locations on the asphalt sample surface were used to drip the liquid droplets, and eight contact angles were evaluated to get reliable findings. Contact angle was measured at the intermediate ambient temperature.

**Table 3**

### *Properties of Probe Liquids*

<b>Probe Liquid SFE (mN/m)</b>	$\gamma^+$	$\gamma^-$	$\gamma^{LW}$	$\gamma^{tot}$
Distilled Water	25.5	25.5	21.8	72.8
Ethanol Glycol	1.92	47.0	29.0	48.0
Formamide	2.28	39.6	39.0	58.0

## **Chapter 4**

### **Experimental Plan**

#### **Introduction**

This chapter outlines the experimental plan used in the laboratory tests conducted for this study. The experimental plan is divided into two main sections: AASHTO T283 testing plan and SFE and FTIR-ATR testing plan. The AASHTO T283 testing plan was performed on asphalt and aggregate compacted specimens, while the SFE was conducted separately for both the asphalt binder and the aggregate. This was done to analyze the surface energy of each material and their compatibility with one another. Furthermore, the FTIR-ATR was carried out specifically on the asphalt binder types, to assess the chemical composition and structure of each type.

#### **AASHTO T283 Experimental Plan**

##### *General Scope*

The experimental plan was designed to evaluate the impact of asphalt mixture oxidative aging and testing temperature on asphalt mixture performance. In general, the experimental plan covered three oxidative conditioning levels: 1) Original Test Conditioning (OTC), 2) Short-Term Oxidative Conditioning (STOC), and 3) Long-Term Oxidative Conditioning (LTOC). Three testing temperatures were also selected: 1) Ambient Laboratory Temperature (ALT) (25°C), 2) Asphalt Intermediate Temperature (AIT), and 3) Climate Intermediate Temperature (CIT). AIT was selected to consider the

intermediate temperature of the asphalt binder as suggested in Note 5 of the IDEAL-CT specification (ASTM D8225). The equation for AIT is expressed in Equation 17.

$$AIT = \frac{PG\ HI + PG\ LT}{2} + 4 \quad (17)$$

Where:

AIT: Asphalt intermediate temperature (°C)

PG HI: Binder high performance grade temperature (°C)

PG LT: Binder low performance grade temperature (°C)

The AASHTO T283 testing temperatures used in this study are shown in Table 4. It is noted that the specimens prepared with PG 64-22 mixture shared both ALT and AIT of 25°C, making it a neutral case. The specimens prepared with PG 76-22 were tested at 25°C and an increased AIT of 31°C. Finally, the specimens prepared with PG 52-34 were evaluated at 25°C as well as a decreased AIT of 13°C. Based on the Long-Term Pavement Performance (LTPPBind) database, PG 52-34 is usually used in cold regions (i.e., Alaska and Canada) where CIT is 13°C. Whereas 25°C is the actual CIT for pavements constructed using PG 76-22 and PG 64-22.

**Table 4**

*Temperatures Used when Conducting AASHTO T283 Testing*

Binder Grade	Ambient Laboratory Temperature (ALT), °C	Asphalt Intermediate Temperature (AIT), °C	Climate Intermediate Temperature (CIT), °C
PG 64-22	25	25	25
PG 76-22	25	31	25
PG 52-34	25	13	13

As shown earlier in Equation 1, the analysis of parameters obtained from load-displacement curves included determining TSR% by dividing the ITS of moisture conditioned (MC) specimens by that of unconditioned (UC) specimens. Further, the UC and MC comparison was carried out for the parameters used in the IDEAL-CT test and cracking tolerance index ( $CT_{index}$ ) calculation (i.e.,  $G_f$ ,  $l_{75}$ , and  $|m_{75}|$ ), according to ASTM D8225. Figure 10 presents an overall flow chart of the experimental plan utilized in this study; specific details regarding specimen preparation, conditioning, and testing are provided in the subsequent sections. In this study, three UC specimens and three MC specimen replicates were created.

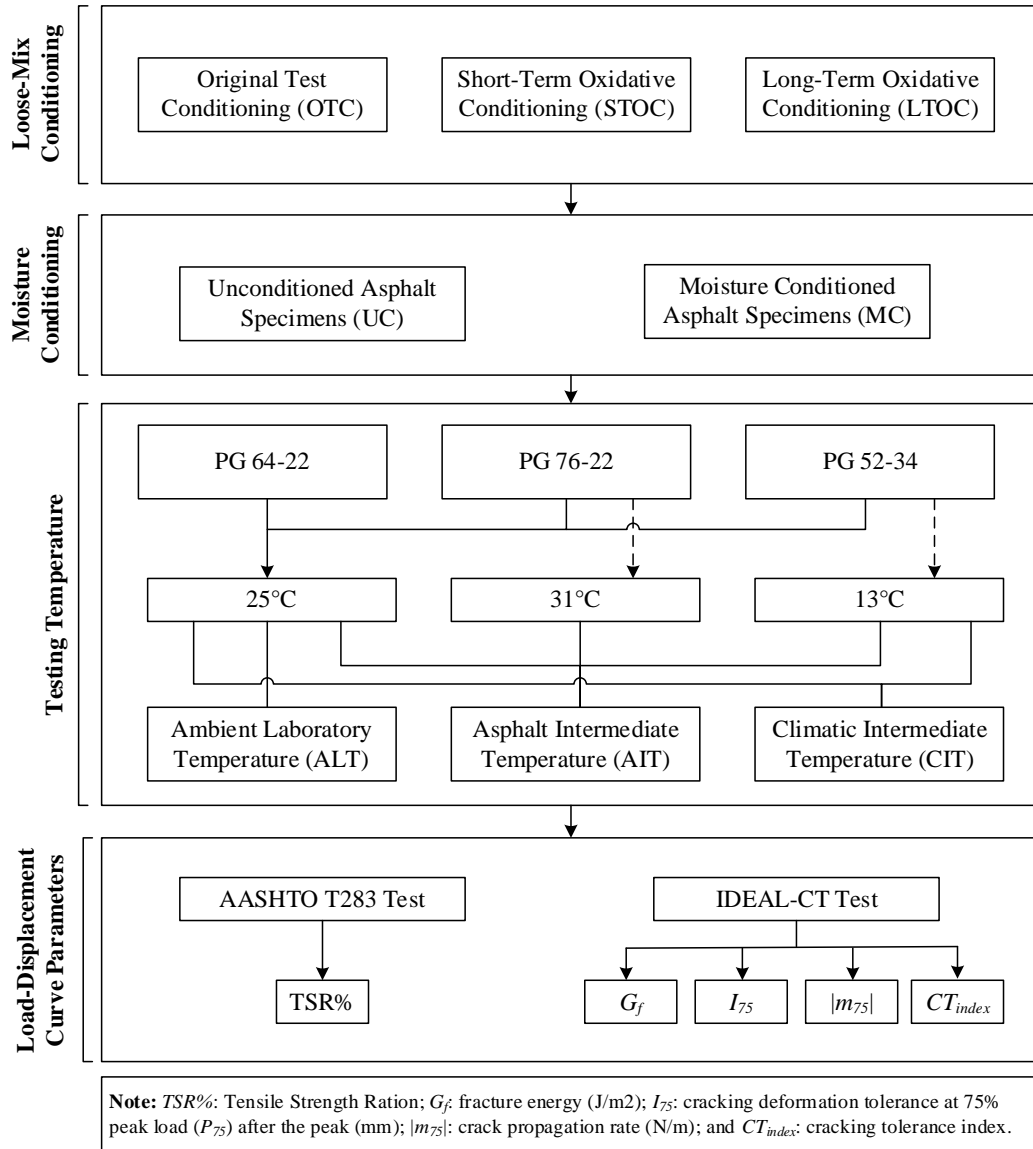


Figure 10. AASHTO T283 Laboratory Experimental Plan

### ***AASHTO T283 Specimen Preparation***

Specimen preparation followed AASHTO T283 specifications. Asphalt binders were heated in an oven and occasionally stirred to maintain homogeneity. The heated asphalt binder was then mixed with preheated aggregates to obtain loose-asphalt mixtures. At this point, loose-mix oxidative conditioning procedures were performed, as applicable, following the oxidation procedures described in the next subsection. Loose-mix samples were then allowed to cool for  $2.0 \pm 0.5$  hours at room temperature. After cooling down, loose-mix samples were placed in a  $60^{\circ}\text{C} \pm 3^{\circ}\text{C}$  oven for  $16 \pm 1$  hours (i.e., AASHTO T283 mix oxidation process). Once loose-mix oxidative conditioning and AASHTO T283 aging were completed, mixes were then heated to the P-401 compaction temperature of  $157^{\circ}\text{C}$  ( $315^{\circ}\text{F}$ ) for  $2.0$  hours  $\pm 10$  minutes and compacted using a SGC targeting  $7.0\% \pm 0.5\%$  AVC%.

### ***AASHTO T283 Conditioning Procedures***

Previous studies have demonstrated that loose-mix oxidation yields more uniform conditioning than oxidation of compacted specimens (Braham et al., 2009; Elwardany et al., 2017; Kim et al., 2018; Partl et al., 2012; Rad et al., 2017). Therefore, loose mix conditioning was selected for use in this paper as follows:

- ***Original Test Procedure (OTC)***: In this level, no additional loose-mix oxidation of asphalt mixtures was conducted. Sample preparation for OTC consisted of cooling the loose-mix after mixing to room temperature, followed by AASHTO T283 oxidation of 16 hours, then heating and compacting the loose-mix at the



compaction temperature. This serves as the control (i.e., standard practice based on typical T283 testing).

- ***Short-Term Oxidative Conditioning (STOC)***: STOC consisted of loose-mix oxidative conditioning for 2.0 hours at the mix compaction temperature (i.e., 157°C or 315°F). Note that STOC was performed during the mix design phase of this work to establish the mix designs.
- ***Long-Term Oxidative Conditioning (LTOC)***: LTOC consisted of loose-mix oxidation at 85°C for 120 hours (5 days). This practice followed procedures in AASHTO R30 for long-term conditioning; however, it is important to note that R30 specifies conditioning of compacted specimens rather than loose mix. This departure from typical R30 practices was an intentional step taken.

#### ***AASHTO T283 Moisture Conditioning***

As in normal AASHTO T283 testing, only a subset of all specimens was set aside for moisture conditioning, including a freeze-thaw cycle, while the other subset was tested without moisture conditioning. Moisture conditioning first required vacuum saturating specimens to 70%-80% saturation. These were then wrapped in plastic film and placed in a plastic bag containing 10 mL  $\pm$  0.5 mL of water. Specimens were subjected to a freeze-thaw cycle in a freezer at  $-18^{\circ}\text{C} \pm 3^{\circ}\text{C}$  for 16 to 24 hours before being removed from the plastic bag and conditioned (thawed) in a 60°C water bath for 24  $\pm$  1 hours.

### ***Additional Parameters for Moisture Damage Evaluation***

To highlight the impacts of oxidation on moisture damage using IDEAL-CT test parameters, the findings were assessed further by plotting average  $G_f$  against average  $l_{75}$  over  $|m_{75}|$  ratio ( $l_{75}/|m_{75}|$ ) on an interaction diagram developed by the National Center for Asphalt Technology (NCAT) (Yin, F et al., 2023). Within the interaction diagram, a series of  $CT_{index}$  contour curves are presented, which serve to connect the initial test parameters of  $G_f$  and  $l_{75}/|m_{75}|$  with the resulting  $CT_{index}$  value.  $G_f$  represents the toughness of asphalt mixtures, while  $l_{75}/|m_{75}|$  describes defines their ductile-brittle nature. Based on Figure 11, and Equation 2, a greater  $CT_{index}$  will result from an increase in  $G_f$  and  $l_{75}/|m_{75}|$ . Consequently, asphalt mixtures with greater  $CT_{index}$  values will be positioned near to the top right corner of the interaction diagram. It is noted that multiple data points on a contour curve can share the same  $CT_{index}$  value but have different  $G_f$  and  $l_{75}/|m_{75}|$  values. A specific mixture combination can produce a high  $G_f$  and a low  $l_{75}/|m_{75}|$ , while another mixture combination can produce a low  $G_f$  and a high  $l_{75}/|m_{75}|$ , with both yielding the same  $CT_{index}$ . As opposed to depending exclusively on the  $CT_{index}$  parameter, the interaction diagram gives a more inclusive perspective for analyzing IDEAL-CT findings.

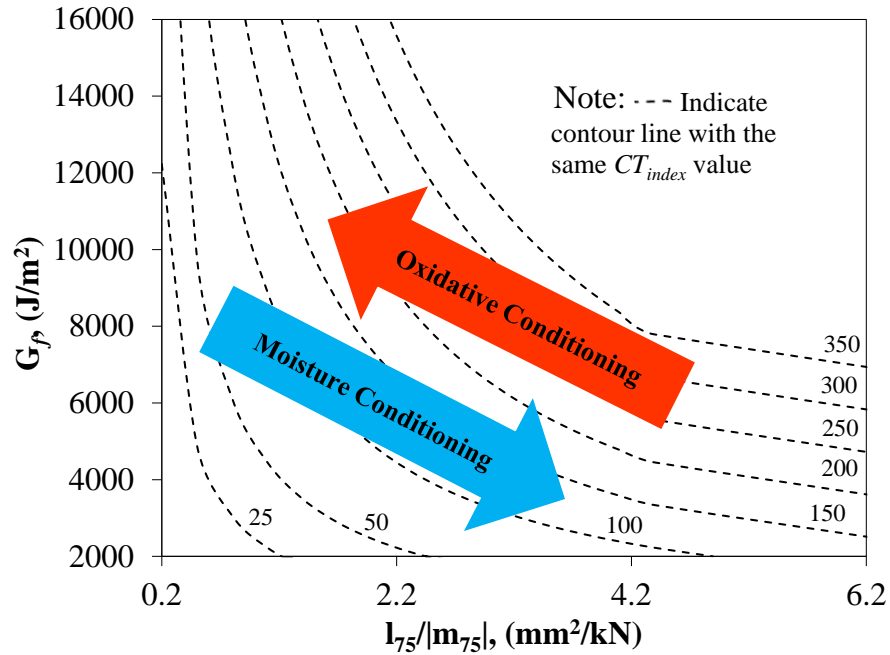


Figure 11. AASHTO T283 Laboratory Experimental Plan

According to Figure 11, it is expected that the influence of oxidative conditioning would result in an increase in  $G_f$  and a reduction in  $l_{75}/|m_{75}|$ , resulting in an expected decrease in  $CT_{index}$ . On the contrary, moisture conditioning is expected to weaken the asphalt mixes, hence, reducing  $G_f$  (weakening the toughness of the mix) and increasing  $l_{75}/|m_{75}|$  (pseudo-enhancing the ductility of the mix). Although it depends on the degree of  $G_f$  reduction, the increased  $l_{75}/|m_{75}|$  may yield a higher  $CT_{index}$ , which is contrary to the anticipated effect of moisture conditioning on asphalt mixtures. Therefore, it is determined that  $l_{75}/|m_{75}|$  and  $CT_{index}$  may not be suitable parameters for evaluating moisture-induced damage, and  $G_f$  may be better suited for moisture damage evaluations.

## SFE and FTIR-ATR Experimental Plan

### General Scope

The testing plan was developed to assess the impact of asphalt oxidative conditioning by evaluating SFE material properties and FTIR-ATR chemical testing. The plan included testing Original Binder (OB), and two levels of oxidation: RTFO, and PAV20. The three asphalt binders (PG 52-34, PG 64-22, and PG 76-22) were tested and analyzed for SFE and FTIR-ATR, at the three oxidation levels, as illustrated in Figure 12. The testing plan utilized in this study is presented in Figure 12, and the subsequent sections provide detailed information on oxidative conditioning procedures and sample preparation.

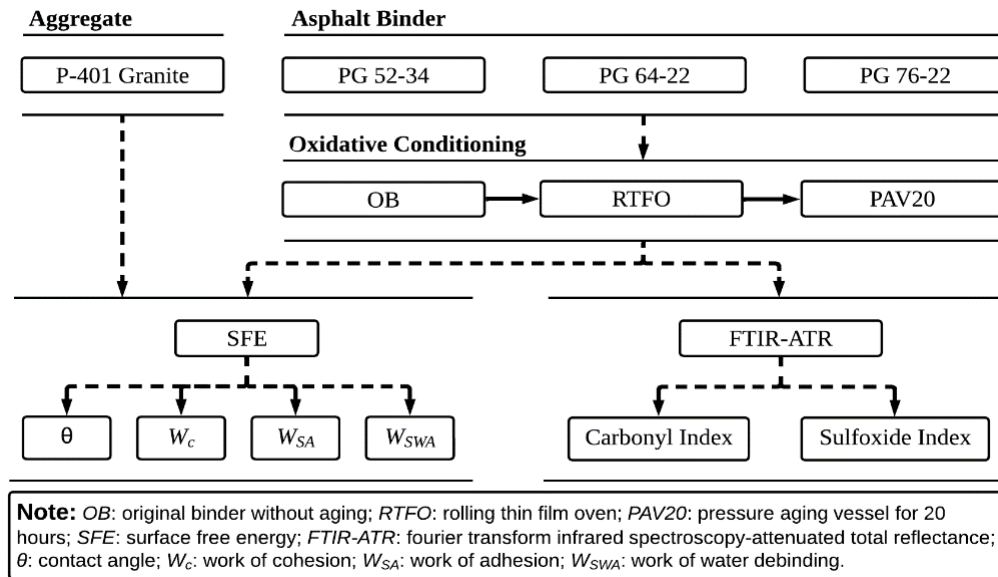


Figure 12. SFE and FTIR-ATR Laboratory Experimental Plan

### ***Binder Oxidation Procedures***

This study analyzed the impact of oxidative conditioning on asphalt binders, with the following levels selected:

- ***Original Binder (OB)***: This level served as the control and did not involve any additional oxidation of asphalt binders.
- ***Rolling Thin Film Oven (RTFO)***: The RTFO level simulated asphalt aging during construction, where the OB binder was placed in an oven set to 325°F (163°C) temperature for 85 minutes, following the procedure specified in AASHTO T 240.
- ***Pressure Aging Vessel (PAV20)***: The PAV20 level simulated long-term aging effects on asphalt binders. The RTFO binder was placed in a heated vessel pressurized to 305 psi (2.10 MPa) and subjected to 212°F (100°C) temperature for 20 hours, following the procedure specified in AASHTO R 28.

### ***SFE Calculations***

SFE is based on the concepts of thermodynamic sorption in which an adhesive will adhere to a substrate if contact is made (CJ Zollinger, 2005). SFE characterization of cohesion and adhesion are associated with the breaking of the asphalt-aggregate interface and the formation of a crack inside the binder, respectively. Characterizing materials and assessing their interfaces allows for the examination of their water susceptibility, healing abilities, and fatigue cracking resistance to predict their long-term performance and durability (Bahmani et al., 2022; Bhasin et al., 2007; Cheng, 2002; Hossain et al., 2019; L. Li et al., 2021; Sarsam, 2021; J. M. Wei et al., 2009; L. Zhou et al., 2021).

According to the thermodynamic adsorption hypothesis, adhesion occurs in moist conditions. Wetting is a bonding condition regardless of the type of material. Wetness is determined by the balance of cohesive and adhesive forces. The contact angle ( $\theta$ ) of a drop of liquid placed on a solid's surface can be used as a quantitative measure of the liquid's surface wetting characteristics. Good wetting and adhesion are indicated by a contact angle less than  $90^\circ$ , whereas a higher contact angle (more than  $90^\circ$ ) suggests non-wetting and inadequate wetting and adhesion. As a result, low wetness surfaces would have a high contact angle, while wet surfaces have a low one. As a result, contact angle is a crucial factor in wetting systems, measuring it provides a reliable method of estimating SFE.

The sessile drop method, which depends on the measurement of contact angle, was used to obtain the SFE components (as shown in Figure 13). The contact angles between the probe liquids and each asphalt binder and material provided three linear equations. These equations were solved for the unknown aggregate and asphalt binder to obtain the components of surface free energy (i.e.,  $\gamma^+$ ,  $\gamma^-$ ,  $\gamma^{LW}$ , and  $\gamma^{tot}$ ). The SFE components were analyzed to obtain the work of cohesion, adhesion, and water-debonding for each combination.

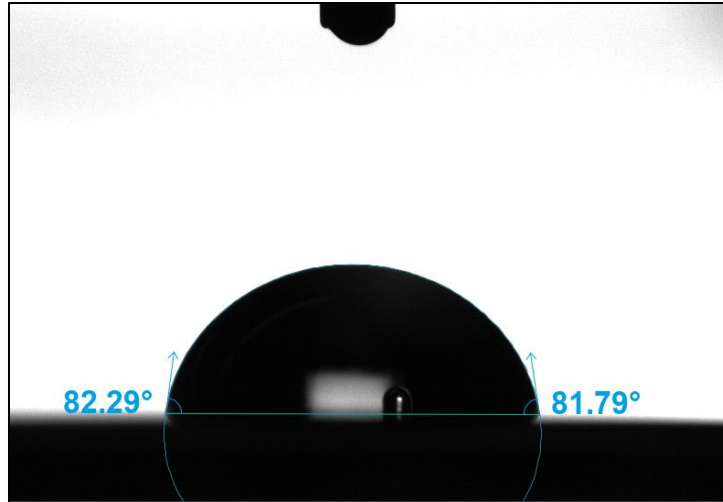


*Figure 13.* Example Of Contact Angle Measurement from Both Right And Left Sides

#### ***SFE Test Equipment and Sample Preparation***

The SFE device will measure the sample's right-to-left contact angle. As shown in Figure 13, the average of the two sides' measurements yields the contact angle.

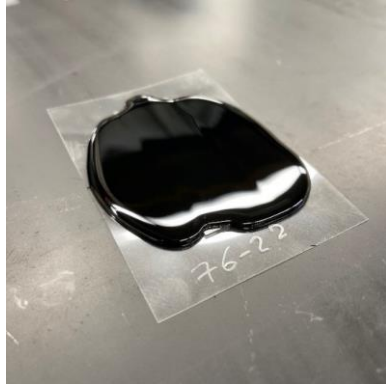
Previous studies measured contact angles by analyzing a picture and reading contact angle. The contact angles in this research will be recorded over 10 seconds at 14 frame rates. This procedure records and averages contact angle measurements.

The preparation of contact angle test samples using the sessile drop method will be performed where asphalt binders are kept in a small container. For the preparation of testing samples, the selected asphalt binder types will be heated in an oven until they liquefied and became pourable. Throughout the preparation of the asphalt sample, the fluid binder will be occasionally stirred to maintain asphalt homogeneity. The heated asphalt binder will then be poured on top of a test strip placed over an unmelting plastic

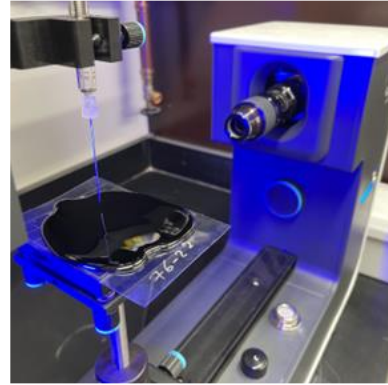
base, creating a flat surface. As seen from Figure 14a, asphalt binder was poured on top of a glass strip to create a flat surface. Samples will then be placed on top of the testing stage (Figure 14b) for contact angle measurement.

The SFE measurement for aggregate was previously conducted using the sessile drop approach. The sessile drop approach for aggregate has been used in previous studies (Sarsam, 2021; Tu et al., 2021). The approach these studies used for aggregate depended on creating a flat surface where an accurate contact angle measurement was obtained. In this study, Asphalt mixture compacted specimens fabricated using granite aggregate were cut and sliced to obtain a flat aggregate surface. As seen in Figure 14c and 11d, asphalt specimens were cut and sanded by hand to create a flat surface for accurate contact angle measurements. This procedure was required to ensure the precision and dependability of the measurements, and to ensure the precision and accuracy of the measurements, despite its labor-intensive nature. Z. Li et al., 2022 also used a similar method to measure the SFE of fiber material by creating a flat surface of the fibers. Similarly, in this study, a flat surface was created for the aggregates to obtain accurate measurements. Five droplets were applied onto the larger aggregates to ensure that they remain confined to the aggregate surface and do not meet the surrounding asphalt (Z. Li et al., 2022).

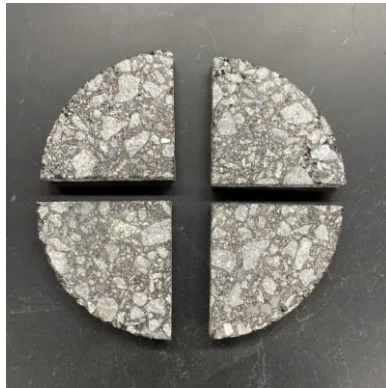




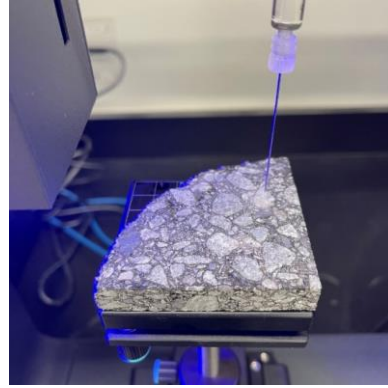
(a) Asphalt Sample



(b) Test Setup for Asphalt



(c) Specimens After Slicing



(d) Test Setup for Aggregate

*Figure 14.* Asphalt binder and Aggregate Preparation for Contact Angle Measurement

### **FTIR-ATR Test Equipment and Sample Preparation**

In this study, carbonyl, and sulfoxide indices for OB, RTFO, and PAV20 oxidation levels were measured using a Spectrum 100 FT-IR Spectrometer. During sample preparation, asphalt binders were placed in a small metal container. The container was sealed with a metal lid and heated to 165°C in a ventilated conventional oven. The

duration of heating varied according to the type of binder used. For example, PG 52-34 required less heating time than PG 64-22 and PG 76-22. The binder was stirred every five minutes to maintain homogeneity. All FTIR-ATR tests were completed within one hour after sample preparation. Following the recommendations of Hofko et al., 2018 and Mirwald et al., 2022 the sample preparation procedure was designed to yield consistent and repeatable results. It is noted that variables such as the temperature of the asphalt binder and the consistency of the stirring can affect the precision with which the sample is prepared. Therefore, throughout the sample preparation process, the asphalt binder temperature was monitored with a thermometer to reduce these potential sources of error.

After the sample preparation, the asphalt binder was analyzed using a Spectrum 100 FT-IR Spectrometer and an FTIR-ATR device. The FTIR-ATR analysis utilizes infrared light wavelengths ( $650\text{-}4000\text{ cm}^{-1}$ ) to determine the chemical composition and structure of the sample based on its ability to absorb different infrared light wavelengths. In this research, each sample was replicated three times. This analysis measured the carbonyl and sulfoxide indices, which are indicators of the change in asphalt binder's chemical composition due to oxidative conditioning.

## Chapter 5

### Laboratory Performance Test Results

#### Introduction

This chapter presents the results of the AASHTO T283, SFE, and FTIR-ATR tests conducted in the study. The AASHTO T283 results show the impact of binder type and testing temperature on ITS and TSR% to observe the conditions where moisture damage has the highest impact. Additionally, the results highlight the impact of binder type and testing temperature on IDEAL-CT to observe parameters that show the impact of moisture damage. Furthermore, a statistical analysis was performed to detect the statistical significance of binder type and testing temperature on the ITS findings. The SFE and FTIR-ATR results shed light on the impact of oxidation on the performance of asphalt components, including asphalt and aggregate. Specifically, the SFE results include contact angle measurements, SFE components ( $\gamma^+$ ,  $\gamma^-$ ,  $\gamma^{LW}$ ,  $\gamma^{tot}$ ), work of cohesion, as well as the work of adhesion, work of debonding, and ER. These measurements provide valuable insights into the surface energy and compatibility of the asphalt components. Furthermore, the FTIR-ATR results include the carbonyl and sulfoxide indices at different oxidation levels. These measurements help to assess the molecular composition and structure of the asphalt binder types and their susceptibility to oxidation. Overall, this chapter presents a detailed analysis of the test results, providing valuable insights into the impact of moisture damage and oxidation on the performance of asphalt components.

## AASHTO T283 Test Results

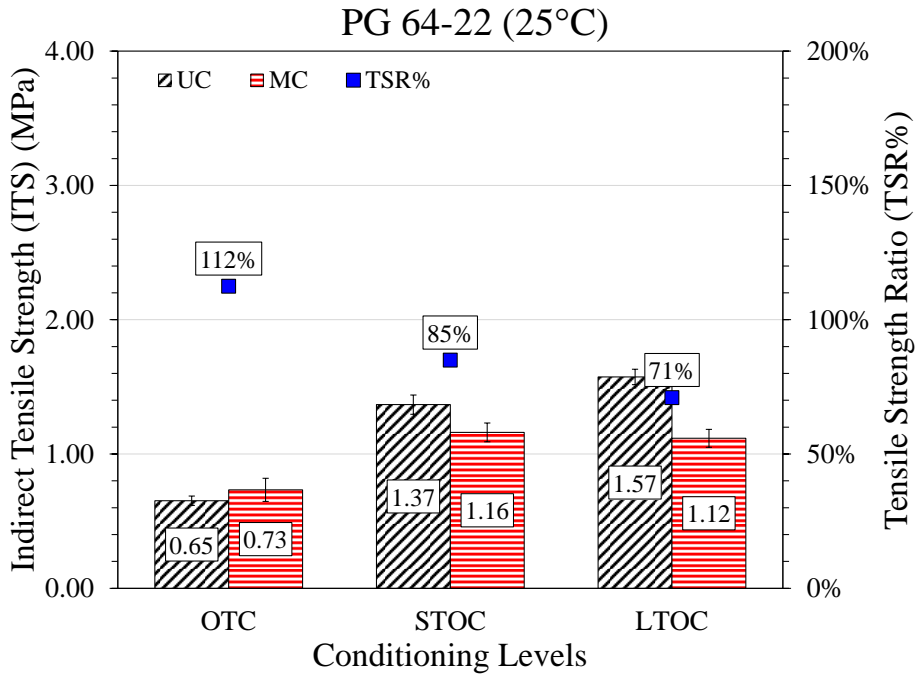
### *Indirect Tensile Strength (ITS) and Tensile Strength Ratio (TSR%)*

**Impact of Binder Type on ITS and TSR%.** Figures 15a, 15b, and 15c present the 25°C (ALT) ITS and TSR% for mixtures prepared using PG 64-22, PG 76-22, and PG 52-34, respectively. As can be seen from Figure 15, the tensile strength of asphalt mixtures increased with higher asphalt grade. Asphalt mixtures prepared using PG 76-22 showed the highest ITS followed by PG 64-22 then PG 52-34. This is expected since PG 76-22 is SBS polymer modified and stiffer than the other binder types. As seen in Figure 15a, oxidative conditioning increased ITS, but this was more prominent in UC mixtures (2-2.4 times of OTC) than MC (1.5-1.6 times of OTC) mixtures. As a result, moisture sensitivity increased meaningfully with TSR% decreasing from above 100% to 85% (STOC) to 71% (LTOC). Figure 15b displays a similar trend for the PG 76-22 mixture with the key difference being that the overall ITS values are higher than for PG 64-22; otherwise, TSR% trends with oxidation are similar (99% to 85% [STOC] to 68% [LTOC]). Similar trends were reported in previous studies (Crucho et al., 2019; Do et al., 2019; Ibrahim, 2019; Ziari et al., 2019) where ITS increased and TSR% decreased as oxidation level increased.

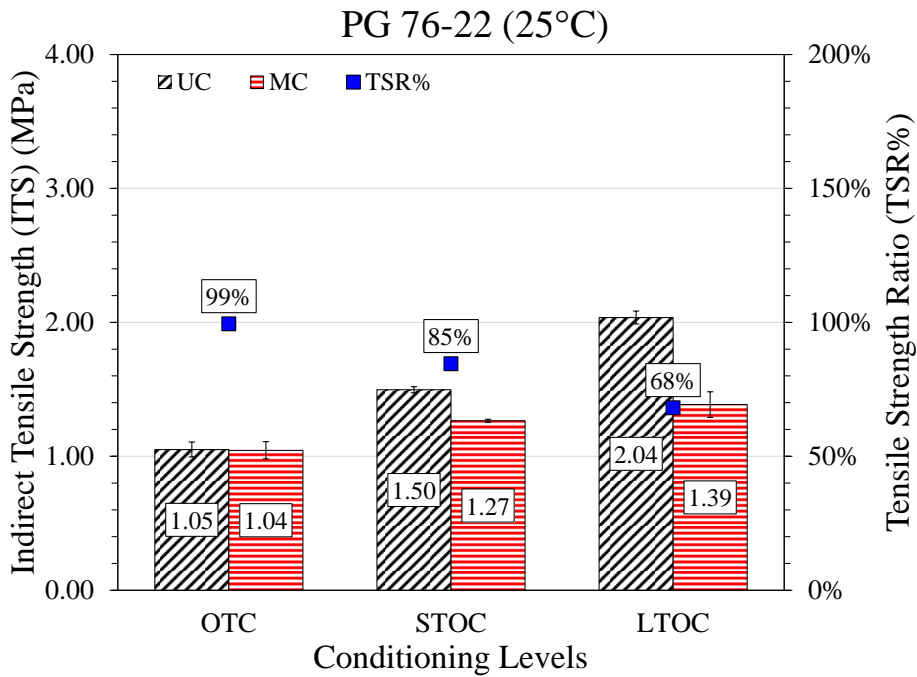
Figure 15c is different from Figures 15a and 15b. The effect of oxidative conditioning showed a slight ITS increase from 0.3 MPa at OTC to approximately 0.6 MPa at STOC and LTOC levels. This suggests that mixtures prepared using the softer PG 52-34 binder and tested at ALT (25°C) were minimally impacted by oxidation as

measured by ITS and TSR%. Interestingly, while TSR% decreased from 97% to 89% when STOC was performed, it increased to above 100% after LTOC, which is not logical. The ITS values for PG 52-34 mixes were consistently lower than those of other asphalt mixes and oxidation levels, ranging from 0.52 to 0.62 MPa for STOC and LTOC, respectively. These values were the lowest across all asphalt mixes and oxidation levels, even lower than the values for the PG 64-22 mixes at OTC (i.e., 0.65 MPa).

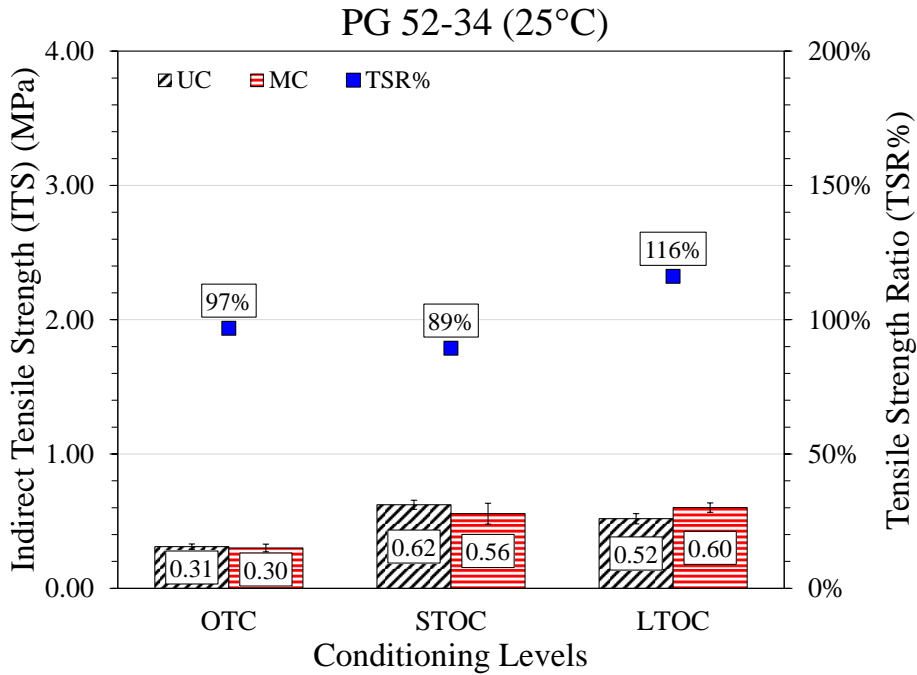
Figure 15c indicates that the oxidation process did not appear to have a significant effect on the ITS values for the PG 52-34 mixes, unlike the PG 64-22 and PG 76-22 mixes, as shown in Figure 15a and 15b, respectively. However, it is noted that the lower ITS values observed for the PG 52-34 mixes may be attributed to the softer nature of the binder, rather than the oxidation process alone. Moreover, the testing of moisture damage for mixes with softer binders such as PG 52-34 at the original intermediate testing temperature of 25°C may not be representative of the actual intermediate temperature of the asphalt binder, which is typically lower (i.e., 13°C in this case). This difference in temperature can affect the performance of the asphalt mix, especially for softer binders. Therefore, while the results suggest that oxidation did not have a substantial impact on the ITS values for the PG 52-34 mixes, it is important to consider other factors such as the stiffness of the binder and testing temperatures when evaluating moisture damage of asphalt mixtures under different oxidation levels.



(a) PG 64-22 at ALT (also AIT and CIT).



(b) PG 76-22 at ALT (also CIT).



(c) PG 52-34 at ALT

Figure 15. ITS And TSR% Results for Asphalt Mixtures Tested At 25°C.

**Impact of Testing Temperature on ITS and TSR%.** Figures 16a and 16b present the ITS and TSR% for mixtures prepared using PG 76-22 and PG 52-34 and tested at the AIT, respectively. As seen from Figure 16a, increasing test temperature from 25°C to 31°C caused a reduction in ITS of PG 76-22 mixes as would be expected.

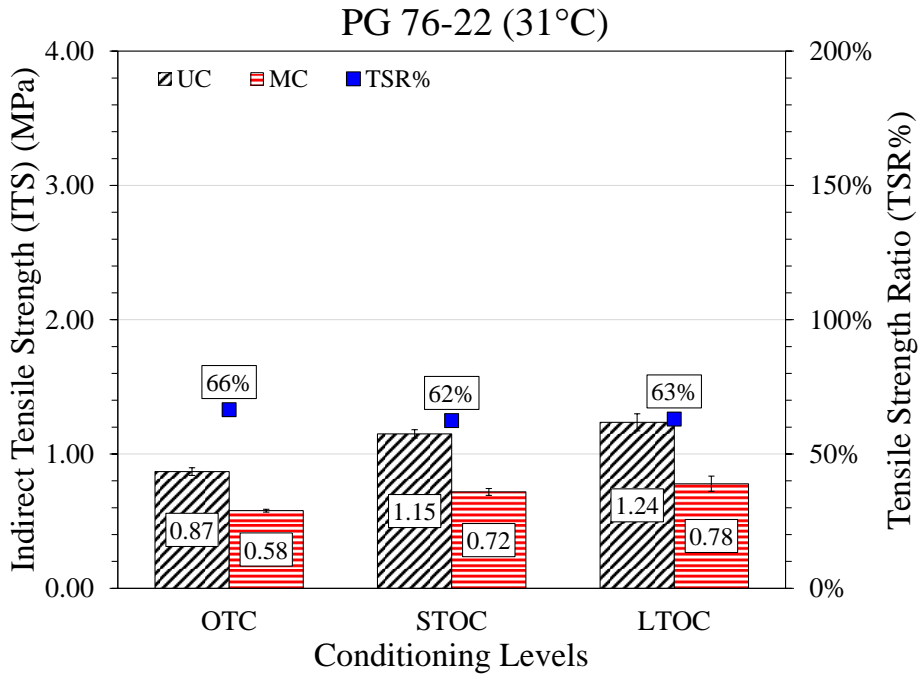
Findings show that with increasing oxidative conditioning level, moisture sensitivity remains the same (within  $\approx 4\%$ ). TSR% was  $64\% \pm 2\%$  indicating that increasing the testing temperature above ALT of 25°C to the AIT negatively impacted the sensitivity of moisture damage to the effect of oxidative conditioning. Interestingly, it is worth noting that the OTC TSR% dropped noticeably from 25°C to 31°C, going from

99% to 66% (Figure 15b compared to Figure 16a). Effectively, the results suggest that changing from ALT to AIT has a meaningful impact on TSR% with no additional oxidation, but testing at the AIT has no sensitivity to oxidation compared to testing at ALT.

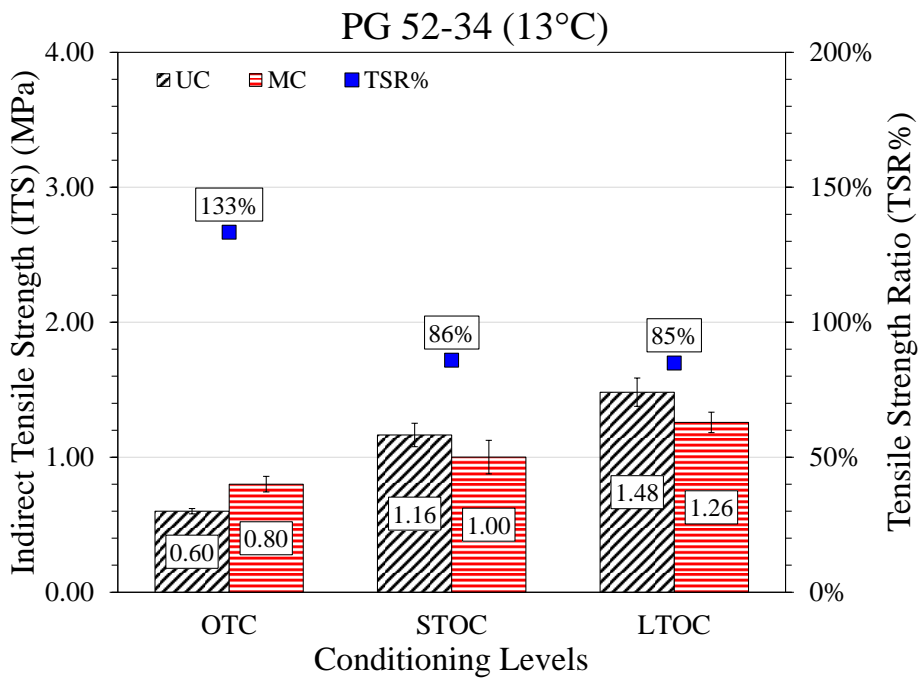
As seen from Figure 16b, reducing the test temperature from 25°C to 13°C led to an increase in ITS values as expected. ITS also progressively increased from 0.60 MPa to 1.48 MPa from OTC to LTOC. Unlike that of 25°C testing, TSR% showed greater and more rational sensitivity to oxidative conditioning when tested at the AIT. TSR% values reduced from 113% (OTC) to a relatively similar TSR% of 86% at the STOC level and 85% at the LTOC level, where higher effect of moisture conditioning can be observed. In the case of PG 52-34, the ALT was less appropriate of a testing temperature, and testing at the AIT greatly alleviated the inconclusive results from ALT testing.

It is important to note that the impact of binder type and testing temperature was limited to the aggregate type and gradation used in this study, as well as the moisture conditioning protocols (i.e., 70 to 80% saturation and one single freeze-thaw cycle) specified in AASHTO T283. However, other factors including temperature, saturation levels, freeze-thaw cycles, moisture diffusion, and other potential moisture-related weather conditions would provide a more accurate correlation with field performance. According to previous studies (Cong et al., 2020; Epps, 2000; K. Yan et al., 2015), increasing the saturation level and the number of freeze-thaw cycles would ultimately lead to a reduction in the ITS and TSR%.





(a) PG 76-22 at AIT



(b) PG 52-34 at AIT (also CIT)

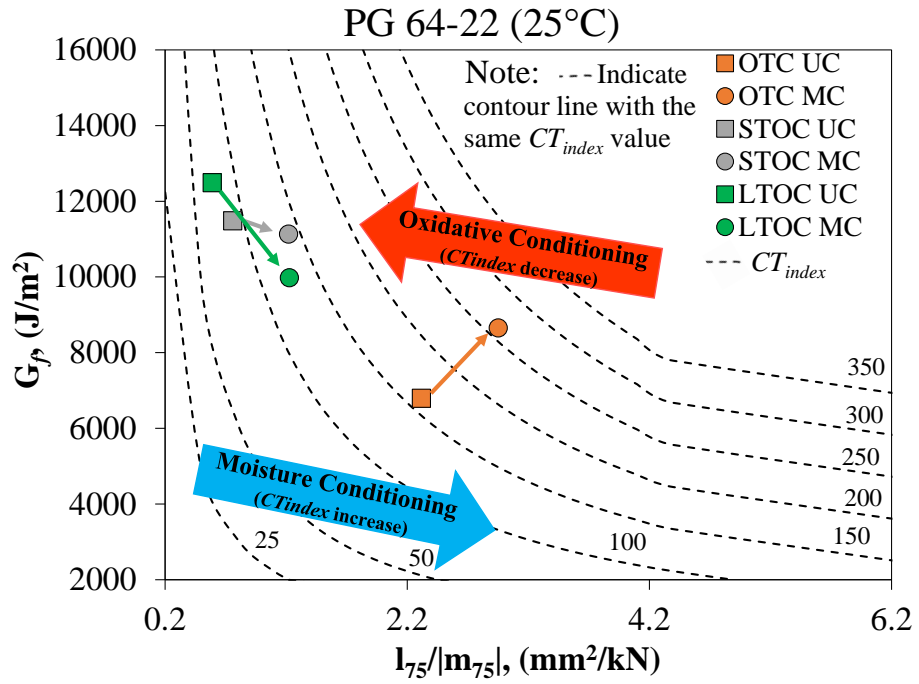
Figure 16. ITS And TSR% Results for Asphalt Mixtures Tested At AIT.

## ***IDEAL-CT Interaction Charts***

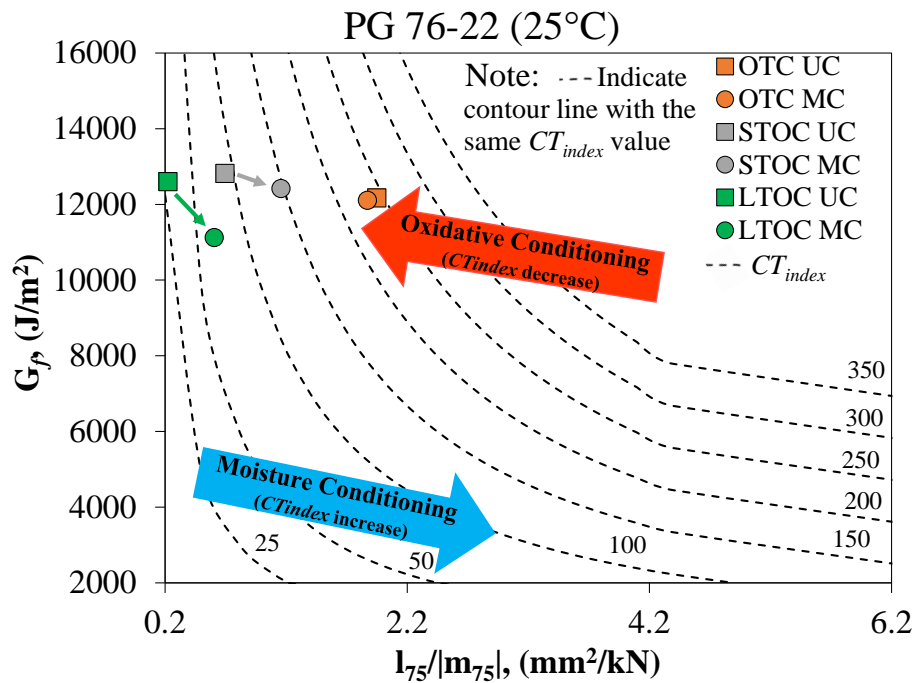
**Impact of Binder Type on IDEAL-CT.** Figure 17 presents IDEAL-CT interaction diagram results at the ALT. Overall, moisture conditioning increased  $CT_{index}$  for all oxidative conditioning levels. Higher  $CT_{index}$  implies mixture fatigue cracking performance has improved although this is not a rational interpretation. In Figure 17, moisture conditioning, which was expected to weaken asphalt strength, increased  $l_{75}/m_{75}$  and  $CT_{index}$ , indicating that moisture conditioning had the contrary anticipated effect of moisture conditioning on asphalt mixtures; Higher  $CT_{index}$  and  $l_{75}/m_{75}$ .

As seen from Figure 17a, unconditioned results for PG 64-22 mixtures showed a reduction in  $CT_{index}$  after STOC and LTOC due to an increase in  $G_f$  (toughness behavior) and a reduction in  $l_{75}/m_{75}$  (more brittle behavior). Moisture conditioning increased  $CT_{index}$  due to increasing  $l_{75}/m_{75}$  (more ductile behavior) and reducing  $G_f$  (low toughness). The highest impact of moisture conditioning was seen at the LTOC level, where the highest drop in  $G_f$  was seen. As can be seen in Figure 17b, PG 76-22 mixtures after oxidative conditioning had high  $G_f$  (between 11000 J/m<sup>2</sup> and 13000 J/m<sup>2</sup>) and low  $l_{75}/m_{75}$  (between 0.2 mm<sup>2</sup>/kN and 2.2 mm<sup>2</sup>/kN). The largest decrease in  $G_f$  due to moisture conditioning was seen after LTOC. Mixtures prepared using the softer PG 52-34 binder (Figure 17c) had low  $G_f$  (between 2900 J/m<sup>2</sup> and 6500 J/m<sup>2</sup>) and high  $l_{75}/m_{75}$  (between 1.8 mm<sup>2</sup>/kN and 6.2 mm<sup>2</sup>/kN). It can be observed that moisture damage behaviors are more evident when  $G_f$  is higher. Moisture conditioning for PG 64-22 and PG 76-22 mixes at the LTOC level had the greatest drop in  $G_f$ . However, PG 52-34 mixes

had increased  $G_f$  at OTC and LTOC oxidation levels (following the above 100% TSR% for these conditions), and equal  $G_f$  at the STOC level.



(a) PG 64-22 at ALT (also AIT and CIT)



(b) PG 76-22 at ALT (also CIT)

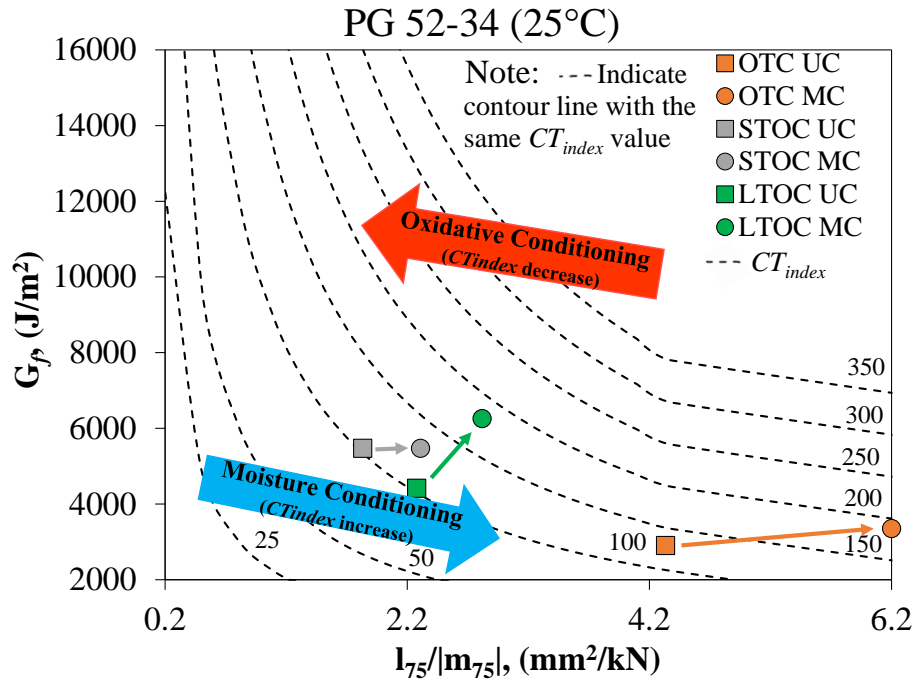
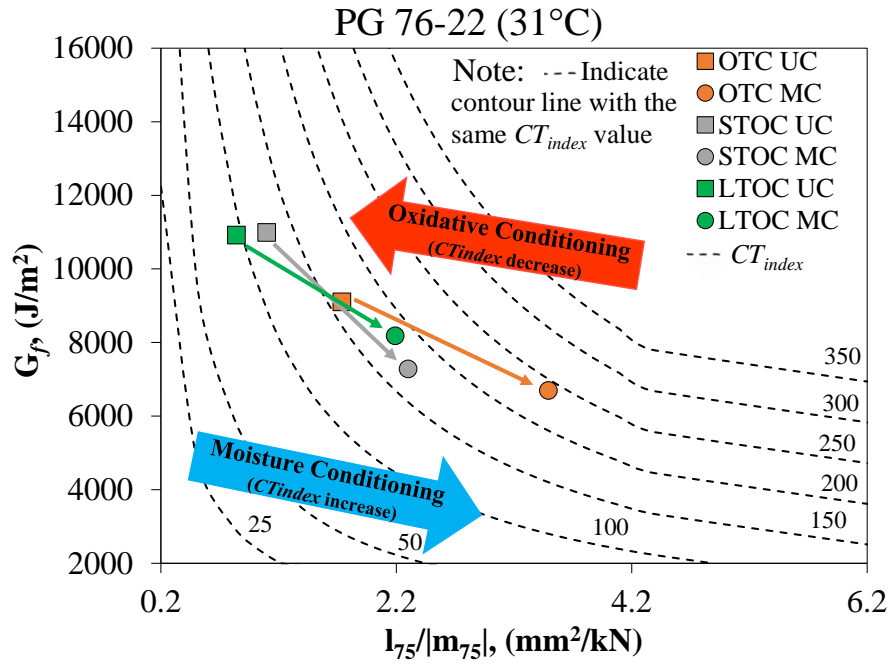


Figure 17. IDEAL-CT Interaction Diagram (25°C) Results

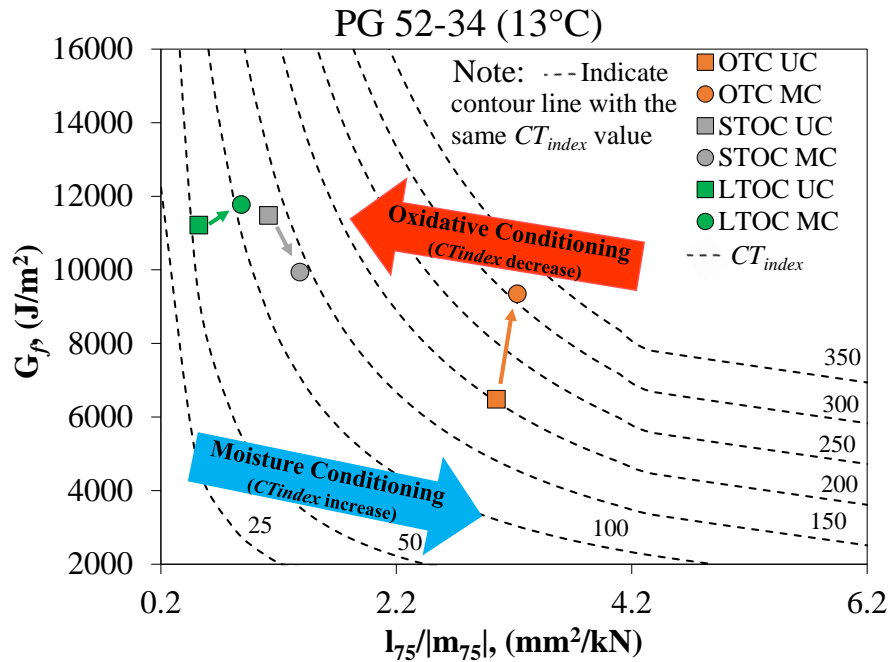
**Impact of Testing Temperature on IDEAL-CT.** Figure 18 presents IDEAL-CT interaction diagrams when testing samples at the AIT. Figure 18a shows that specimens prepared using PG 76-22 and tested at 31°C presented lower  $CT_{index}$  sensitivity due to oxidation and moisture conditioning. Moisture conditioning reduced  $G_f$  and increased  $l_{75}/|m_{75}|$  which is the expected behavior. However, impacts of oxidation were less evident when tested at AIT rather than ALT.

Mixes with PG 52-34 showed that decreasing the testing temperature from 25°C to 13°C (Figure 18b) led to an increase in  $G_f$  and reduction in  $l_{75}/|m_{75}|$ . In contrast to testing at 25°C, higher sensitivity to oxidation and moisture conditioning, reflected in  $G_f$

and  $l_{75}/m_{75}$ , resulted in greater impacts to  $CT_{index}$  ( $CT_{index}$  values range from as low as 60 to as high as 310). Moisture conditioning only impacted PG 52-34 mixes at the STOC oxidation level. However,  $G_f$  was the only parameter that demonstrated susceptibility to moisture damage. Although moisture conditioning for LTOC oxidation and PG 52-34 mixes obtained slightly higher  $G_f$ , higher oxidation had higher impact when testing at 13°C than 25°C. As 13°C is the CIT for PG 52-34 and 25°C is the CIT for PG 76-22, the results suggest that, compared to ALT and AIT, CIT is the testing temperature at which asphalt mixtures exhibited the highest moisture susceptibility.



(a) PG 76-22 at AIT



(b) PG 52-34 at AIT (also CIT)

Figure 18. IDEAL-CT Interaction Diagram AIT Results

## Statistical Analysis

A multi-factor Analysis of Variance (ANOVA) and Tukey's Honestly Significant Difference (HSD) post-hoc analysis were conducted to detect the statistical significance of binder type, oxidative conditioning, and testing temperature to the sensitivity of moisture conditioning. The analysis was performed on two stages; the first analysis was with the goal of evaluating the statistical significance between three oxidative conditioning levels (i.e., OTC, STOC, and LTOC) with ITS as the response variable, the second analysis was performed to compare the difference between the three different binder types (ITS used as the response variable) to evaluate the effect of moisture conditioning on asphalt performance. ANOVA and Tukey's HSD analysis were performed on both the ALT of 25°C and the AIT. The analysis was conducted at 95% confidence level (or p-value  $\leq 0.05$  for a significant impact). Tables 5 and 6 presents the results for ANOVA and Tukey's HSD post-hoc analysis, respectively.

As seen in Table 5, ANOVA results had a statistical significance with a p-value of  $<.001$  at different binder types, oxidation levels, and moisture conditioning, whereas the testing temperature's p-value was 0.309 indicating no statistical significance; however, this comparison included all binder types (ITS range between 0.3 MPa and 2.04 MPa), whereas comparing the testing temperature for the binder types individually (i.e., Binder\_Type\*Testing\_Temperature) shows a significance of testing temperature with a p-value of  $<.001$ . This indicates that when PG 76-22 and PG 52-34 were tested at different temperatures, the values were statistically significant. In Table 6, Tukey's HSD analysis showed that all oxidation levels (OTC, STOC, and LTOC) are showing



significantly different ITS results from each other. This indicates that ITS is significantly affected by the loose-mix conditioning at all oxidation levels. Tukey’s HSD post-hoc results confirms data analysis results where all combinations were significantly affected at different oxidation levels. The impact of binder types showed that mixes prepared using PG 64-22 were statistically significant from mixes prepared using PG 52-34. This indicates that only PG 52-34 were statistically significant at both testing temperatures.

**Table 5**

*ANOVA Results for Indirect Tensile Strength (ITS)*

<b>Analysis of Variance (ANOVA)</b>		
<b>Factor</b>	<b>F-value</b>	<b>p-value</b>
Binder_Type	114.032	<.001*
Oxidation_Level	216.103	<.001*
Moisture_Conditioning	74.523	<.001*
Testing_Temperature	1.046	0.309
Binder_Type*Oxidation_Level	6.283	<.001*
Binder_Type*Moisture_Conditioning	18.622	<.001*
Binder_Type*Testing_Temperature	196.219	<.001*
Oxidation_Level*Moisture_Conditioning	24.549	<.001*
Testing_Temperature*Oxidation_Level	0.144	0.866
Testing_Temperature*Moisture_Conditioning	1.919	0.169

**Table 6***Tukey's HSD Results for Indirect Tensile Strength (ITS)*

<b>Tukey's HSD Post-Hoc</b>			
<i>Impact of Oxidative Conditioning</i>			
Oxidative Conditioning (I)	Oxidative Conditioning (J)	Mean Difference (I-J)	p-value
OTC	STOC	-.3967*	<.001*
	LTOC	-.5296*	<.001*
STOC	LTOC	-.1329*	<.001*
<i>Impact of Binder Type</i>			
Binder Type (I)	Binder Type (J)	Mean Difference (I-J)	p-value
PG 64-22	PG 52-34	.3289*	<.001*
	PG 76-22	-0.0332	0.425
PG 52-34	PG 76-22	-.3621*	<.001*

**Additional Load-Displacement Parameters**

To assess moisture damage in asphalt mixtures in greater detail, additional parameters were evaluated beyond the standard IDEAL-CT parameters ( $G_f$  and  $l_{75}/m_{75}$ ). Specifically, the analysis considered these parameters at different load levels, both before and after the peak load (pre-peak and post-peak), at 75%, 50%, and 25% of the load. The load-displacement curve presented in Figure 11 revealed that all post-peak parameters exhibited an increase due to moisture conditioning. This suggests that post-peak parameters may not be suitable indicators of moisture damage. On the other hand, pre-peak parameters may be more suitable for moisture damage evaluation. The asphalt

mixes with PG 64-22 are suitable for testing at all temperatures (ALT, AIT, and CIT), and LTOC level showed the highest impact of moisture damage. Therefore, this study analyzed the load and displacement data for these mixes, and the results are presented in Figure 19.

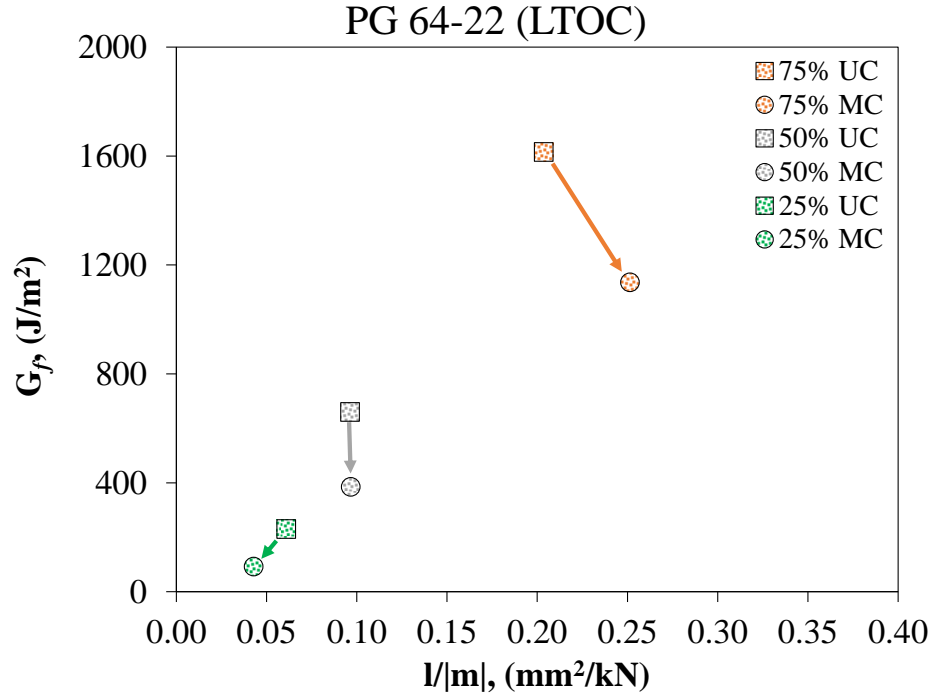


Figure 19. Results For Pre-Peak Parameters of PG 64-22 At The LTOC.

As seen in Figure 16, the  $G_f$  showed sensitivity to moisture conditioning at all pre-peak levels, consistent with the analysis of the original IDEAL-CT parameters. In terms of  $l_{75}/m_{75}$ , as the analysis level was lowered from 75% pre-peak to 25% pre-peak, the parameters showed the effect of moisture conditioning by decreasing from a UC value of 0.06 mm<sup>2</sup>/kN to an MC value of 0.04 mm<sup>2</sup>/kN, while remaining constant at 50% (0.1

mm<sup>2</sup>/kN for both UC and MC), and increasing at 75% (from 0.2 mm<sup>2</sup>/kN for UC to 0.25 mm<sup>2</sup>/kN for MC). Since all IDEAL-CT parameters 25% pre-peak showed higher response to moisture conditioning for mixes with PG 64-22 at the LTOC, additional analysis was carried out to validate this case across all asphalt binder types, oxidation levels, and testing temperatures with the results shown in Table 7.

**Table 7**

*Pre-Peak Parameters Analysis Results at 25%*

25% pre-peak	UC → MC		
	Oxidation Level	$G_{p25}$	$I_{25} /  m_{25} $
PG 64-22 (25°C)	OTC	Higher	Higher
	STOC	Lower	Lower
	LTOC	Lower	Lower
PG 76-22 (25°C)	OTC	Higher	Higher
	STOC	Lower	Higher
	LTOC	Lower	Equal
PG 52-34 (25°C)	OTC	Higher	Higher
	STOC	Lower	Equal
	LTOC	Higher	Higher
PG 76-22 (31°C)	OTC	Lower	Higher
	STOC	Lower	Higher
	LTOC	Lower	Higher
PG 52-34 (13°C)	OTC	Higher	Lower
	STOC	Lower	Higher
	LTOC	Lower	Higher

As seen in Table 7, although mixes with PG 64-22 at the LTOC consistently showed lower values of IDEAL-CT parameters after moisture conditioning, other mixes did not exhibit a reduction in all parameters. The changes in the  $G_{f25}$  and  $l_{25}/m_{25}$  values varied depending on the asphalt binder type, oxidation level, and testing temperature.

The findings presented in Figure 16 and Table 7 indicate that analyzing the pre-peak parameters at a lower analysis level allowed a greater number of parameters to reveal the impact of moisture conditioning on asphalt mixtures. Specifically, in PG 64-22 and LTOC, the analysis showed that at 25% pre-peak, both  $G_f$  and  $l_{75}/m_{75}$  were sensitive to moisture damage, and all IDEAL-CT parameters were affected, while other mixes did not show this impact in reducing all parameters.

## **SFE and FTIR-ATR Results**

### ***SFE Results***

**Contact Angle Measurements.** Contact angle measurements were taken from OB, RTFO, and PAV20 asphalt binders, and results for contact angle and corresponding coefficient of variance (COV%) are presented in Table 8. The results demonstrate a low average COV% of 1.0% compared to values seen in literature (Bionghi et al., 2021; Chen et al., 2020), indicating the reliability of the measurements taken in this study. Table 8 also shows that the contact angle measured for PG 64-22 and PG 76-22 increased with higher oxidative conditioning levels, apart from ethanol glycol for PG 76-22, for which

an inconsistent trend was observed. Specifically, the contact angle was higher at the RTFO but lower at the PAV20 conditioning. Results indicate that the wettability of asphalt binder reduces as a higher level of oxidation is applied, which causes an increase in the contact angle. This means that the asphalt binder becomes less susceptible to moisture damage because it becomes more viscous and less fluid, which reduces its ability to absorb moisture.

**Table 8**

*Contact Angle Measurements*

Mixture Constitute	Oxidation level	Distilled Water		Formamide		Ethylene Glycol	
		Average, °	COV, %	Average, °	COV, %	Average, °	COV, %
P-401 Granite Aggregate	-	57.1	1.2	31.5	0.9	24.8	0.7
PG 52-34	OB	100.9	0.8	75.4	0.7	81.1	0.7
	RTFO	103.4	2.8	79.1	2.2	82.5	2.4
	PAV20	97.6	0.7	76.0	0.4	83.1	0.6
PG 64-22	OB	93.1	0.7	76.8	0.7	79.2	0.6
	RTFO	95.8	0.6	78.2	0.5	78.4	0.5
	PAV20	96.9	0.7	79.8	0.3	79.1	0.5
PG 76-22	OB	101.8	0.6	84	0.4	81.3	0.4
	RTFO	102.4	0.7	85.5	0.2	81.7	0.4
	PAV20	102.7	0.4	85.3	0.2	79.8	0.1

With regards to PG 52-34 (Table 8), contact angle for distilled water and formamide increased moving from OB to RTFO level. The contact angle measurement, however, decreased at PAV20. Ethylene glycol's contact angle increased with oxidation.

**Surface Free Energy Components.** Table 9 presents the calculation of SFE components that were determined using the measured contact angles for all asphalt binder types at all oxidative conditioning levels, as well as that for P-401 granite aggregate. Asphalt binder results showed that for PG 52-34,  $\gamma^+$  was higher than that for PG 64-22 and PG 76-22 across all oxidative conditioning levels.  $\gamma^+$  decreased from OB level to RTFO level, then increased at the PAV20 level. Similar trends were overall seen for all PG 52-34's SFE components, as these measurements were calculated from the contact angle values. For PG 64-22, the incremental increase in contact angle with the effect of oxidative conditioning reflected a corresponding incremental decrease in all SFE components ( $\gamma^+$ ,  $\gamma^-$ ,  $\gamma^{LW}$ , and  $\gamma^{tot}$ ). In the case of PG 76-22, different trends are seen for every SFE component; however,  $\gamma^{tot}$  overall decreased with the effect of oxidative conditioning.

Additionally, results for the tested P-401 granite aggregate were reported and compared with two other granite aggregate types (Snyder granite and MMMC granite) obtained from Xu et al., 2018. It was found that the  $\gamma^+$  for the P-401 granite aggregate tested in this study was similar to the MMMC granite result (i.e., 0.4 mN/m).  $\gamma^-$  for the P-401 granite aggregate was 17.1 mN/m which was between that of the Snyder granite (i.e., 8.4 mN/m) and the MMMC granite (i.e., 37.0 mN/m).  $\gamma^{LW}$  component value was higher for the P-401 granite aggregate, compared to the Snyder and MMMC granite types.

Overall, results reveal that the sessile drop that was employed on aggregate is compatible with previous research done by Xu et al., 2018.

**Table 9**

*SFE Components Results*

Mixture Constitute	Oxidation Level	$\gamma^+$ (mN/m)	$\gamma^-$ (mN/m)	$\gamma^{LW}$ (mN/m)	$\gamma^{tot}$ (mN/m)
<u><b>Aggregate</b></u>					
P-401 Granite	N/A	0.4	17.1	67.7	62.6
Snyder Granite	N/A	0.1	8.4	35.2	37.0
MMMC Granite	N/A	0.4	37.0	35.8	43.7
<u><b>Asphalt Binder</b></u>					
PG 52-34	OB	6.55	0.71	67.13	62.8
	RTFO	3.53	0.53	52.41	49.7
	PAV20	7.51	2.04	66.89	59.0
PG 64-22	OB	2.79	4.58	47.14	40.0
	RTFO	1.00	3.13	38.20	34.7
	PAV20	0.55	2.99	33.67	31.1
PG 76-22	OB	0.01	1.64	24.06	23.9
	RTFO	0.07	1.69	19.65	20.3
	PAV20	0.37	1.46	17.02	18.5

**Work of Cohesion.** Work of cohesion ( $W_c$ ) results are shown in Figure 17. As can be seen from Figure 17, lower  $W_c$  was seen when increasing high PG grade of asphalt binders. Also,  $W_c$  for PG 64-22 and PG 76-22 generally decreased with increasing oxidative conditioning, with the lowest  $W_c$  seen at the PAV20 conditioning, but oxidation effects were inconsistent for PG 52-34 where  $W_c$  was lowest at the RTFO conditioning,



and higher  $W_c$  was seen at the PAV20 conditioning. These findings suggest that PG 52-34 may become more susceptible to moisture damage at the RTFO conditioning, while PG 64-22 and PG 76-22 may show higher susceptibility to moisture damage at the PAV20 conditioning. This is due to the reduced ability of PG 64-22 and PG 76-22 to resist internal deformation and fracture, shown in lower  $W_c$  at these oxidation conditions. Similar observations were reported by J. Wei & Zhang, 2010 where unjustified fluctuations in  $W_c$  were observed with the increase of oxidative conditioning level.

PG 52-34 is a softer asphalt binder. Due to its rubbery and elastic consistency, the PG 52-34 asphalt binder has a higher work of cohesion than the asphalt binders with a stiffer consistency (i.e., PG 64-22 and PG 76-22) at an equivalent ambient temperature. This contributes to the material's cohesive properties and makes it harder to separate. In addition to its flexibility, it is possible that the PG 52-34 may also have a greater degree of crosslinking between its asphalt molecules, which could further increase its cohesive strength. Because asphalt binders with greater rigidity, such as PG 64-22 and PG 76-22, require longer time to flow and deform under load, they may be more susceptible to moisture damage over time. This is because their reduced ability to accommodate stresses from traffic loading and temperature changes may lead to higher susceptibility to moisture damage. Because asphalt binders with greater rigidity, such as PG 64-22 and PG 76-22, require longer time to flow and deform under load, they may be more susceptible to moisture damage.

As seen, STOC had a greater impact on the cohesion of the PG 52-34 binder than PAV20 oxidation. Furthermore, the softer PG 52-34, required more energy to fail

cohesively when compared to stiffer binders. The chemical composition of the asphalt binder may be related to the behavior of SFE results (Howson et al., 2011; J. Wei et al., 2014; J. Wei & Zhang, 2010). In certain instances, variations in the total SFE component results have been observed in the literature (Federal Highway Administration (FHWA), 2001; Howson et al., 2011). According to a comprehensive study conducted by the Western Research Institute (WRI) on asphalt oxidation, these variations were attributed to the effect of asphalt oxidation on the chemistry and properties of the original unoxidized (OB) binder, which can vary depending on the severity of the oxidation process (Federal Highway Administration (FHWA), 2001).

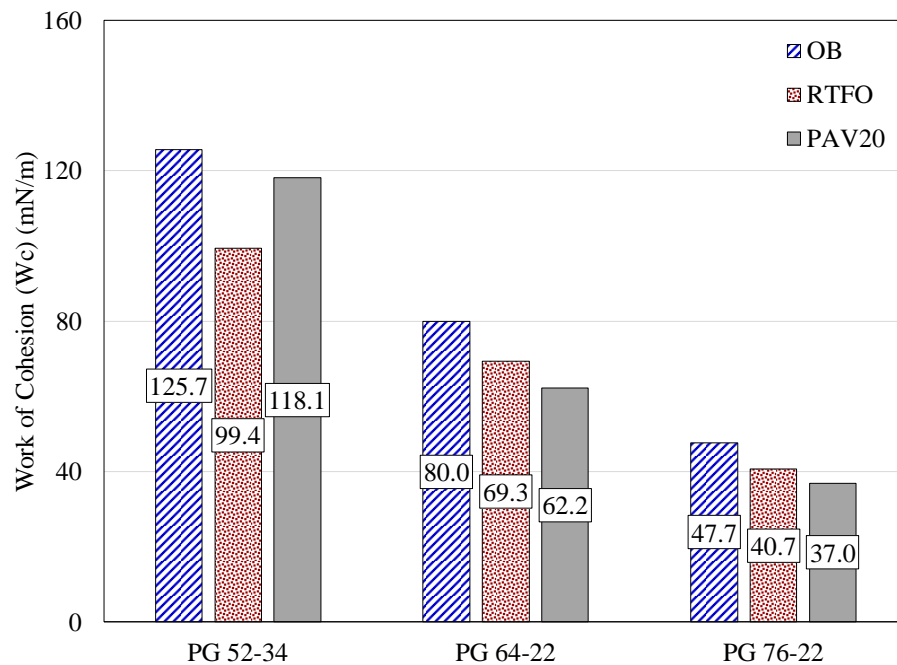


Figure 20. Work Of Cohesion Results

**Work of Adhesion, Water-Debonding, and Energy Ratio (ER).** Figure 18 presents the results for work of adhesion, water-debonding, and ER. Work of adhesion ( $W_{SA}^a$ ) results followed a similar trend like  $W_c$ . Consistent drop in  $W_{SA}^a$  was seen with the increase in asphalt stiffness and oxidative conditioning level, where PG 64-22 and PG 76-22 had the lowest  $W_{SA}^a$  seen at the PAV20 conditioning, and inconsistency in oxidation effect was seen for PG 52-34, where the lowest  $W_{SA}^a$  seen at the RTFO level. Results show that adhesion failure at the contact surface of softer asphalt binder and aggregate was less likely to occur, where higher resistance to moisture damage was observed.

Work of water-debonding ( $W_{SWA}^a$ ) values decreased with the increase in stiffness and oxidative conditioning levels (including PG 52-34). The ER did not follow a specific trend of oxidation and/or stiffness, as it fluctuated for PG 52-34, decreased for PG 64-22, and increased for PG 76-22. The ER after long-term oxidation of PAV20 for PG 52-34, PG 64-22, and PG 76-22 were 2.6, 2.6, and 1.9, respectively. Results of Figure 17 show that at the PAV20 conditioning, there is a tendency for the ER to decrease as the PG grade of the asphalt binder increases.

The results suggest that softer asphalt binders (i.e., PG 52-34) required a higher energy of water to separate the asphalt-aggregate interface, indicating better adhesion between the binder and aggregate, which reduces moisture damage. As a result, the lower ER required for separation of stiffer asphalt binders (i.e., PG 64-22 and PG 76-22) from the aggregate indicates a higher susceptibility to moisture damage.

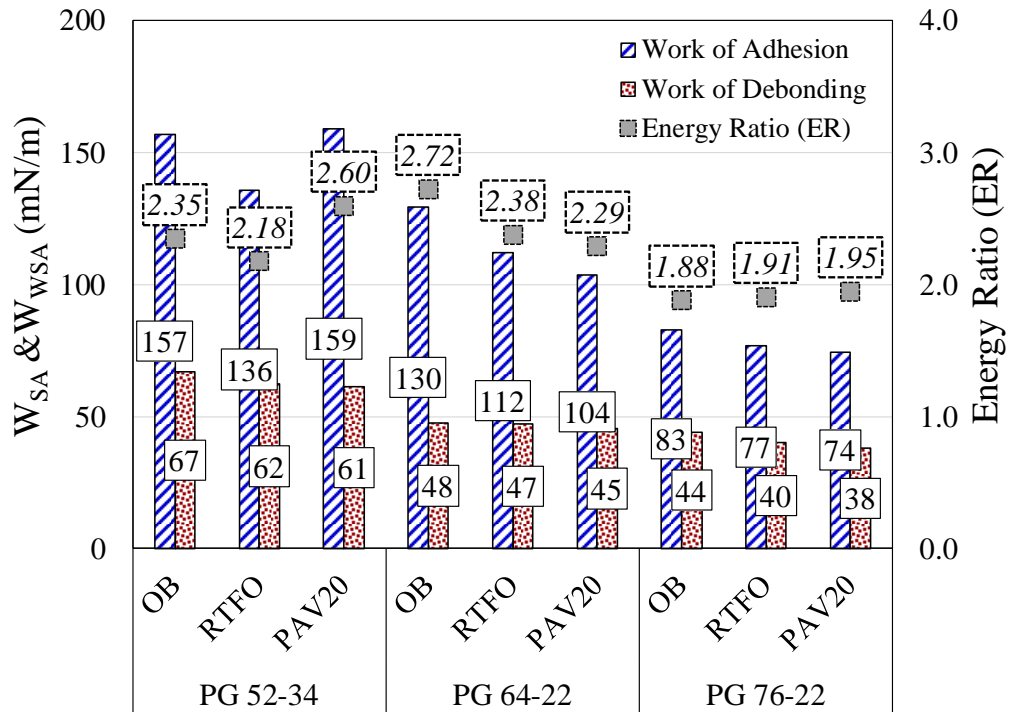
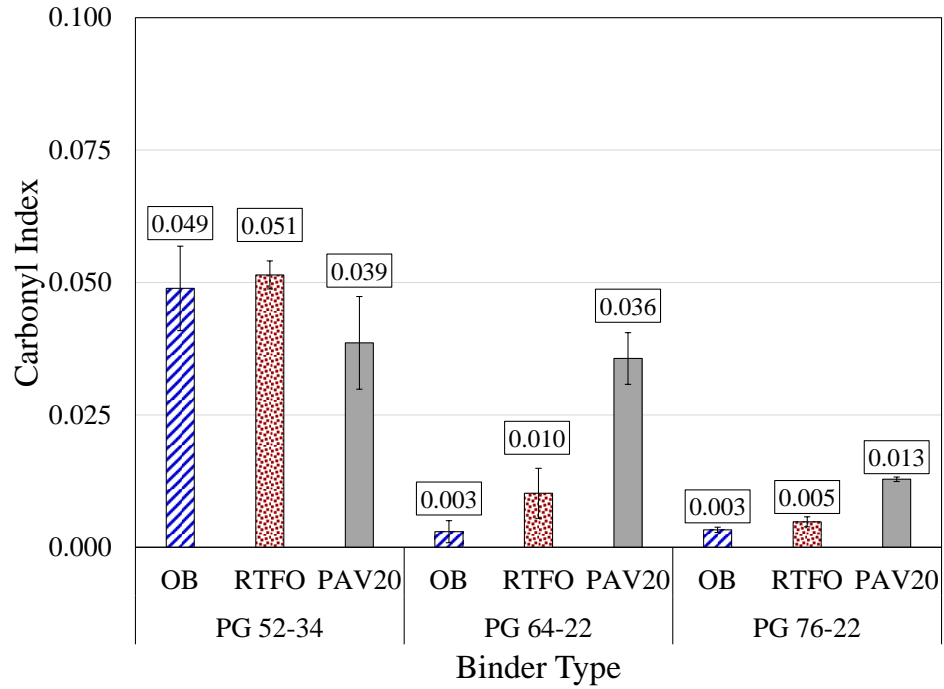


Figure 21. Work Of Adhesion, Debonding, And Energy Ratio Results

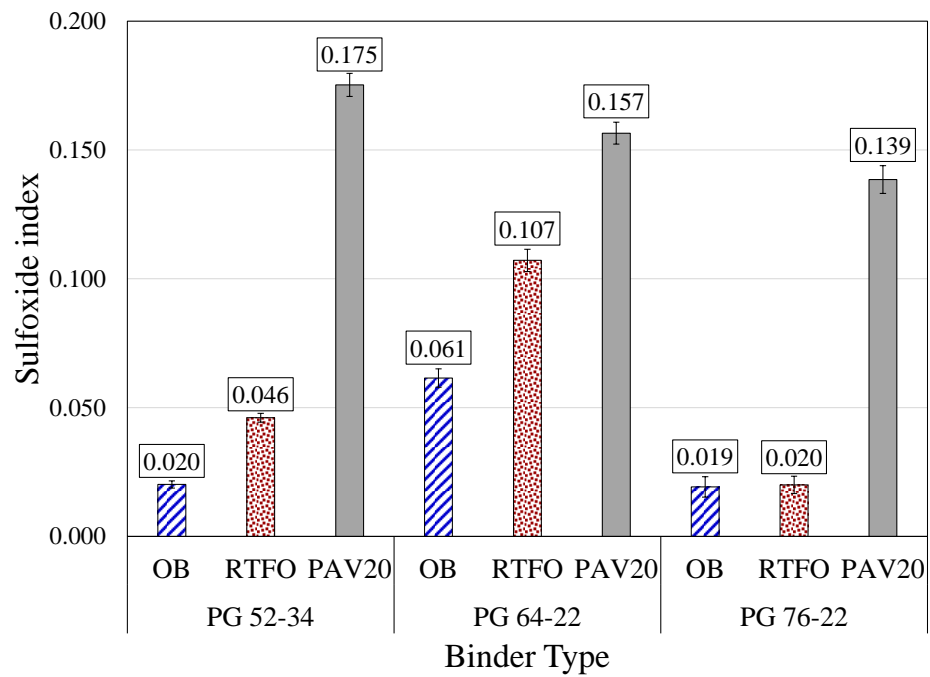
### FTIR-ATR Results

Figures 19a and 19b present the growth in carbonyl and sulfoxide indices, respectively. The overall trend shows an increase in carbonyl and sulfoxide indices with the increase of oxidation, and a decrease in these indices with the increase in the stiffness of the asphalt binder. As illustrated in Figure 19a, when evaluating the change in carbonyl index across the oxidative conditioning levels, it was found that all asphalt binder types generally showed lower susceptibility to oxidation, with a higher carbonyl index for RTFO than OB and for PAV20 than RTFO. However, this was not the case for

PAV20 where conditioning PG 52-34 showed reduced susceptibility to oxidation by obtaining a carbonyl index of 0.039 at the PAV20 conditioning, and the highest impact of oxidation (highest carbonyl index) was seen at the RTFO conditioning. These results correspond with the SFE results where PAV20 aged PG 52-34 showed higher work of cohesion (Figure 17) and work of adhesion (Figure 18). Similar observations between carbonyl index and SFE components were reported in literature (Mullapudi & Sudhakar Reddy, 2020). As illustrated in Figure 19b, sulfoxide index showed an increase in the susceptibility of oxidation for all combinations. PG 52-34 and PG 64-22 had higher susceptibility of oxidation than PG 76-22 at all conditioning levels.



(a) Carbonyl Index



(b) Sulfoxide Index

Figure 22. FTIR-ATR Test Results

## **Regression Analysis Between Mixture and Binder Tests**

In this study, a multiple linear regression analysis using ANOVA was conducted to better understand the relationship between asphalt mixture testing results (TSR%) and asphalt components (SFE and FTIR-ATR). The objective of the analysis was to provide researchers with a relatively simple and reliable method for estimating the TSR% of different types of asphalt binder and at various oxidation levels using SFE and FTIR-ATR tests.

To ensure accuracy, the laboratory oxidation conditionings applicable for asphalt binder were taken into consideration. Specifically, OB at the binder level was used to simulate OTC at the mixture level, RTFO at the binder level was used to simulate STOC at the mixture level, and PAV20 at the binder level, which is equivalent to LTOC at the mixture level and simulates long-term pavement aging, was used. These conditionings are shown in Table 10.

The approach offered researchers a quick and reliable method for estimating TSR% in different asphalt binder types and oxidation levels. This information was essential for pavement design and construction, as well as for understanding the long-term performance of asphalt pavement. In this study, TSR% was used as the dependent variable, and the work of cohesion representative of the SFE component, along with the carbonyl and sulfoxide indices, were included as the independent variables. The analysis was initiated by ensuring that  $W_c$ , carbonyl index, and sulfoxide indices were statistically significant in differentiating binder types and oxidation levels. An ANOVA analysis was

conducted with a significance level of 95% (or a p-value < 0.05), and the results are presented in Table 11.

**Table 10**

*Aging Levels for Regression Analysis*

<b>Binder Type</b>	<b>Field Aging</b>	<b>Binder Oxidation</b>	<b>Mixture Oxidation</b>
PG 52-34	Without aging	OB	OTC
	Short-term aging	RTFO	STOC
	Long-term aging	PAV20	LTOC
PG 64-22	Without aging	OB	OTC
	Short-term aging	RTFO	STOC
	Long-term aging	PAV20	LTOC
PG 76-22	Without aging	OB	OTC
	Short-term aging	RTFO	STOC
	Long-term aging	PAV20	LTOC

**Table 11**

*ANOVA Results for Tests Performed on Asphalt Binders*

<b>Factor</b>	<b>Work of Cohesion</b>		<b>Carbonyl Index</b>		<b>Sulfoxide Index</b>	
	F-value	p-value	F-value	p-value	F-value	p-value
Binder_Type	90.866	<.001*	184.613	<.001*	428.39	<.001*
Oxidation_Level	4.152	<b>0.033*</b>	12.724	<.001*	3006.14	<.001*
Binder_Type * Oxidation_Level	1.239	<b>0.033*</b>	20.361	<.001*	129.26	<.001*



Table 11 displays the ANOVA results for tests performed on asphalt binders, where the F-value and p-value were calculated for each factor, including Binder Type, Oxidation Level, and Binder Type \* Oxidation Level. The table shows that the values of  $W_c$ , carbonyl index, and sulfoxide index were all statistically significant, with a p-value below 0.05. This indicates the feasibility of these parameters to distinguish different binder types and oxidation levels. The results of the regression analysis for each significant parameter ( $W_c$ , carbonyl index, and sulfoxide index) separately and combined were examined for their relationship with TSR% at the CIT, and the findings are presented in Table 12.

**Table 12**

*Regression Analysis ( $R^2$ ) Between TSR% with SFE and FTIR-ATR Components*

Dependent Variable	Independent Variables	Multiple Linear Regression			
		(ANOVA Results)			
		Regression n	Regression p-value	$R^2$	Adjusted $R^2$
TSR% at CIT	$W_c$	10.491	<b>0.003*</b>	0.296	0.267
	Carbonyl Index	8.964	<b>0.001*</b>	0.428	0.380
	Sulfoxide Index	29.656	<b>&lt;.001*</b>	0.712	0.688
	All combined	25.678	<b>&lt;.001*</b>	0.878	0.740

Table 12 exhibits the Regression Analysis ( $R^2$ ) between TSR% at CIT with SFE and FTIR-ATR Components, where the dependent variable was TSR% at CIT, and the independent variables were  $W_c$ , carbonyl index, sulfoxide index, and all combined. The ANOVA results of the multiple linear regression for each interaction showed a significant p-value below 0.05. However, when applied to the regression separately, the adjusted  $R^2$ , which is the deciding factor, was lower for  $W_c$ , carbonyl index, and sulfoxide index. Nevertheless, the adjusted  $R^2$  for the combined parameters was the highest (0.740). The equation from the regression analysis is provided in Equation 18, which can be used to estimate TSR%:

$$\begin{aligned}
 \text{TSR}\% = & 78.93 + 0.491 \times W_c - 351.56 \times \text{Carbonyl Index} \\
 & - 197.346 \times \text{Suloxide Index}
 \end{aligned}
 \tag{18}$$

To validate the accuracy of the regression model, predicted TSR% values were compared with actual TSR% values for different binder types and oxidation conditioning, as shown in Table 13. The predicted TSR% values were obtained using the regression equation, and the actual TSR% values were measured in the laboratory. The standard deviation of the actual TSR% values was also provided, and it was observed that some predicted versus actual TSR% values exhibited a high standard deviation, particularly for PG 52-34 without aging, and at the short-term aging. However, the prediction was accurate long-term aging condition shown by the low absolute difference. While the regression model generally provided relatively accurate predictions of TSR% values at LTOC; where moisture conditioning had the highest effect, there were small differences between predicted and actual values. These findings have significant implications for

pavement design and construction, as well as for understanding the long-term performance of asphalt pavement.

**Table 13**

*Predicted And Actual TSR% Values*

<b>Binder Type</b>	<b>Field Aging</b>	<b>Predicted TSR%</b>	<b>Actual TSR%</b>	<b>Absolute Difference</b>
PG 52-34	Without aging	119.4%	133%	9.9%
	Short-term aging	100.5%	86%	10.4%
	Long-term aging	88.5%	85%	2.7%
PG 64-22	Without aging	105.0%	112%	5.1%
	Short-term aging	88.2%	85%	2.4%
	Long-term aging	66.0%	71%	3.5%
PG 76-22	Without aging	97.4%	99%	1.4%
	Short-term aging	93.2%	85%	6.1%
	Long-term aging	65.1%	86%	2.0%

The combined parameters of  $W_c$ , carbonyl index, and sulfoxide index offer a more reliable method for estimating TSR% compared to using these parameters separately. However, further research and validation efforts may be needed to ensure the accuracy and applicability of the regression model in different asphalt binder types and oxidation levels. It is important to note that the results and findings presented in this study are specific to the conditions and parameters used in the analysis, and caution should be exercised when applying the regression model to different binder types or oxidation conditioning. Further research and validation may be needed to ensure the

accuracy and applicability of the regression model in different asphalt binder types and oxidation levels, especially considering the observed high standard deviation for PG 52-34 without aging and at short-term aging.

## Chapter 6

### Summary of Findings, Conclusions, Recommendations & Future Work

#### Summary of Findings

This study evaluated the effect of asphalt oxidation and testing temperature on asphalt mixture moisture damage using AASHTO T283 and Surface Free Energy (SFE). Asphalt mixtures used in AASHTO T283 assessment were evaluated using two New Jersey asphalt binder grades (PG 64-22 and PG 76-22) and one Alaska and Canada asphalt binder grade (PG 52-34). Testing was conducted at the ambient laboratory temperature (ALT) of 25°C, asphalt intermediate temperature (AIT), and climatic intermediate temperature (CIT). Additionally, three oxidation levels (original test conditioning [OTC], short-term oxidative conditioning [STOC], and long-term oxidative conditioning [LTOC]) were evaluated to determine an appropriate level of oxidation and testing temperature to be applied in AASHTO T283 at which moisture damage is the highest. Additional analysis was conducted using the AASHTO T283 load displacement curve and IDEAL-CT parameters. As opposed to relying on  $CT_{index}$  parameter (final IDEAL-CT parameter), an interaction diagram was established to better study and comprehend the effects of oxidation and moisture conditioning on the load-displacement parameters. Furthermore, a statistical analysis was conducted to evaluate the effect of oxidation on moisture susceptibility of asphalt mixtures. The evaluation using SFE included original unaged binder (OB) and two oxidation levels—rolling thin film oven (RTFO) and 20 hours pressure aging vessel (PAV20)—that were applied to determine the short-term and long-term oxidative effects

on moisture damage susceptibility of asphalt mixtures, respectively. Additional chemical testing was adopted to quantify the functional group concentration in asphalt binder. In specific, the Fourier transform infrared spectroscopy (FTIR) attenuated total reflectance (ATR) test was used to quantify the effect of oxidative conditioning on the carbonyl and sulfoxide groups indices of various asphalt binders. Based on the results of this study, the following findings were drawn:

- **Tensile Strength Ratio (TSR%)**

- Based on the AASHTO T283 test results at ALT, moisture damaged the asphalt mixtures more as the level of oxidation increased. The biggest impact of oxidation on TSR% was seen at the LTOC level. This was seen for mixes prepared using PG 64-22 and PG 76-22 and tested at 25°C, where TSR% were 71% and 68%, respectively. However, testing PG 52-34 mixes at 25°C yielded increased TSR% after LTOC level where TSR% was 116%. The biggest impact on PG 52-34 mixes at 25°C was seen at the STOC level.
- Based on AASHTO T283 test results at AIT, impact of oxidation was better discerned when evaluating TSR% for mixes prepared using PG 52-34 at the AIT (i.e., 13°C), where the lowest TSR% was seen at the STOC (86%) and LTOC (85%). PG 76-22 mixes when tested at the AIT (i.e., 31°C), the TSR values were maintained around 64% across all oxidation conditioning, showing minimum impact of oxidation on TSR%.
- The TSR% was observed to be the lowest when the CIT testing temperature was applied, including PG 64-22 and PG 76-22 mixes when tested at the ALT (i.e.,

25°C), and PG 52-34 when tested at the AIT (i.e., 13°C). These findings suggest that the CIT is the appropriate testing temperature that shows higher susceptibility to moisture damage.

- ANOVA and Tukey's post-hoc statistical analysis also support the conclusion that moisture conditioning had the most significant impact at CIT, all at the STOC and LTOC levels, where a statistical significance (i.e., p-value < 0.05) was seen for PG 64-22, PG 76-22 at 25°C, and PG 52-34 at 13°C.
- **IDEAL-CT Parameters**
  - Based on IDEAL-CT test results, it was found that moisture conditioning had a positive impact on  $CT_{index}$ , with an average increase of 58.1% for all oxidation levels. The increase in  $CT_{index}$  due to moisture conditioning was mainly attributable to an increase of  $l_{75}/|m_{75}|$ , with an average increase of 66.2%. On the other hand, oxidation had a negative impact on  $CT_{index}$ , with an average reduction of 2.3% for all oxidation levels.
  - The IDEAL-CT results showed that moisture conditioning had an impact only on  $G_f$ , with reductions observed at different oxidation levels. For mixes with PG 64-22, the impact was observed at the LTOC, resulting in an average decrease of 20.1%. Similarly, for mixes with PG 76-22, the impact was also observed at the LTOC, resulting in an average decrease of 11.7%. The highest impact was seen in mixes with PG 52-34 at the STOC, with an average decrease of 13.4%. Overall, moisture conditioning primarily affected  $G_f$  and showed varying effects on different asphalt mixes.

- The IDEAL-CT data analysis at lower level than the peak (75%, 50%, and 25% pre-peak) showed that compared to the analysis at 75% and 50%, the moisture conditioning analysis at 25% pre-peak performance resulted in a decrease in pre-peak  $l_{25}/m_{25}$ , from 0.06 mm<sup>2</sup>/kN to 0.04 mm<sup>2</sup>/kN. Although there was a decline in certain IDEAL-CT parameters, not all binder types, oxidative conditioning, and testing temperatures were affected. These results indicate that moisture conditioning at 25% did not have a uniform effect on all IDEAL-CT parameters.
  
- **Surface Free Energy (SFE)**
  - The sessile drop method was utilized to determine the SFE of aggregate materials. It was found that the values obtained using this method were comparable to those reported in the literature. The  $\gamma^+$  value for the P-401 granite aggregate was like that of MMMC granite (i.e., 0.4 mN/m), and the  $\gamma^-$  value (i.e., 8.4 mN/m) was between that of Synder granite (8.4 mN/m) and MMMC granite (i.e., 37.0 mN/m), supporting the accuracy of the test method.
  - The study found that an increase in asphalt stiffness and oxidative conditioning led to a decrease in total surface free energy and the work of cohesion of the asphalt. This reduction in surface energy and cohesion, in turn, led to a decrease in the asphalt's susceptibility to moisture damage. Interestingly, PG 52-34 asphalt had the lowest total surface free energy (measured at 49.7 mN/m) after RTFO conditioning compared to the OB (i.e., 62.8 mN/m) and PAV20 (i.e., 59.0 mN/m) conditioning. On the other hand, PG 64-22 and PG 76-22 showed the highest moisture damage,



indicated by their lowest total SFE of 31.1 mN/m and 18.5 mN/m, respectively, at the PAV20 oxidative conditioning level. In comparison, their values were higher at the OB conditioning (i.e., 40.0 mN/m and 23.9 mN/m for PG 64-22 and PG 76-22, respectively), and RTFO conditioning (i.e., 34.7 mN/m and 20.3 mN/m for PG 64-22 and PG 76-22, respectively). The work of debonding followed the trends seen for the work of adhesion.

- The Energy Ratio (ER) showed no consistent trend in terms of asphalt stiffness or level of oxidation. Specifically, ER was lowest at the RTFO for PG 52-34 (i.e., 2.2) compared to OB (i.e., 2.3) and PAV20 (i.e., 2.6). At the PAV20, PG 64-22 had the lowest ER (i.e., 2.3) compared to OB (i.e., 2.7) and RTFO (i.e., 2.4). In contrast, PG 76-22 asphalt was minimally affected by the impact of oxidation, as all oxidation levels showed a similar ER of 1.9. These results suggest that the ER is a complex measure affected by various factors, including the asphalt's composition and the type and level of conditioning.

- **FTIR-ATR**

- There is an overall trend of increase in carbonyl and sulfoxide indices with the increase of oxidation and a decrease with the increase in asphalt binder stiffness.
- All asphalt binder types generally showed lower susceptibility to oxidation, with a higher carbonyl index for RTFO than OB and for PAV20 than RTFO.
- The study found that the increase in binder stiffness corresponded to higher carbonyl and sulfoxide indices, indicating greater susceptibility to oxidation. PG

52-34 had the highest carbonyl index of 0.049 at the RTFO level, and highest sulfoxide index and sulfoxide index of 0.175 at the PAV20 level. In contrast, PG 64-22 had a higher susceptibility to oxidation than PG 76-22 had higher susceptibility of oxidation at the PAV20 level, with carbonyl indices of 0.036 and 0.013 and sulfoxide indices of 0.157 and 0.139, respectively.

- The results suggest that PG 52-34 had reduced susceptibility to oxidation with the highest carbonyl index seen at the RTFO conditioning. These results correspond with the SFE results where PAV20 aged PG 52-34 showed higher work of cohesion and work of adhesion.

- **Regression Analysis**

- A regression analysis was performed between TSR% at CIT with SFE and FTIR-ATR Components. The dependent variable was TSR% at CIT, and the independent variables were  $W_c$ , carbonyl index, sulfoxide index, and all combined. ANOVA results of the multiple linear regression for each interaction were significant with a p-value below 0.05. However, adjusted R2 was lower for  $W_c$ , carbonyl index, and sulfoxide index when applied to the regression separately. The adjusted R2 for the combined parameters was the highest (0.740).

## **Conclusions**

Based on the findings from this study, the following conclusions can be found:

- **Effect of Oxidation on TSR%:** The long- and short-term oxidation had a greater impact on moisture damage compared to the original test procedure when characterizing moisture damage of asphalt mixtures.
- **Effect of Testing Temperature on TSR%:** To assess the highest susceptibility to moisture damage, it is recommended to test mixes for TSR% at the climatic intermediate temperature applicable for each binder, rather than at a constant 25°C. This is because TSR% results were consistently lower at the climatic intermediate temperature, indicating a greater vulnerability to moisture damage.
- **Load-Displacement Curves Parameters:** The study found that  $G_f$ , as well as all IDEAL-CT parameters at 25% pre-peak obtained from the IDEAL-CT test method, has good potential for characterizing moisture damage of asphalt mixtures.
- **SFE:** An increase in asphalt stiffness and oxidative conditioning led to a decrease in total surface free energy and work of cohesion, as well as a reduction in susceptibility to moisture damage. However, PG 52-34 had the lowest total surface free energy at the RTFO conditioning compared to the OB, while PG 64-22 and PG 76-22 showed the highest moisture damage (lowest total SFE) at the PAV20 oxidative conditioning level.
- **FTIR-ATR:** There is an overall trend of an increase in carbonyl and sulfoxide indices with the increase of oxidation and a decrease with the increase in asphalt binder stiffness. All asphalt binder types generally showed lower susceptibility to oxidation, with a higher carbonyl index for RTFO than OB and for PAV20 than RTFO.
- **Regression Analysis:** a regression analysis was conducted to develop a linear model that predicts TSR% at the CIT, based on the work of cohesion, carbonyl, and sulfoxide

indices. Using the SFE, carbonyl, and sulfoxide indices, an equation was established to forecast the TSR% at the CIT. This model can provide a quick and non-destructive approach for estimating the TSR% at various oxidation levels.

## **Recommendations**

Based on the conclusions from this study, the following recommendations were drawn:

- **Effect of Oxidation on TSR%:** It is recommended to revise AASHTO T283 to consider alternative oxidation conditioning for characterizing moisture damage in asphalt mixtures when conducting TSR% testing.
- **Effect of Testing Temperature on TSR%:** It is recommended that the testing for TSR% should be conducted at the climatic intermediate temperature applicable for each binder, instead of at a fixed temperature of 25°C.
- **Load-Displacement Curves Parameters:** It is recommended that the IDEAL-CT parameters should be considered when evaluating moisture damage in asphalt mixtures, and parameters such as  $G_f$  and all IDEAL-CT parameters at 25% pre-peak can be included in the evaluation of asphalt mixtures.
- **Estimation of TSR% using SFE and FTIR-ATR:** The estimation of TSR% of asphalt mixtures at CIT is applicable using the range of work of cohesion, and the carbonyl and sulfoxide indices. These parameters can be easily measured using the SFE method and FTIR. Further validation is needed using a larger dataset of asphalt mixtures. Additionally, the model can be implemented by incorporating it into existing laboratory protocols. Future

work should expand the model to include additional asphalt mixture components that affect TSR%, such as air void content, aggregate types and gradation, and binder types.

### **Study Limitations and Future Work**

It is recommended that future research consider assessing the laboratory performance of various asphalt mixtures produced by different plants, particularly those that incorporate recycled asphalt pavement (RAP), which is commonly used in pavement construction today. This would provide a more comprehensive representation of the performance of asphalt pavements currently in use. Additionally, while this study did not investigate the impacts of factors such as saturation levels and freeze-thaw cycles on the performance of this study's specific mixtures at different oxidation levels, it is possible that these factors could affect asphalt performance at other oxidation levels. Further investigation would be needed to fully understand the relationship between these factors and asphalt performance under different aging levels. Future research should acknowledge and carefully consider the limitations of this study, particularly with regards to the equivalence of the SFE and FTIR-ATR methods for predicting TSR% at the climatic intermediate temperature. The validity of these methods may depend on various factors such as binder types and aggregate materials and may require modifications or adaptations to suit specific conditions or materials. To better comprehend the relationship between oxidative conditioning level and susceptibility to moisture damage, future research should consider a wider variety of asphalt binders and aggregate materials. This model may involve evaluating different types modified and unmodified asphalt binders

and analyzing the effect of different aggregate types on the susceptibility to moisture damage could also provide valuable insights.

## References

- AASHTO. (2009). AASHTO Standard Specifications for Transportation Materials and Methods of Sampling and Testing (Part 1 – Specifications), Twenty-Ninth Edition, American Association of State Highway and Transportation Officials, Washington, DC. 2009.
- Abdulrahman, S., Hainin, M. R., Satar, M., Hassan, N. A., & Usman, A. (2019). Rutting and moisture damage evaluation of warm mix asphalt incorporating POFA modified bitumen. *Int. J. Eng. Adv. Technol*, 9(1).
- Abo-Qudais, S. (2007). The effects of damage evaluation techniques on the prediction of environmental damage in asphalt mixtures. *Building and Environment*, 42(1), 288–296.
- Ahmad N. (2011). Asphalt mixture moisture sensitivity evaluation using surface energy parameters. University of Nottingham.
- Airey, G. D., Choi, Y. K., Collop, A. C., Moore, A. J. v, & Elliott, R. C. (2005). Combined laboratory ageing/moisture sensitivity assessment of high modulus base asphalt mixtures (with discussion). *Journal of the Association of Asphalt Paving Technologists*, 74.
- Airey, G. D., & Choi, Y.-K. (2002). State of the art report on moisture sensitivity test methods for bituminous pavement materials. *Road Materials and Pavement Design*, 3(4), 355–372.
- Airey, G. D., Collop, A. C., Zoorob, S. E., & Elliott, R. C. (2008). The influence of aggregate, filler and bitumen on asphalt mixture moisture damage. *Construction and Building Materials*, 22(9), 2015–2024.
- Alam, M. M. (1998). A test method for identifying moisture-susceptible asphalt concrete mixes. The University of Texas at El Paso.
- Al-Badr, B. K. (2021). High Polymer Modified of Investigation Laboratory A Asphalt Mixtures With Softening Agent.
- Alfalah, A., Offenbacher, D., Ali, A., Decarlo, C., Lein, W., Mehta, Y., & Elshaer, M. (2020). Assessment of the impact of fiber types on the performance of fiber-reinforced hot mix asphalt. *Transportation Research Record*, 2674(4), 337–347.
- Alfalah, A., Offenbacher, D., Ali, A., Mehta, Y., Elshaer, M., & Decarlo, C. (2021). Evaluating the impact of fiber type and dosage rate on laboratory performance of Fiber-Reinforced asphalt mixtures. *Construction and Building Materials*, 310, 125217.

- Ali, A., Kabir, S. F., Al-Badr, B., Alfalah, A., Xie, Z., Decarlo, C., Elshaer, M., & Mehta, Y. (2022). Laboratory performance of dense graded asphalt mixtures prepared using highly polymer modified binders containing corn oil as softening agent. *Construction and Building Materials*, 345, 128336.
- Al-Swailmi, S. H. (1992). Development of a test procedure for water sensitivity of asphalt concrete mixtures.
- Al-Swailmi, S., & Terrel, R. L. (1992). Evaluation of water damage of asphalt Concrete mixtures using the environmental conditioning system (Ecs)(with discussion). *Journal of the Association of Asphalt Paving Technologists*, 61.
- Amelian, S., Abtahi, S. M., & Hejazi, S. M. (2014). Moisture susceptibility evaluation of asphalt mixes based on image analysis. *Construction and Building Materials*, 63, 294–302.
- Ameri, M., Vamegh, M., Naeni, S. F. C., & Molayem, M. (2018). Moisture susceptibility evaluation of asphalt mixtures containing Evonik, Zycotherm and hydrated lime. *Construction and Building Materials*, 165, 958–965.
- Aschenbrener, T. (1995). Evaluation of Hamburg wheel-tracking device to predict moisture damage in hot-mix asphalt. *Transportation Research Record*, 1492, 193.
- ASTM. (2011). Standard test method for effect of water on compressive strength of compacted bituminous mixtures.
- Azari, H. (2010). Precision estimates of AASHTO T283: Resistance of compacted hot mix asphalt (HMA) to moisture-induced damage. *Citeseer*.
- Badal, A., Carvajal-Munoz, J. S., & Airey, G. (2020). Comparison of the Effects of Hydrated Lime on the Moisture-Induced Damage of Stone Mastic Asphalt (SMA) Mixtures. *RILEM International Symposium on Bituminous Materials*, 465–471.
- Bahmani, H., Sanij, H. K., & Peiravian, F. (2022). Estimating Moisture Resistance of asphalt mixture containing epoxy resin using Surface Free Energy Method and Modified Lottman test. *International Journal of Pavement Engineering*, 23(10), 3492–3504.
- Bausano, J., & Williams, R. C. (2009). Transitioning from AASHTO T283 to the simple performance test using moisture conditioning. *Journal of Materials in Civil Engineering*, 21(2), 73–82.



- Bazuhair, R. W., Howard, I. L., Middleton, A., Jordan III, W. S., & Cox, B. C. (2020). Combined Effects of Oxidation, Moisture, and Freeze–Thaw on Asphalt Mixtures. *Transportation Research Record*, 2674(12), 409–424.
- Bhasin, A., Little, D. N., Vasconcelos, K. L., & Masad, E. (2007). Surface free energy to identify moisture sensitivity of materials for asphalt mixes. *Transportation Research Record*, 2001(1), 37–45.
- Bhasin, A., Masad, E., Little, D., & Lytton, R. (2006). Limits on adhesive bond energy for improved resistance of hot-mix asphalt to moisture damage. *Transportation Research Record*, 1970(1), 2–13.
- Bionghi, R., Shahraki, D., Ameri, M., & Karimi, M. M. (2021). Correlation between bond strength and surface free energy parameters of asphalt binder-aggregate system. *Construction and Building Materials*, 303, 124487.
- Birgisson, B., Roque, R., Tia, M., & Masad, E. A. (2005). Development and evaluation of test methods to evaluate water damage and effectiveness of antistripping agents.
- Braham, A. F., Buttlar, W. G., Clyne, T. R., Marasteanu, M., & Turos, M. I. (2009). The effect of long-term laboratory aging on asphalt concrete fracture energy. *Asphalt Paving Technology: Association of Asphalt Paving Technologists-Proceedings of the Technical Sessions*, 78, 417–445.
- Brown, E. R., Kandhal, P. S., & Zhang, J. (2001). Performance testing for hot mix asphalt. *NCAT Report*, 1(05).
- Buchanan, M. S., Moore, V., Mallick, R., O'Brien, S., & Regimand, A. (2004). Accelerated moisture susceptibility testing of hot mix asphalt (HMA) mixes. 83rd *Transportation Research Board Annual Meeting*. Washington, DC.
- Caputo, P., Miriello, D., Bloise, A., Baldino, N., Mileti, O., & Ranieri, G. A. (2020). A comparison and correlation between bitumen adhesion evaluation test methods, boiling and contact angle tests. *International Journal of Adhesion and Adhesives*, 102, 102680.
- Chen, Y., Dong, S., Wang, H., Gao, R., & You, Z. (2020). Using surface free energy to evaluate the fracture performance of asphalt binders. *Construction and Building Materials*, 240, 118004.
- Cheng, D. (2002). Surface free energy of asphalt-aggregate system and performance analysis of asphalt concrete based on surface free energy. Texas A&M University.

- Cheng, D., Little, D. N., Lytton, R. L., & Holste, J. C. (2002). Use of surface free energy properties of the asphalt-aggregate system to predict moisture damage potential (with discussion). *Journal of the Association of Asphalt Paving Technologists*, 71.
- Chindaprasirt, P., Hatanaka, S., Mishima, N., Yuasa, Y., & Chareerat, T. (2009). Effects of binder strength and aggregate size on the compressive strength and void ratio of porous concrete. *International Journal of Minerals, Metallurgy and Materials*, 16(6), 714–719.
- CJ Zollinger. (2005). Application of surface energy measurements to evaluate moisture susceptibility of asphalt and aggregates. Texas A&M University.
- Collop, A. C., Choi, Y. K., Airey, G. D., & Elliott, R. C. (2004). Development of the saturation ageing tensile stiffness (SATS) test. *Proceedings of the Institution of Civil Engineers-Transport*, 157(3), 163–171.
- Cong, L., Ren, M., Shi, J., Yang, F., & Guo, G. (2020). Experimental investigation on performance deterioration of asphalt mixture under freeze–thaw cycles. *International Journal of Transportation Science and Technology*, 9(3), 218–228.
- Copeland, A. R., Youtcheff, J., & Shenoy, A. (2007). Moisture sensitivity of modified asphalt binders: Factors influencing bond strength. *Transportation Research Record*, 1998(1), 18–28.
- Crucho, J., Picado-Santos, L., Neves, J., & Capitão, S. (2019). A review of nanomaterials' effect on mechanical performance and aging of asphalt mixtures. *Applied Sciences*, 9(18), 3657.
- Das, A. K., & Singh, D. (2017). Investigation of rutting, fracture and thermal cracking behavior of asphalt mastic containing basalt and hydrated lime fillers. *Construction and Building Materials*, 141, 442–452.
- Dave, E. v, Daniel, J. S., & Mallick, R. B. (2018). Moisture susceptibility testing for hot mix asphalt pavements in New England. Final Report for New England Transportation Consortium, Project, 13–15.
- Diab, A., & You, Z. (2013). Development of a realistic conditioning and evaluation system to study moisture damage of asphalt materials. In *Airfield and Highway Pavement 2013: Sustainable and Efficient Pavements* (pp. 1008–1017).
- Do, T. C., Tran, V. P., Lee, H. J., & Kim, W. J. (2019). Mechanical characteristics of tensile strength ratio method compared to other parameters used for moisture susceptibility evaluation of asphalt mixtures. *Journal of Traffic and Transportation Engineering (English Edition)*, 6(6), 621–630.

- Dupré, A. (1869). *Théorie mécanique de la chaleur*. Gauthier-Villars.
- Eid, Z. A. (2000). Evaluation of anti-stripping additives in asphalt mixtures. University of Nevada, Reno.
- Elwardany, M. D., Rad, F. Y., Castorena, C., & Kim, Y. R. (2018). Climate-, depth-, and time-based laboratory aging procedure for asphalt mixtures. *Journal of the Association of Asphalt Paving Technologists*, 87, 467–511.
- Elwardany, M. D., Yousefi Rad, F., Castorena, C., & Kim, Y. R. (2017). Evaluation of asphalt mixture laboratory long-term ageing methods for performance testing and prediction. *Road Materials and Pavement Design*, 18(sup1), 28–61.
- Emery, J., & Seddik, H. (1997). Moisture damage of asphalt pavements and antistripping additives: Background document.
- Epps, J. A. (2000). Compatibility of a test for moisture-induced damage with superpave volumetric mix design (Issue 444). Transportation Research Board.
- FAA. (2020). AC 150/5370-10H, Standard Specifications for Construction of Airports, 21 December 2018 (updated by errata 19 August 2020). <http://www.faa.gov/airports/aip/procurement/>.
- Yin, F., West, R., Powell, B., & DuBois, C. J. (2023). Short-Term Performance Characterization and Fatigue Damage Prediction of Asphalt Mixtures Containing Polymer-Modified Binders and Recycled Plastics. *Transportation Research Record*, 03611981221143119.
- Federal Highway Administration (FHWA). (2001). *Fundamental Properties of Asphalts and Modified Asphalts, Volume 1; Interpretive Report*.
- Giwa, I., Sadek, H., & Zaremotekhas, F. (2021). Evaluation of different analysis approaches for Hamburg Wheel-Tracking testing (HWTT) data. *Construction and Building Materials*, 280, 122420.
- Good, R. J. (1992). Contact angle, wetting, and adhesion: a critical review. *Journal of Adhesion Science and Technology*, 6(12), 1269–1302.
- Grenfell, J., Ahmad, N., Airey, G., Collop, A., & Elliott, R. (2012). Optimising the moisture durability SATS conditioning parameters for universal asphalt mixture application. *International Journal of Pavement Engineering*, 13(5), 433–450.

- Grenfell, J., Ahmad, N., Liu, Y., Apeageyi, A., Large, D., & Airey, G. (2014). Assessing asphalt mixture moisture susceptibility through intrinsic adhesion, bitumen stripping and mechanical damage. *Road Materials and Pavement Design*, 15(1), 131–152.
- Grenfell, J., Apeageyi, A., & Airey, G. (2015). Moisture damage assessment using surface energy, bitumen stripping and the SATS moisture conditioning procedure. *International Journal of Pavement Engineering*, 16(5), 411–431.
- Hajj, E. Y., Aschenbrener, T. B., & Nener-Plante, D. (2021). Case Studies on the Implementation of Balanced Mix Design and Performance Tests for Asphalt Mixtures: Maine Department of Transportation (MaineDOT). UNR Pavement Engineering & Science Program.
- Hefer, A. W. (2004). Adhesion in bitumen-aggregate systems and quantification of the effects of water on the adhesive bond. Texas A&M University.
- Hicks, R. G., Santucci, L., & Aschenbrener, T. (2003). Introduction and seminar objectives. Moisture Sensitivity of Asphalt Pavements-A National Seminar California Department of Transportation; Federal Highway Administration; National Asphalt Pavement Association; California Asphalt Pavement Alliance; and Transportation Research Board.
- Hofko, B., Alavi, M. Z., Grothe, H., Jones, D., & Harvey, J. (2017). Repeatability and sensitivity of FTIR ATR spectral analysis methods for bituminous binders. *Materials and Structures*, 50(3), 1–15.
- Hofko, B., Porot, L., Falchetto Cannone, A., Poulidakos, L., Huber, L., Lu, X., Mollenhauer, K., & Grothe, H. (2018). FTIR spectral analysis of bituminous binders: Reproducibility and impact of ageing temperature. *Materials and Structures*, 51(2), 1–16.
- Hossain, K., Karakas, A., & Hossain, Z. (2019). Effects of aging and rejuvenation on surface-free energy measurements and adhesion of asphalt mixtures. *Journal of Materials in Civil Engineering*, 31(7), 04019125.
- Howson, J., Bhasin, A., Masad, E., Lytton, R., & Little, D. (2009). Development of a database for surface energy of aggregates and asphalt binders. Texas Transportation Institute.
- Howson, J., Masad, E., Bhasin, A., Little, D., & Lytton, R. (2011). Comprehensive analysis of surface free energy of asphalts and aggregates and the effects of changes in pH. *Construction and Building Materials*, 25(5), 2554–2564.

- Ibrahim, A.-H. A. (2019). Laboratory investigation of aged HDPE-modified asphalt mixes. *International Journal of Pavement Research and Technology*, 12, 364–369.
- Jakarni, F. M., Rosli, M. F., Yusoff, N. I. M., Aziz, M. M. A., Muniandy, R., & Hassim, S. (2016). An overview of moisture damage performance tests on asphalt mixtures. *Jurnal Teknologi*, 78(7–2).
- Jemere, Y. (2010). Development of a laboratory ageing method for bitumen in porous asphalt. *Constr. Build. Mater*, 204–210.
- Kandhal, P. S. (1992). Moisture susceptibility of HMA mixes: identification of problem and recommended solutions. National Asphalt Pavement Association Lanham, MD.
- Karlsson, R., & Isacson, U. (2003). Application of FTIR-ATR to characterization of bitumen rejuvenator diffusion. *Journal of Materials in Civil Engineering*, 15(2), 157–165.
- Kaukuntla, P. R. (2014). Standard ruggedness study on moisture induced sensitivity tester (MIST). Oklahoma State University.
- Khan, R., Grenfell, J., Collop, A., Airey, G., & Gregory, H. (2013). Moisture damage in asphalt mixtures using the modified SATS test and image analysis. *Construction and Building Materials*, 43, 165–173.
- Kim, Y. R., Castorena, C., Elwardany, M. D., Rad, F. Y., Underwood, S., Akshay, G., Gudipudi, P., Farrar, M. J., & Glaser, R. R. (2018). Long-term aging of asphalt mixtures for performance testing and prediction.
- Kringos, N., Azari, H., & Scarpas, A. (2009). Identification of parameters related to moisture conditioning that cause variability in modified Lottman test. *Transportation Research Record*, 2127(1), 1–11.
- Kringos, N., Scarpas, A., & Azari, H. (2009). Combined experimental and numerical analysis of moisture infiltration in the modified Lottman test. In *Advanced Testing and Characterization of Bituminous Materials, Two Volume Set* (pp. 277–286). CRC Press.
- LaCroix, A., Regimand, A., & James, L. (2016). Proposed approach for evaluation of cohesive and adhesive properties of asphalt mixtures for determination of moisture sensitivity. *Transportation Research Record*, 2575(1), 61–69.
- Li, H., Yu, J., Wu, S., Liu, Q., Wu, Y., Xu, H., & Li, Y. (2020). Effect of moisture conditioning on mechanical and healing properties of inductive asphalt concrete. *Construction and Building Materials*, 241, 118139.

- Li, L., Yang, Y., Gao, Y., & Zhang, Y. (2021). Healing characterisations of waste-derived bitumen based on crack length: Laboratory and modelling. *Journal of Cleaner Production*, 316, 128269.
- Li, Z., Li, K., Chen, W., Liu, W., Yin, Y., & Cong, P. (2022). Investigation on the characteristics and effect of plant fibers on the properties of asphalt binders. *Construction and Building Materials*, 338, 127652.
- Liang, R. (2008). Refine AASHTO T283 resistance of compacted bituminous mixture to moisture induced damage for superpave. United States. Federal Highway Administration.
- Liu, Z., Cao, L., Zhou, T., & Dong, Z. (2020). Multiscale Investigation of Moisture-Induced Structural Evolution in Asphalt–Aggregate Interfaces and Analysis of the Relevant Chemical Relationship Using Atomic Force Microscopy and Molecular Dynamics. *Energy & Fuels*, 34(4), 4006–4016.
- Maadani, O., Shafiee, M., & Egorov, I. (2021). Climate change challenges for flexible pavement in Canada: an overview. *Journal of Cold Regions Engineering*, 35(4), 03121002.
- Masad, E., Zollinger, C., Bulut, R., Little, D., Lytton, R., Khalid, H., Davis, R., Scarpas, T., Fini, E., & Guarin, A. (2006). Characterization of HMA moisture damage using surface energy and fracture properties. *Asphalt Paving Technology: Association of Asphalt Paving Technologists-Proceedings of the Technical Sessions*, 75, 713–754.
- Mirwald, J., Nura, D., & Hofko, B. (2022). Recommendations for handling bitumen prior to FTIR spectroscopy. *Materials and Structures*, 55(2), 1–17.
- Mohammad, L. (2015). NCHRP project 20-07/task 361: hamburg wheel-track test equipment requirements and improvements to AASHTO T 324: research project capsule. Louisiana Transportation Research Center.
- Mullapudi, R. S., & Sudhakar Reddy, K. (2020). An investigation on the relationship between FTIR indices and surface free energy of RAP binders. *Road Materials and Pavement Design*, 21(5), 1326–1340.
- Nazirizad, M., Kavussi, A., & Abdi, A. (2015). Evaluation of the effects of anti-stripping agents on the performance of asphalt mixtures. *Construction and Building Materials*, 84, 348–353.
- Nicholls, J. C., Prime, J., Meitei, B., & Lowe, A. (2011). Review of Saturation Ageing Tensile Stiffness (SATS) test for use in Ireland.

- Partl, M. N., Bahia, H. U., Canestrari, F., de la Roche, C., di Benedetto, H., Piber, H., & Sybilski, D. (2012). Advances in interlaboratory testing and evaluation of bituminous materials: state-of-the-art report of the RILEM technical committee 206-ATB (Vol. 9). Springer Science & Business Media.
- Petersen, J. C. (2000). Chemical composition of asphalt as related to asphalt durability. In *Developments in petroleum science* (Vol. 40, pp. 363–399). Elsevier.
- Polaczyk, P., Ma, Y., Xiao, R., Hu, W., Jiang, X., & Huang, B. (2021). Characterization of aggregate interlocking in hot mix asphalt by mechanistic performance tests. *Road Materials and Pavement Design*, 22(sup1), S498–S513.  
<https://doi.org/10.1080/14680629.2021.1908408>
- Rad, F. Y., Elwardany, M. D., Castorena, C., & Kim, Y. R. (2017). Investigation of proper long-term laboratory aging temperature for performance testing of asphalt concrete. *Construction and Building Materials*, 147, 616–629.
- Radeef, H. R., Hassan, N. A., Abidin, A. R. Z., Mahmud, M. Z. H., Yaacob, H., Mashros, N., & Mohamed, A. (2021). Effect of aging and moisture damage on the cracking resistance of rubberized asphalt mixture. *Materials Today: Proceedings*, 42, 2853–2858.
- Rafiq, W., Napiah, M. Bin, Sutanto, M. H., Alaloul, W. S., Khan, M. I., & Al-Sabaei, A. (2020). Performance evaluation for rutting and moisture damage of hot asphalt mixtures using high percentage of recycled asphalt pavement material. *IOP Conference Series: Earth and Environmental Science*, 498(1), 012010.
- Rahman, F., & Hossain, M. (2014). Review and analysis of Hamburg Wheel Tracking device test data.
- Rahman, M. A., Ghabchi, R., Zaman, M., & Ali, S. A. (2021). Rutting and moisture-induced damage potential of foamed warm mix asphalt (WMA) containing RAP. *Innovative Infrastructure Solutions*, 6(3), 1–11.
- Rahmani, E., Darabi, M. K., Little, D. N., & Masad, E. A. (2017). Constitutive modeling of coupled aging-viscoelastic response of asphalt concrete. *Construction and Building Materials*, 131, 1–15.
- Saedi, S., & ORUÇ, Ş. (2020). The Effects of Nano Bentonite and Fatty Arbocel on Improving the Behavior of Warm Mixture Asphalt against Moisture Damage and Rutting. *CIVIL ENGINEERING JOURNAL-TEHRAN*, 6(5).

- Saltibus, N. E., & Wasiuddin, N. M. (2017). Moisture damage in asphalt: Analysis based on the dewetting mechanism. *Journal of Materials in Civil Engineering*, 29(6), 04017002.
- Samara, M., Offenbacher, D., Mehta, Y., Ali, A., Elshaer, M., & Decarlo, C. (2022). Performance Evaluation and Characterization of Extracted Recycled Asphalt Binder With Rejuvenators. *Transportation Research Record*, 03611981221097091.
- Sarsam, S. (2021). Assessing the surface free energy of modified asphalt binder with image processing technique. *International Journal of Intelligent Networks*, 2, 70–76.
- Schrader, M. E. (1995). Young-dupre revisited. *Langmuir*, 11(9), 3585–3589.
- Schram, S., & Williams, R. C. (2012). Ranking of HMA moisture sensitivity tests in Iowa. Iowa Department of Transportation Ames, IA.
- Shackil, G. J. (2020). EVALUATING CRACKING PERFORMANCE OF POLYMER ENHANCED AND FIBER REINFORCED MICROSURFACE MIXTURES USING ASPHALT LABORATORY TESTING.
- Shanahan, M. E. R. (1991). Adhesion and wetting: similarities and differences. *Rubber World;(United States)*, 205(1).
- Sirin, O., Paul, D. K., & Kassem, E. (2018). State of the art study on aging of asphalt mixtures and use of antioxidant additives. *Advances in Civil Engineering*, 2018.
- Solaimanian, M., Bonaquist, R. F., & Tandon, V. (2007). Improved conditioning and testing procedures for HMA moisture susceptibility (Vol. 589). *Transportation Research Board*.
- Solaimanian, M., Harvey, J., Tahmoressi, M., & Tandon, V. (2003). Test methods to predict moisture sensitivity of hot-mix asphalt pavements. *Transportation Research Board National Seminar*. San Diego, California, 77–110.
- Swiertz, D., Ling, C., Teymourpour, P., & Bahia, H. (2017). Use of the Hamburg wheel-tracking test to characterize asphalt mixtures in cool weather regions. *Transportation Research Record*, 2633(1), 9–15.
- Taib, A., Jakarni, F. M., Rosli, M. F., Yusoff, N. I. M., & Abd Aziz, M. (2019). Comparative study of moisture damage performance test. *IOP Conference Series: Materials Science and Engineering*, 512(1), 012008.
- Tandon, V., & Nazarian, S. (2001). *Modified Environmental Conditioning System: Validation and Optimization*.



- Tandon, V., Vemuri, N., Nazarian, S., & Tahmoressi, M. (1996). A comprehensive evaluation of environmental conditioning system. Center for Geotechnical and Highway Materials Research, University of Texas.
- Tarefder, R. A., Weldegiorgis, M. T., & Ahmad, M. (2014). Assessment of the effect of pore pressure cycles on moisture sensitivity of hot mix asphalt using MIST conditioning and dynamic modulus. *Journal of Testing and Evaluation*, 42(6), 1530–1540.
- Tavassoti, P., & Baaj, H. (2020). Moisture Damage in Asphalt Concrete Mixtures: State of the Art and Critical Review of the Test Methods. Transportation Association of Canada 2020 Conference and Exhibition-The Journey to Safer Roads.
- Tayebali, A. A., Guddati, P. M., Yadav, S., & LaCroix, A. (2017). Use of moisture induced stress tester (MiST) to determine moisture sensitivity of asphalt mixtures. North Carolina Department of Transportation (NCDOT) Project, 1.
- Terrel, R. L., & Al-Swailmi, S. (1994). Water sensitivity of asphalt-aggregate mixes: test selection (Issue SHRP-A-403).
- The M.I.S.T.TM. (2022). The M.I.S.T.TM. <https://www.instrotek.com/products/the-m-i-s-t>
- Tu, C., Luo, R., & Huang, T. (2021). Influence of Infiltration Velocity on the Measurement of the Surface Energy Components of Asphalt Binders Using the Wilhelmy Plate Method. *Journal of Materials in Civil Engineering*, 33(9), 04021243.
- Twagira, M. E., & Jenkins, K. J. (2009). Moisture damage on bituminous stabilized materials using a MIST device. In *Advanced Testing and Characterization of Bituminous Materials, Two Volume Set* (pp. 299–310). CRC Press.
- van Oss, C. J., Chaudhury, M. K., & Good, R. J. (1987). Monopolar surfaces. *Advances in Colloid and Interface Science*, 28, 35–64.
- Vemuri, N. (1996). Evaluation and modification of environmental conditioning system to predict the moisture susceptibility of hot mix asphalt concrete. The University of Texas at El Paso.
- Vinet-Cantot, J., Gaudefroy, V., Delfosse, F., Chailleux, E., & Crews, E. (2019). Stripping at the bitumen–aggregate interface: A laboratory method To assess the loss of chemical adhesion. *Energy & Fuels*, 33(4), 2641–2650.

- Wei, J., Dong, F., Li, Y., & Zhang, Y. (2014). Relationship analysis between surface free energy and chemical composition of asphalt binder. *Construction and Building Materials*, 71, 116–123.
- Wei, J. M., Zhang, Y. Z., & Youtcheff, J. (2009). Determination of the surface free energy of asphalt binders by sessile drop method. *Acta Petrolei Sinica (Petroleum Processing Section)*, 25(2), 207–215.
- Wei, J., & Zhang, Y. (2010). Influence of aging on surface free energy of asphalt binder. *International Journal of Pavement Research and Technology*, 3(6), 343.
- Wei, J., & Zhang, Y. (2012). Application of sessile drop method to determine surface free energy of asphalt and aggregate. ASTM International.
- Xiao, R., Polaczyk, P., & Huang, B. (2022). Measuring moisture damage of asphalt mixtures: The development of a new modified boiling test based on color image processing. *Measurement*, 190, 110699.
- Xiao, R., Polaczyk, P., Wang, Y., Ma, Y., Lu, H., & Huang, B. (2022). Measuring moisture damage of hot-mix asphalt (HMA) by digital imaging-assisted modified boiling test (ASTM D3625): Recent advancements and further investigation. *Construction and Building Materials*, 350, 128855.
- Xu, W., Luo, R., Zhang, K., Feng, G., & Zhang, D. (2018). Experimental investigation on preparation and performance of clear asphalt. *International Journal of Pavement Engineering*, 19(5), 416–421.
- Yan, C., Zhang, Y., & Bahia, H. U. (2020). Comparison between SCB-IFIT, un-notched SCB-IFIT and IDEAL-CT for measuring cracking resistance of asphalt mixtures. *Construction and Building Materials*, 252. <https://doi.org/10.1016/j.conbuildmat.2020.119060>
- Yan, K., Ge, D., You, L., & Wang, X. (2015). Laboratory investigation of the characteristics of SMA mixtures under freeze–thaw cycles. *Cold Regions Science and Technology*, 119, 68–74.
- Yin, F., Chen, C., West, R., Martin, A. E., & Arambula-Mercado, E. (2020). Determining the relationship among hamburg wheel-tracking test parameters and correlation to field performance of asphalt pavements. *Transportation Research Record*, 2674(4), 281–291.
- Young, T. (1805). III. An essay on the cohesion of fluids. *Philosophical Transactions of the Royal Society of London*, 95, 65–87.

- Yusoff, N. I. M., Breem, A. A. S., Alattug, H. N. M., Hamim, A., & Ahmad, J. (2014). The effects of moisture susceptibility and ageing conditions on nano-silica/polymer-modified asphalt mixtures. *Construction and Building Materials*, 72, 139–147.
- Zaidi, S. B. A., Airey, G. D., Grenfell, J., Ahmad, N., & Ahmed, I. (2022). Moisture susceptibility assessment of hydrated lime modified asphalt mixture and surface energy. *International Journal of Pavement Engineering*, 23(3), 599–611.
- Zhang, D., & Luo, R. (2019). Using the surface free energy (SFE) method to investigate the effects of additives on moisture susceptibility of asphalt mixtures. *International Journal of Adhesion and Adhesives*, 95, 102437.
- Zhou, F., Im, S., Sun, L., & Scullion, T. (2017). Development of an IDEAL cracking test for asphalt mix design and QC/QA. *Road Materials and Pavement Design*, 18(sup4), 405–427.
- Zhou, L., Huang, W., Zhang, Y., Lv, Q., & Sun, L. (2021). Mechanical evaluation and mechanism analysis of the stripping resistance and healing performance of modified asphalt-basalt aggregate combinations. *Construction and Building Materials*, 273, 121922.
- Ziari, H., Moniri, A., Bahri, P., & Saghafi, Y. (2019). The effect of rejuvenators on the aging resistance of recycled asphalt mixtures. *Construction and Building Materials*, 224, 89–98.

## Appendix

### List of Abbreviations

Abbreviation	Definition	Abbreviation	Definition
ITS	Indirect Tensile Strength`	$\gamma^{LW}$	Lifshitz-van der Waals Component
TSR	Tensile Strength Ratio	$\gamma^{AB}$	Acid-Base Component
IDEAL-CT	Indirect Tensile Asphalt Cracking Test	GvOC	Good-van Oss-Chaudhury
SFE	Surface Free Energy	$\gamma^+$	Lewis Acid Surface Interaction Component
FTIR-ATR	Fourier Transform Infrared Spectroscopy – Attenuated Total Reflectance	$\gamma^-$	Lewis Base Surface Interaction Component
HWTT	Hamburg Wheel Tracking Test	$\theta$	Contact Angle
SATS	Saturated Ageing Tensile Stiffness	$\gamma_s$	Solid Surface Free Energy
ECS	Environmental Conditioning System	$\gamma_{SL}$	Solid-Liquid Interface Free Energy
M.I.S.T	Moisture Induced Sensitivity Test	$\gamma_L$	Liquid Surface Tension
SIP	Stripping Inflection Point	$W_c$	Work of Cohesion
NTEC	Nottingham Transportation Engineering Centre	$W_a$	Work of Adhesion
SSD	Saturated Surface Dry	$W_{SA}^a$	Work of Adhesion
ITSM	Indirect Tensile Stiffness Modulus	$W_{SWA}^a$	Work of Debonding

SHRP	Strategic Highway Research Program	ER	Energy Ratio
OSU	Oregon State University	NMAS	Nominal Maximum Aggregate Size
SCB	Semi-Circular Bending Test	FAA	Federal Aviation Administration
HMA	Hot-Mix Asphalt	USACE	US Army Corps of Engineers
NCHRP	National Cooperative Highway Research Program	JMF	Job Mix Formula
AVC	Air Void Content	Ndes	Number of Design Gyration
FHWA	Federal Highway Administration	VMA	Voids in Mineral Aggregate
TxDOT	Texas Department of Transportation	OBC	Optimum Binder Content
AFM	Atomic Force Microscopy	OTC	Original Test Conditioning
USD	Universal Sorption Device	STOC	Short-Term Oxidative Conditioning
RTFO	Rolling Thin Film Oven	LTOC	Long-Term Oxidative Conditioning
PAV20	Pressure Aging Vessel for 20 Hours	ALT	Ambient Laboratory Temperature
ITSMC	The Indirect Tensile Strength for Moisture Conditioned Specimens	AIT	Asphalt Intermediate Temperature
ITSUC	The Indirect Tensile Strength for Unconditioned Specimens	CIT	Climate Intermediate Temperature
$CT_{index}$	Cracking Tolerance Index	PG HI	Binder High Performance Grade Temperature

$G_f$	Fracture Energy	PG LT	Binder Low Performance Grade Temperature
$ m_{75} $	Absolute Slope of Load and Displacement from 85% to 65% Post-Peak Load	LTPP	Long-Term Pavement Performance
$l_{75}$	Displacement Corresponding To 75% of the Peak Load at the Post-Peak Stage	NCAT	National Center for Asphalt Technology
$t$	Specimen Thickness	OB	Original Unaged Binder
$D$	Specimen Diameter	PG	Performance Grade
$P_{100}$	Peak Load	ANOVA	Analysis of Variance
$W_f$	Work of Fracture	HSD	Honestly Significant Difference
$P_{70}$	75% Peak Load	WRI	Western Research Institute
$\gamma^{tot}$	Total SFE		